UNIVERSITY OF SOUTHAMPTON

Natural Dark Matter within

the Minimal Supersymmetric

Standard Model

by

Jonathan Peter Roberts

A thesis submitted for the degree of

Doctor of Philosophy

School of Physics and Astronomy

August 2006

To Kate and my family

UNIVERSITY OF SOUTHAMPTON

ABSTRACT

FACULTY OF SCIENCE

SCHOOL OF PHYSICS AND ASTRONOMY

Doctor of Philosophy

Natural Dark Matter within the Minimal Supersymmetric Standard Model

Jonathan Peter Roberts

It is often claimed that supersymmetry naturally explains the observed dark matter relic density. We provide a quantitative study of the fine-tuning required to fit the observed dark matter relic density within the Minimal Supersymmetric Standard Model (MSSM) and a semi-realistic type I string model. Within the MSSM we find the degree of tuning to be closely correlated to the dominant annihilation channel of neutralinos in the early universe. Some annihilation channels, such as t-channel slepton exchange, can require no fine-tuning at all whereas others, such as annihilation via an on-shell Higgs h^0, can require tuning at the 0.1% level. We go on to consider a semi-realistic type I string model. We find many of the regions require the same degree of tuning as in the MSSM. Where there are large variations we find that they can be explained by relations between the input parameters of the string model and those of the MSSM. This opens up the possibility of guiding research into models of SUSY breaking by attempting to minimise fine-tuning.

Contents

List of Figures

List of Tables

Preface

The work described in this thesis was carried out in collaboration with Prof.
S. F. King. The following details the original work and gives references for
the material.

- Chapter 3: S. F. King and J. P. Roberts, arXiv:hep-ph/0603095.

- Chapter 4: S. F. King and J. P. Roberts, arXiv:hep-ph/0608135.

No claims of originality are made for Chapter 1 and much of Chapter 2
which were compiled from a number of sources.

Acknowledgements

I would like to thank Steve for his help and encouragement throughout. I would like to thank my family and Kate for their support.

I have had a good time at Southampton, thanks to the friendly nature of all the students in the postgrad offices. Special thanks go to Iain, for teaching me C++ and SOFTSUSY, James and Martin W. for answers to endless computing questions and Oli and Martin N. for much appreciated distraction techniques.

Chapter 1

Introduction

1.1 Motivation

The Standard Model of particle physics (SM) has survived extensive testing
throughout the 20th century. At the beginning of the 21st, the discovery of
neutrino masses, the observed relic density of non-baryonic dark matter and
extreme sensitivity of the Higgs mass to Planck scale physics all suggest that
era of the Standard Model is coming to an end. To solve these problems we
must look for physics Beyond the Standard Model (BSM).

One of the leading contenders for BSM physics is supersymmetry (SUSY).
Low energy SUSY stabilises the Higgs mass, provides an excellent dark mat-
ter candidate, naturally generates electroweak symmetry breaking (EWSB)
and has close ties to string theory. Unfortunately the Minimal Supersym-
metric Standard Model (MSSM) has 124 free parameters, so concrete pre-
dictions are hard to make. This freedom comes from our ignorance about
the source of SUSY breaking. To make contact with experiment it is im-
portant to constrain these free parameters using present experimental data

or to derive SUSY and the mechanism of SUSY breaking from some more fundamental theory, such as a string model, with fewer degrees of freedom.

Different regions of the remaining parameter space correspond to different mechanisms of SUSY breaking. Though each of these regions satisfy present experimental bounds, they are not all equally well-motivated. Two primary motivations of SUSY are that it provides a mechanism for breaking electroweak symmetry and that it provides a natural explanation for dark matter. Different structures of SUSY breaking can provide more or less natural explanations of these phenomena. This is quantified in terms of the fine-tuning of the parameters that is required to produce both radiative electroweak symmetry breaking of the correct form, and the tuning required to produce the observed dark matter density.

Models that require large fine-tuning are not ruled out. The MSSM is not proposed as a complete theory, rather it is an effective theory that arises from some more fundamental physics. It is this more fundamental theory that should remove any fine-tuning present within the MSSM, just as SUSY removes the tuning of the Higgs mass required within the Standard Model. Therefore if evidence for a model that requires large fine-tuning were discovered by experiment, the degree and type of fine-tuning should provide a clue as to the structure of the more fundamental theory.

Therefore by studying the experimental constraints on MSSM models and the fine-tuning required to produce EWSB and dark matter:

- We constrain the parameter space allowing predictions for the phenomenology of supersymmetric theories at future collider and direct dark matter detection experiments.

- Studying the fine-tuning allows us to compare how naturally different regions explain EWSB and dark matter.

- SUSY is motivated by its removal of the fine-tuning in the Standard Model. Equally, if the Large Hadron Collider (LHC) finds evidence for a finely tuned region of the MSSM parameter space we can use this fine-tuning to motivate a theory of SUSY breaking.

1.2   Thesis structure

This thesis is organised as follows. In Chapter 1 we introduce the Standard Model (SM) and motivate the need to move beyond it. We specifically consider $\mathcal{N} = 1$ supersymmetry (SUSY) in the form of the Minimal Supersymmetric Standard Model (MSSM). We highlight the reasons for taking SUSY seriously as well as noting the open questions.

In Chapter 2 we look at the methods used to constrain supersymmetric models. We summarise the most restrictive experimental bounds and look at the patterns of input parameters that are required to satisfy them. We focus particularly on the calculation of the dark matter relic density. There are a few distinct channels by which supersymmetric models can reproduce the observed relic density. Each has their own distinct signature. We also introduce means of measuring the fine-tuning required to provide electroweak symmetry breaking and dark matter. This allows us to quantify how naturally any given SUSY model explains two of the significant problems that plague the Standard Model.

In Chapter 3 we study the MSSM with different boundary conditions.

We begin by looking at the simplest case, the Constrained Minimal Supersymmetric Standard Model (CMSSM), before going on to study less restricted models. We catalogue the parameter space that satisfies all experimental bounds and analyse the fine-tunings required in each case. This allows us to study the tunings required to produce the observed dark matter density through different annihilation channels. Once we move beyond the CMSSM we find regions that require no tuning to account for the observed dark matter density whereas others require tuning at the 0.1% level.

In Chapter 4 we extend this analysis to a semi-realistic type I string theory. We introduce the model and the relevant aspects of model building within type I string theories. Using experimental bounds we once again constrain the parameter space. We study the phenomenology of the remaining regions, finding distinctive experimental signatures. By studying the fine-tuning required for EWSB and dark matter within we once again find natural dark matter. This also allows us to study the variation of fine-tuning between the MSSM and more fundamental theories, highlighting the use of fine-tuning as a guide to model building.

The overall conclusions of this thesis are presented in Chapter 5.

1.3   The Standard Model

Before we consider SUSY, we must understand why there is a need for new physics. This means considering the present theory of particle physics, the Standard Model. The Standard Model (SM) of particle physics is a renormalisable gauge quantum field theory based on the gauge group $G_{\text{SM}} =$

Field	Spin	$SU(3)_c$	$SU(2)_L$	$U(1)_Y$
Left-handed quarks, $Q_{iL} \equiv (u_{iL}, d_{iL})$	1/2	**3**	**2**	1/6
Right-handed up quarks u_{iR}	1/2	**3**	**1**	2/3
Right-handed down quarks d_{iR}	1/2	**3**	**1**	$-1/3$
Left-handed leptons $L_{iL} \equiv (\nu_{iL}, e_{iL})$	1/2	**1**	**2**	$-1/2$
Right-handed electrons e_{iR}	1/2	**1**	**1**	-1
Gluons, g^α, $\alpha \in \{1, \ldots, 8\}$	1	**8**	**1**	0
Weak bosons, W^a, $a \in \{1, 2, 3\}$	1	**1**	**3**	0
Hypercharge boson, B	1	**1**	**1**	0
Higgs boson, $\phi \equiv (\phi^+, \phi_0)$	0	**1**	**2**	1/2

Table 1.1: Gauge representations of the Standard Model fields. Note that left-handed (right-handed) fields transform as doublets (singlets) under $SU(2)_L$. There are three generations of fermionic matter. These are designated by the subscript i on the quark and lepton fields where $u_i \in \{u, c, t\}$, $d_i \in \{d, s, b\}$, $e_i \in \{e, \mu, \tau\}$, $\nu_i \in \{\nu_e, \nu_\mu, \nu_\tau\}$.

$SU(3)_c \otimes SU(2)_L \otimes U(1)_Y$[1]. Every fundamental particle observed to date corresponds to a field within this quantum field theory. Table 1.1 lists these particles along with their gauge quantum numbers.

The Standard Model has been fantastically successful in accounting for experimental data. All the leptons have been directly observed. The quark model accounts for the wide spectrum of hadrons observed. Quarks and gluons also explain data from deep inelastic scattering (DIS) experiments. The hypercharge and weak bosons mix when electroweak symmetry is broken to form the photon, Z and $W^\pm$. These have been directly produced at colliders, and of course the existence of the photon was proved long ago. Beyond such direct evidence there is a wealth of precision data such as the measured rates of rare decays that test quantum corrections to processes from loop diagrams involving the Standard Model fields. From this data there are only a handful of signals that cannot be clearly accounted for by the fields in Table 1.1. The only particle that remains unobserved is the

---

[1]Here we summarise the Standard Model and introduce the features that are important to motivate the search for new physics. For the technical details of the Standard Model see for example [1], [2].

Higgs boson.

1.3.1   The Higgs mechanism

Though it has yet to be observed, the Higgs boson is an integral component of the Standard Model. Without the Higgs, all the particles would be massless. We are forbidden from writing down a mass term for the gauge bosons and the fermions by the requirement that the Lagrangian be gauge invariant. Through the Higgs boson we can break electroweak symmetry and generate masses in a gauge invariant way.

The Higgs mechanism is somewhat ad hoc within the Standard Model. One of the primary motivations for SUSY is that it naturally results in electroweak symmetry breaking (EWSB). As EWSB is both a key feature of SUSY and one of its primary motivations, we summarise EWSB in the Standard Model here. First we notice that we are allowed to write down a gauge invariant Yukawa interaction term of the form:

$$\mathcal{L}_{\text{Yukawa}} = \overline{Q}_{iL}\left(-i\tau_2\phi^*\right)u_{jR}Y^u_{ij} + \overline{Q}_{iL}\phi d_{jR}Y^d_{ij} + \overline{L}_{iL}\phi e_{jR}Y^e_{ij} + h.c. \quad (1.1)$$

If the Higgs field develops a non-zero vacuum expectation value (VEV), such terms give rise to masses for the quarks and leptons. In the Standard Model we postulate the Higgs potential to have the form:

$$\mathcal{L}_{\text{Higgs}} = (D^\mu\phi)^\dagger (D_\mu\phi) - \left[-m_H^2\phi^\dagger\phi + \frac{\lambda}{2}\left(\phi^\dagger\phi\right)^2\right], \quad (1.2)$$

6

where D^μ is the covariant derivative:

$$D_\mu = \partial_\mu - ig'YB_\mu - igW_\mu^a T^a. \tag{1.3}$$

Here g' is the $U(1)_Y$ hypercharge coupling and g is the $SU(2)_L$ gauge coupling.

Now consider the form of the potential Eq. 1.2. If $m_H^2 > 0$ and $\lambda > 0$ the minimum of the potential is no longer at $\phi = 0$. This results in the Higgs field developing a non-zero VEV:

$$\langle \phi \rangle = \sqrt{\frac{m_H^2}{\lambda}}. \tag{1.4}$$

Such a VEV spontaneously breaks electroweak symmetry (EWSB):

$$SU(2)_L \otimes U(1)_Y \to U(1)_{\text{em}}. \tag{1.5}$$

To perform calculations in quantum field theory we must take perturbations around the minima of the potential. Therefore we rewrite the Higgs field:

$$\phi(x) = \frac{1}{\sqrt{2}} \begin{pmatrix} 0 \\ v + h(x) \end{pmatrix}, \tag{1.6}$$

where v is the VEV, $\langle \phi \rangle$, and $h(x)$ is the physical Higgs field. If we substitute Eq. 1.6 into Eq. 1.2, the first term of Eq. 1.2 gives rise to mass terms[2] for $W^\pm$ and the Z^0. In the process of giving mass to the gauge bosons three

---

[2]The physical fields $W^\pm$, Z^0, γ are formed of linear combinations of W^a and B that have definite electric charge. We do not cover this step here as it is well described in textbooks and somewhat off the spine of the argument. Similarly note that Eq. 1.1 does not lead directly to the physical masses of the fermions, we must perform a rotation first.

of the Higgs bosons develop Goldstone modes and are "eaten", leaving one real physical Higgs boson, three massive gauge bosons and a massless photon. Equally when we substitute Eq. 1.6 into Eq. 1.1 the Yukawa couplings generate a mass for the fermions.

The Higgs mechanism provides a very clean method of providing mass to the Standard Model particles. Unfortunately no mechanism within the Standard Model naturally generates a Higgs potential of the form in Eq. 1.2, we must put it in by hand. The various free parameters are set by experiment. The size of the Higgs VEV is set by the gauge boson masses. The entries in the Yukawa matrices are set by the observed masses of the fermions. In all, the Standard Model has 27 free parameters that must be set by experiment.

1.3.2   Successes of the Standard Model

The Standard Model has been rigorously tested since its inception and accounts for the vast wealth of experimental data [3] almost without exception. However it does more than accommodate the observed experimental data. It explains the observed phenomena and has a long list of predictions that have been borne out by experiment.

Measurements of the Z^0 width at LEP have constrained the number of active neutrinos with masses $m_\nu < M_Z/2$ to be three. This requires that there be three generations of quarks and leptons which is in agreement with observations. The quark model successfully predicts the mass spectra of light mesons and baryons. The unitarity of the Cabibbo-Kobayashi-Maskawa (CKM) matrix [4] results in the Glashow-Iliopoulos-Maiani (GIM) mechanism [5] for the suppression of flavour changing processes and allowed

for the prediction of the charm quark. The Higgs mechanism explains how the bosons and fermions can acquire mass in a gauge invariant way. This in turn explains the short range of the weak force. The process of renormalisation allows us to understand the running of physical parameters with energy which, when applied to the strong force, allows us to understand the confinement of quarks into hadrons. Finally, perturbative calculations allow us to calculate quantities to successively higher degrees of accuracy. These calculations are then tested by precision experiments and allow us to continually test the accuracy of the Standard Model.

This phenomenal agreement with experiment coupled with a long list of accurate predictions makes the Standard Model one of the most robust theories in physics.

1.3.3   Problems of the Standard Model

Having survived many years of testing it is now becoming clear that the Standard Model will not be a valid description of particle physics at higher energies. In other words it appears to be an effective field theory. There are also good reasons to believe that major discrepancies with Standard Model predictions should appear at energies just above those currently probed by experiment. These expectations will be tested by the Large Hadron Collider (LHC) at CERN which is due to turn on in 2008. Until then, our best guide to physics beyond the Standard Model is in the few areas where the Standard Model already comes up short.

- **Neutrino masses**

9

The Sudbury Neutrino Observatory (SNO) measured the flux of electron neutrinos from the Sun, ν_e, and the total flux of neutrinos from the Sun. Though the total neutrino flux agreed with the predictions of the Standard Solar Model (SSM), the flavours of the observed neutrinos were in clear disagreement [6]. The observations could only be accounted for if neutrinos could oscillate between different flavour eigenstates between their creation in the Sun and their detection on Earth. Such oscillations can only occur if neutrinos have mass. However within the Standard Model, massive neutrinos are forbidden.

- **Dark matter abundance**

The success of the Standard Model is founded in the fact that all matter observed in experiment can be explained in terms of the fundamental fields in Table 1.1. Unfortunately astrophysics experiments have shown that this is not true of all the matter in the universe. In 1933 Zwicky postulated [7] the existence of a large quantity of dark matter in galaxy clusters to account for their motions. More recently, the measurement of the velocity of stars within galaxies has been shown to require a substantial quantity of dark matter. Finally, proof of a large quantity of non-baryonic dark matter in the universe was provided by measurements of the anisotropies in the cosmic microwave background (CMB) by the Wilkinson Microwave Anisotropy Probe (WMAP) [8, 9]. WMAP precisely measures the CMB, the radiation emitted at the surface of last scattering when photons decoupled from matter and the universe became transparent to electromagnetic radiation. This data provides a wealth of information about the physics of the early uni-
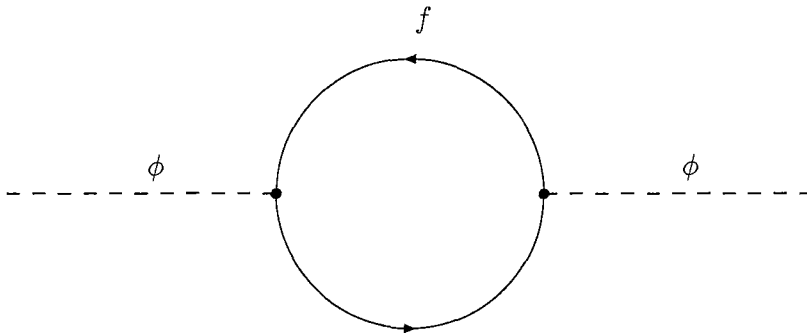
Figure 1.1: The form of the loop corrections to the Higgs (mass)^2 from Standard Model fermions f.

verse. With regards to dark matter, it shows that dark matter is not only required to account for observations, but that it is non-baryonic and that it makes up roughly 23% of the energy density of the universe. Unfortunately for the Standard Model, SM matter only accounts for 4%. Thus the majority of the matter in the universe is beyond the Standard Model[3].

- **The hierarchy problem**

In the Standard Model the size of the Higgs VEV determines the particle masses. From Eq. 1.4 the magnitude of the VEV is determined by m_H^2 and λ. Therefore we can directly constrain the size of m_H^2 through the experimentally measured particle masses. This requires the Higgs (mass)^2 to have a size of the order $m_H^2 = \mathcal{O}\left(-(100\ \text{GeV})^2\right)$. At the tree level we can set the mass to have this size by hand. However as soon as we allow for quantum corrections we must add in corrections to the Higgs mass from diagrams such as Fig. 1.1. Each such diagram introduces a correction to the

---

[3]It could be objected that the rotation curves of galaxies can be accounted for via modifications of Newtonian gravity (MOND) [10]. Such modifications are empirically motivated alterations rather than arising from a solid theoretical framework. However the theory is under active research and may well prove to be a fruitful contender to dark matter explanations of rotation curves. Nevertheless modifications of gravity still have a very hard time accounting for the WMAP data.

Higgs mass of the form:

$$\Delta m_H^2 = \frac{|\lambda_f|^2}{16\pi^2} \left[-2\Lambda_{UV}^2 + 6m_f^2 \ln\left(\Lambda_{UV}/m_f\right) + \ldots \right], \qquad (1.7)$$

where λ_f is the coupling between the Higgs and the fermion in the loop. Λ_{UV} is the high energy cut-off, the energy at which new physics enters. As the Standard Model does not incorporate gravity, new physics must enter at or near the reduced Planck scale $M_P = 2.4 \times 10^{18}$ GeV. Unfortunately if $\Lambda_{UV} \approx M_P$ these loop corrections mean that the natural size of the Higgs mass is of the order of the Planck scale[4], 16 orders of magnitude larger than the scale required by experiment.

To end up with m_H^2 of the correct size after quantum corrections we must set the tree-level mass to almost completely cancel out the quadratic divergences:

$$m_H^2 = m_{H,0}^2 - \Delta m_H^2 \approx (100 \text{ GeV})^2, \qquad (1.8)$$

where $m_{H,0}^2$ is the tree-level Higgs (mass)^2. As $\Delta m_H^2 \sim \Lambda_{UV}^2$, we require that the tree-level Higgs mass and the quantum loop corrections cancel exactly to 16 decimal places. As these quantities are fundamentally unrelated within the Standard Model, such a cancellation can only be achieved through extreme fine-tuning of the parameters by hand. Such a massive conspiracy between two unrelated quantities hints strongly at some deeper physical mechanism at work.

---

[4]One option would be to set Λ_{UV} very low. However it proves extremely difficult to shield the Higgs mass from Planck scale corrections. See [16] for a good discussion of this point.

Therefore there are two problems with the Higgs mechanism within the Standard Model. Firstly we have we have to set the form of the Higgs potential by hand rather than it being a natural result of the theory. Secondly quantum corrections to m_H^2 quickly destroy such a potential unless we indulge in some extreme fine-tuning.

- **Gauge unification**

When we calculate the running of the gauge couplings with the energy scale, using the Standard Model renormalisation group equations (RGEs), we find that they appear to converge at some high energy scale. This, coupled with previous successful attempts at unifying forces, prompted attempts to build Grand Unified Theories (GUTs) in which the Standard Model gauge group G_{SM} is a subgroup of some much larger group G_{GUT}. Such models have many benefits, yet they all require the gauge couplings to unify. Unfortunately for such a programme, further work showed that, with the Standard Model RGEs, the gauge couplings do not unify.

These problems have spawned a number of theories of BSM physics. Within this work we study one of the leading candidates for BSM physics, SUSY.

1.4 Supersymmetry

SUSY is a symmetry that relates fermions and bosons:

$$Q \left| Boson \right\rangle \approx \left| Fermion \right\rangle$$

$$Q \left| Fermion \right\rangle \approx \left| Boson \right\rangle.$$

As fermions and bosons have different spins, the generator Q must carry spin-1/2. This means supersymmetry is a spacetime symmetry and as such extends the Poincaré group to the super-Poincaré group. The form of such algebras are limited by the Haag-Lopuszanski-Sohnius extension of the Coleman-Mandula theorem [11, 12]. This theorem requires the generators Q and $Q^\dagger$ to have the commutation properties:

$$\{Q, Q^\dagger\} = P^\mu \tag{1.9}$$

$$\{Q, Q\} = \{Q^\dagger, Q^\dagger\} = 0, \tag{1.10}$$

$$[P^\mu, Q] = 0 \tag{1.11}$$

where P^μ is the momentum generator. As we intend only to provide a broad overview of SUSY rather than a technical introduction[5], all spinor indices, and hence all spinor matrices, have been suppressed throughout.

From the commutation properties we can see that one application of Q transforms a fermion (boson) to a boson (fermion), but two applications reverts it back to the original boson (fermion). Therefore the particle content of a supersymmetric theory naturally divides into groups of particles related to each other by the SUSY transformations. These are referred to as supermultiplets. As $-P^2$, the mass generator, commutes with the operators Q and $Q^\dagger$, particles in the same supermultiplet must have the same mass. Equally, Q and $Q^\dagger$ commute with the generators of gauge transformations so particles within the same supermultiplet must have the same gauge quantum numbers.

---

[5]There are many good sources for a technical introduction to SUSY, see for example [13, 14, 15, 16]

Under SUSY transformations particles with different spins transform separately. A single Weyl fermion has two helicity states, each of which transform differently under Q and $Q^\dagger$. Therefore a single Weyl fermion will have two scalar partners. This is required for supermultiplets to have the same number of bosonic and fermionic degrees of freedom.

If we wanted, we could have a theory in which there were more than one copy of the generators Q and $Q^\dagger$. In such a theory we would have more than one set of bosonic partners for each fermion and vice versa. Though such models are interesting, especially in models with extra dimensions, they are not phenomenologically feasible in $D = 4$. Here we only consider $\mathcal{N} = 1$ SUSY in which there is only one set of generators.

1.4.1 The MSSM

We can use this new symmetry to extend the Standard Model by creating supersymmetric partners (superpartners) for all the Standard Model fields. Superpartners are represented by adding a tilde to the Standard Model notation. The naming convention depends on whether the new particle is a fermion or a boson. If the superpartner is a bosonic partner to a Standard Model fermion we prepend an s- (short for scalar) to the name of the SM particle. If the superpartner is a fermionic partner of a Standard Model boson, we append an -ino. So the partner of the gluon is called the gluino and is written $\tilde{g}$ whereas the partner to the right-handed charm quark is called the scharm and is written $\tilde{c}_R$. Note that though the subscript indicates a handedness the scharm is a spin-0 particle and thus it has no handedness. Instead the subscript designates the handedness of its fermionic partner.

Spin 0	Spin-1/2	Spin-1	$SU(3)_c$	$SU(2)_L$	$U(1)_Y$
$\widetilde{Q}_{iL}$	Q_{iL}	$-$	**3**	**2**	$1/6$
$\widetilde{\overline{u}}_{iR}$	$\overline{u}_{iR}$	$-$	**3**	**1**	$-2/3$
$\widetilde{\overline{d}}_{iR}$	$\overline{d}_{iR}$	$-$	**3**	**1**	$1/3$
$\widetilde{L}_{iL}$	L_{iL}	$-$	**1**	**2**	$-1/2$
$\widetilde{\overline{e}}_{iR}$	$\overline{e}_{iR}$	$-$	**1**	**1**	1
$-$	$\widetilde{g}^{\alpha}$	g^{α}	**8**	**1**	0
$-$	$\widetilde{W}^{a}$	W^{a}	**1**	**3**	0
$-$	$\widetilde{B}$	B	**1**	**1**	0
H_u	$\widetilde{H}_u$	$-$	**1**	**2**	$1/2$
H_d	$\widetilde{H}_d$	$-$	**1**	**2**	$-1/2$

Table 1.2: The G_{SM} representations of the field content of the MSSM. Note that right-handed field degrees of freedom have been CP-conjugated to make them transform as left-handed fields.

However, merely adding a superpartner for every SM particle introduces problems. In the Standard Model there are no triangle anomalies as the contributions of the fermions in loops cancel exactly. When we supersymmetrise the Higgs doublet we produce higgsinos, fermions with hypercharge $Y = +1/2$. This introduces a non-zero triangle anomaly. To cancel this anomaly we need to introduce a second Higgs doublet with $Y = -1/2$. In this case the contributions from the $Y = 1/2$ and $Y = -1/2$ higgsinos cancel exactly leaving the theory anomaly free. It turns out that the extra Higgs doublet is also are required for the supersymmetric analogue of electroweak symmetry breaking. The doublet with hypercharge $Y = +1/2$ gives mass to the up-type quarks and leptons whereas the doublet with $Y = -1/2$ gives mass to the down-type quarks and leptons. For this reason they are often designated as H_u and H_d respectively.

This completes the minimal field content required to create a consistent supersymmetric field theory that contains all the fields of the Standard Model. This is known as the Minimal Supersymmetric Standard Model
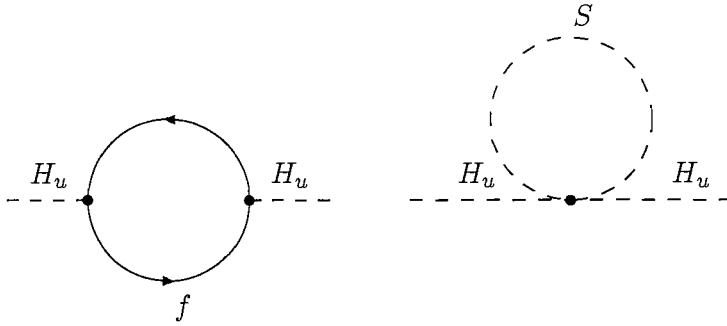
Figure 1.2: In SUSY the correction to the Higgs (mass)^2 comes from both fermion and scalar loops.

(MSSM). The particle content is summarised in Table 1.2.

1.4.2 The hierarchy problem revisited

By supersymmeterising the Standard Model we more than double the number of fundamental fields in our theory. What do we get in return? The most immediate result is that we solve the hierarchy problem of the Standard Model. In the Standard Model fermions in loops provide corrections to the Higgs mass of the form:

$$\Delta m_H^2 = \frac{|\lambda_f|^2}{16\pi^2} \left[-2\Lambda_{UV}^2 + 6m_f^2 \ln\left(\Lambda_{UV}/m_f\right) + \ldots \right]. \qquad (1.12)$$

In section 1.3.3 we noted that there must be some conspiracy at work cancelling out the quadratically divergent terms to the Higgs (mass)^2. It happens that if a theory contains a scalar particle that couples to the Higgs through a term of the form $-\lambda_S |\phi|^2 |S|^2$, then it will provide a loop correction to the Higgs (mass)^2 via processes such as that shown in the right hand diagram of Fig. 1.2. The size of the correction from such processes is:

$$\Delta m_H^2 = \frac{\lambda_S}{16\pi^2} \left[\Lambda_{UV}^2 - 2m_S^2 \ln\left(\Lambda_{UV}/m_S\right) + \ldots \right], \qquad (1.13)$$

17

where m_S is the mass of the scalar particle. Note that the quadratically divergent Λ_{UV}^2 term cancels exactly *if and only if* (i) there are two such contributions for every fermion and (ii) $|\lambda_f|^2 = \lambda_S$.

Within the MSSM we guarantee both of these conditions are fulfilled. Firstly, to even out the fermionic and bosonic degrees of freedom in each supermultiplet SUSY requires that there be two scalars partnering every Standard Model fermion, satisfying the first criteria. Secondly, when we construct our Lagrangian we find that the coupling strength to the Higgs of particles in the same supermultiplet must satisfy $|\lambda_f|^2 = \lambda_S$. Thus, via SUSY, we automatically remove quadratic divergences to the Higgs mass. There will still be a contribution to Δm_H^2 that is sensitive to Λ_{UV} but this sensitivity is only logarithmic. Therefore supersymmetric theories remove the need to tune the tree level Higgs mass to 16 orders of magnitude.

1.4.3 Breaking supersymmetry

Within the MSSM as presented so far there is a serious problem. If SUSY is an exact symmetry, superpartners must have the same mass as their Standard Model counterparts. This cannot be the case. A light selectron, for example, should have a mass of 0.511 MeV and would have been spotted years ago in collider experiments. Therefore SUSY must be broken.

Despite many years of hard work, there is no leading model of SUSY breaking[6]. To make progress we must parameterise our ignorance. We do this by adding SUSY breaking terms to the Lagrangian with coefficients that we set by hand. We require that a theory of SUSY breaking determine these

---

[6]The mechanism behind SUSY breaking has been the focus of a lot of work over the years and has given rise to a substantial literature. For a recent review of work in this field see [17].

parameters, until then we consider them as free inputs. As we do not want to reintroduce quadratic divergences to the Higgs (mass)^2 we limit the SUSY breaking terms we can include. Terms that avoid quadratic divergences are called *soft* terms. The soft SUSY breaking Lagrangian is:

$$
\begin{aligned}
-\mathcal{L}_{soft}^{MSSM} \;=\; & \frac{1}{2}\left(M_1 \tilde{B}\tilde{B} + M_2 \tilde{W}\tilde{W} + M_3 \tilde{g}\tilde{g}\right) + h.c. \\
& + \; \tilde{\bar{u}}_R \,\mathbf{\tilde{A}_u}\, \tilde{Q}_L H_u - \tilde{\bar{d}}_R \,\mathbf{\tilde{A}_d}\, \tilde{Q}_L H_d - \tilde{\bar{e}}_R \,\mathbf{\tilde{A}_e}\, \tilde{L}_L H_d + h.c. \\
& + \; \tilde{Q}_L^\dagger \,\mathbf{m_Q^2}\, \tilde{Q}_L + \tilde{L}_L^\dagger \,\mathbf{m_L^2}\, \tilde{L}_L + \tilde{\bar{u}}_R \,\mathbf{m_u^2}\, \tilde{\bar{u}}_R^\dagger + \tilde{\bar{d}}_R \,\mathbf{m_d^2}\, \tilde{\bar{d}}_R^\dagger + \tilde{\bar{e}}_R \,\mathbf{m_e^2}\, \tilde{\bar{e}}_R^\dagger \\
& + \; m_{H_u}^2 H_u^* H_u + m_{H_d}^2 H_d^* H_d - \left(b H_u H_d + h.c.\right), \qquad (1.14)
\end{aligned}
$$

where the terms in bold are 3×3 complex matrices in family space. Once again we have suppressed spinor indices.

As these terms explicitly involve the superpartners without their Standard Model counterparts they clearly break SUSY. In the first line we have explicit mass terms for the gauginos. In the second line we have trilinear couplings between three scalar fields that parallel the Yukawa couplings. In the third line we write masses for the squarks and sleptons. Finally in the fourth line we write a mass term for the two Higgs doublets as well as a bilinear term (b) that couples H_u and H_d. By varying these soft mass terms we are able to set the superpartners masses to lie beyond the present reach of experiment and so satisfy present experimental bounds.

As we do not know how SUSY breaking occurs, in principle all of the coefficients of fields in Eq. 1.14 are arbitrary. As many of the coefficients are complex matrices, this introduces an enormous number of free parameters into the MSSM. After rotating away unphysical phases, we are left with 124

free parameters within the MSSM.

If all these parameters were actually free then SUSY would have a serious problem. It is very hard for a theory with this degree of freedom to make any meaningful predictions. Only after enough data were collected to fix the majority of these parameters could the theory make solid predictions and thus be truly falsifiable.

Thankfully we do not need to deal with the full 124 dimensional parameter space. Firstly, the parameters of Eq. 1.14 are not *a priori* free. They should be generated dynamically through some mechanism of SUSY breaking. Even without an explicit model of SUSY breaking, there are many well motivated proposals for the form the parameters of $\mathcal{L}_{soft}$ should take, often specified at some high energy scale such as $m_{GUT} \approx 2 \times 10^{16}$ GeV. In these models the parameters of $\mathcal{L}_{soft}$ are determined by a small set of more fundamental parameters at the high energy scale. We then use the renormalisation group equations (RGEs) to run their values to the low energy scale. It is these low energy values that then determine the phenomenology that would be observed in experiments. Secondly, in precision testing the Standard Model, a lot of possible BSM physics was ruled out. This experimental evidence tightly constrains many of the parameters in Eq. 1.14. In particular, the lack of observation of exotic flavour changing neutral currents (FCNCs) constrains the off-diagonal elements of the sfermion $(mass)^2$ matrices to be vanishingly small.

Within this work we make a number of assumptions to simplify the process of studying the MSSM parameter space. We take all of the parameters in $\mathcal{L}_{soft}$ to be real. This is not ideal but the numerical codes presently

available are unable to cope with complex phases. We take sfermion and squark mass matrices to be diagonal to suppress dangerous FCNCs. Finally we take the trilinear terms to be proportional to the Yukawa matrices:

$$\tilde{\mathbf{A}}_{\mathbf{u}} = A_u \mathbf{Y}_{\mathbf{ij}}, \ \tilde{\mathbf{A}}_{\mathbf{d}} = A_d \mathbf{Y}_{\mathbf{ij}}, \ \tilde{\mathbf{A}}_{\mathbf{e}} = A_e \mathbf{Y}_{\mathbf{ij}}. \tag{1.15}$$

This minimal flavour violating scenario (MFV) helps in suppressing FCNCs and CP violating processes in addition to greatly simplifying the parameter space. However the MFV scenario is not a necessary condition FCNC and CP violation bounds. Therefore there are no hard phenomenological or theoretical reasons to expect that such a scenario must be realised.

1.4.4 Breaking electroweak symmetry

As well as SUSY, electroweak symmetry must be broken. However, whereas we have no good model of SUSY breaking, electroweak symmetry occurs naturally within the MSSM for most choices of the parameters in $\mathcal{L}_{soft}$. Not only does this answer one of the questions left open in the Standard Model, by requiring that electroweak symmetry be broken we fix some of the soft parameters. To understand electroweak symmetry breaking within the MSSM we need to consider the form of the Higgs potential. At the tree level this is:

$$
\begin{aligned}
V_{Higgs} &= \left(|\mu|^2 + m_{H_u}^2\right)|H_u|^2 + \left(|\mu|^2 + m_{H_d}^2\right)|H_d|^2 \\
&+ \frac{1}{8}\left(g^2 + g'^2\right)\left(|H_u|^2 - |H_d|^2\right)^2 + \frac{1}{2}g^2|H_u H_d^*|^2 \\
&- \left(B\mu H_d H_u + h.c.\right),
\end{aligned}
\tag{1.16}
$$

where g is the $SU(2)_L$ gauge coupling, g' is the $U(1)_Y$ hypercharge coupling as before, μ is a SUSY preserving Higgs mass and $B\mu = b$.

For this potential to break electroweak symmetry the Higgs doublets must acquire non-zero VEVs. Via $SU(2)_L$ gauge transformations we are always allowed to rotate the fields such that the VEVs appear in the neutral components of the fields:

$$\langle H_u \rangle = \begin{pmatrix} 0 \\ v_u \end{pmatrix}, \quad \langle H_d \rangle = \begin{pmatrix} v_d \\ 0 \end{pmatrix}. \tag{1.17}$$

To give the correct masses to the Standard model particles we also require that $v^2 = v_u^2 + v_d^2 = (174 \text{ GeV})^2$. Though this fixes the magnitude of v^2, it does not fix the ratio of v_u to v_d. This ratio is written $\tan\beta = v_u/v_d$ and is an important quantity in phenomenological studies of the MSSM.

For the Higgs potential to develop the correct symmetry breaking minimum we must satisfy the relation:

$$\mu^2 = \frac{m_{H_d}^2 - m_{H_u}^2 \tan^2\beta}{\tan^2\beta - 1} - \frac{1}{2}m_Z^2. \tag{1.18}$$

For large $\tan\beta$ or small $m_{H_d}^2$ this reduces to:

$$\mu^2 \approx -m_{H_u}^2 - \frac{m_Z^2}{2}. \tag{1.19}$$

In this limit electroweak symmetry is only broken if $m_{H_u}^2$ is negative and has a magnitude slightly larger than μ. In general, negative $m_{H_u}^2$ is not necessary to achieve electroweak symmetry breaking, but it helps.

For SUSY to naturally provide electroweak symmetry breaking it must

naturally generate soft Higgs masses with values that satisfy Eq. 1.18. In specifying our parameterisation of SUSY breaking we specify $m^2_{H_{u,d}}$ at some high energy scale, taken to be m_{GUT} throughout this work. To find their low energy values we run them down using the MSSM RGEs. However within the MSSM the Higgs RGEs are dominated by quantum corrections from the 3rd family squarks. These corrections naturally push $m^2_{H_{u,d}}$ to values that satisfy Eq. 1.18. Thus SUSY provides a mechanism that generates electroweak symmetry breaking. This is known as radiative electroweak symmetry breaking (REWSB).

Through the requirement that a SUSY model must exhibit REWSB and give the correct mass to Standard Model gauge bosons, we can fix the size of μ (up to a sign) and exchange the soft parameter b for $\tan\beta$. This is common in phenomenological studies and we do this throughout. We must sound a note of caution here. If $m^2_{H_{u,d}}$ are much larger than m^2_Z (as they must be), we must have a degree of cancellation between the soft Higgs (mass)^2 and μ^2. This would suggest that μ^2 and $m^2_{H_{u,d}}$ are related in some way. Unfortunately as μ is a SUSY preserving mass term, it cannot be related to the parameters of $\mathcal{L}_{soft}$. If we are forced to consider soft masses $m_{soft} > 10$ TeV, the degree of tuning required becomes large. We consider this point in more detail in Chapter 2.

1.4.5 The physical particle spectrum

In the Standard Model the W^a and B fields mix to create the physical $W^\pm$, Z^0 and γ. In the MSSM a similar process occurs. As in the Standard Model, after electroweak symmetry breaking three Higgs bosons develop Goldstone

modes and are "eaten" to give masses to the $W^{\pm}$ and Z^0. However, as the MSSM contains 2 complex Higgs doublets we have 5 remaining real physical Higgs bosons rather than 1:

- h^0, H^0, the light and heavy neutral CP-even Higgs bosons ($m_{h^0} < m_{H^0}$).

- A^0, the CP-odd Higgs boson.

- $H^{\pm}$, the charged Higgs bosons.

After electroweak symmetry breaking fields with the same quantum numbers mix. This allows mixing between the $SU(2)_L$ and $U(1)_Y$ gauginos, and the higgsinos. The neutral states mix to form the neutralinos:

$$\left(\tilde{B}, \tilde{W}^0, \tilde{H}_u^0, \tilde{H}_d^0 \right) \to \left(\tilde{\chi}_i^0 \right), \ i \in \{1, 2, 3, 4\}, \tag{1.20}$$

where conventionally $i = 1$ designates the lightest neutralino and $i = 4$ designates the heaviest. Equally the charged states mix to form the charginos:

$$(\tilde{W}^+, \tilde{H}_u^+) \to \left(\tilde{\chi}_i^+ \right), \ i \in \{1, 2\}$$

$$(\tilde{W}^-, \tilde{H}_d^-) \to \left(\tilde{\chi}_i^- \right), \ i \in \{1, 2\}. \tag{1.21}$$

Again $i = 1$ conventionally designates the lighter chargino.

As the lightest neutralino is often the lightest superpartner (LSP), and will turn out to be the best MSSM candidate for particulate dark matter, it is worth considering in more detail here. The exact composition of the

neutralinos is found by diagonalising the mass matrix:

$$
\begin{pmatrix}
M_1 & 0 & -m_Z c_\beta s_w & m_Z s_\beta s_w \\
0 & M_2 & m_Z c_\beta c_w & -m_Z s_\beta c_w \\
-m_Z c_\beta s_w & m_Z c_\beta c_w & 0 & -\mu \\
m_Z s_\beta s_w & -m_Z s_\beta c_w & -\mu & 0
\end{pmatrix},
\tag{1.22}
$$

where $c_\beta = \cos\beta$, $s_\beta = \sin\beta$, $c_w = \cos\theta_w$, $s_w = \sin\theta_w$.

The equivalent mass matrix for the charginos is:

$$
\begin{pmatrix}
M_2 & \sqrt{2}m_w s_\beta \\
\sqrt{2}m_w c_\beta & \mu
\end{pmatrix}.
\tag{1.23}
$$

There are three limiting cases that will be of interest. If $M_1 \ll M_2, \mu$ at the electroweak scale, the lightest neutralino will be pure $\tilde{B}$, or bino. The charginos will be significantly heavier as their masses depend on M_2 and μ. If $M_2 \ll M_1, \mu$ at the electroweak scale, the lightest neutralino will be $\tilde{W}$ or wino, as will the lightest chargino. As a result $\tilde{\chi}_1^0$ and $\tilde{\chi}_1^+$ will be almost degenerate in mass. Finally, if $\mu \ll M_1, M_2$ at the electroweak scale $\tilde{\chi}_1^0$, $\tilde{\chi}_2^0$ and $\tilde{\chi}_1^+$ will be higgsino and close in mass. Therefore the ratio of $M_1 : M_2 : \mu$ at the low energy scale entirely determines the masses and properties of the spectrum of neutralinos and charginos. Through this mechanism, these three parameters have a large effect on the phenomenology of MSSM models.

As mentioned, the lightest neutralino is the best candidate for dark matter within the MSSM. It is uncoloured, electrically neutral, weakly interacting, massive and non-baryonic. However, before we can conclude that it is a good candidate we must ensure that it is stable.
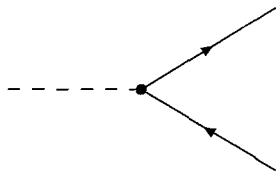
Figure 1.3: A process forbidden by R-parity conservation. The superpartner (dashed) has $P_R = -1$ whereas the final state SM fermions (solid) have $P_R = 1$.
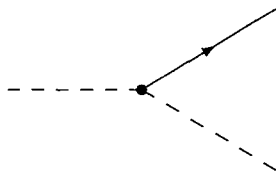
Figure 1.4: A process allowed by R-parity conservation. The superpartner (dashed) has $P_R = -1$ and the final state with one SM fermion (solid) and a superpartner (dashed) has $P_R = 1$.

1.4.6 R-parity

Supersymmetry on its own does not forbid terms of the Lagrangian that violate baryon or lepton number. If such terms were allowed there would be a number of unfortunate consequences, such as proton decay. To rule out such terms we introduce a discrete symmetry to the theory called R-parity. It is a multiplicatively conserved quantum number defined as:

$$P_R = (-1)^{3(B-L)+2S},\qquad(1.24)$$

where B is baryon number and L is lepton number. Under this parity, superpartners have $P_R = -1$, whereas all Standard Model fields and Higgs bosons have $P_R = 1$.

R-parity conservation guarantees baryon and lepton number conservation. It also forbids processes such as those of Fig. 1.3 while allowing processes of the form shown in Fig. 1.4. Thus though SUSY particles can decay to lighter SUSY particles, no one SUSY particle can decay entirely to Standard Model matter. This means the lightest superpartner is absolutely stable. Superpartners can only annihilate in pairs.

With this final piece of information, required to avoid proton decay, the LSP finally fulfils all the criteria required of a good dark matter candidate.

1.4.7 Motivations for SUSY

We have now introduced the entire MSSM spectrum, highlighted the physical low energy states and noted the input parameters that will define the phenomenology. However, at time of writing, no supersymmetric particles have been directly observed. Before we introduce the methods we use to study MSSM phenomenology in Chapter 2, we pause to review the motivations for SUSY, and summarise the new questions that it raises.

- **The hierarchy problem**

Within the Standard Model it is very hard to avoid quadratically divergent corrections to the Higgs mass via fermion loops (particularly the top). By introducing scalar partners to the SM fermions, SUSY automatically cancels the quadratically divergent terms exactly. This removes the need to fine-tune the tree level Higgs $(\text{mass})^2$ to 16 decimal places.

- **Dark matter**

When we construct the minimal supersymmetric extension of the Standard Model, and require that it conserve Baryon and Lepton number, we automatically end up with a massive, non-baryonic, weakly interacting, stable particle. If we choose our soft parameters to ensure that it is neutral as well we have an excellent dark matter candidate. However, just having a candidate is not enough to explain the observed dark matter relic density. Any candidate particle must occur in the right amounts to explain the experimental observations. In Chapter 2 we look at how such a relic density is generated and we address the question of whether SUSY really provides a natural explanation for dark matter.

- **Unifying the fundamental forces**

In the Standard Model, if we run the gauge couplings to high energies they fail to unify. Within SUSY, the β-function coefficients that govern the running are different. To run the gauge couplings in the MSSM to high energies we use the Standard Model β-functions until we reach the mass scale of the supersymmetric particles and then we switch to the MSSM β-functions. If the mass of the supersymmetric particles is $\mathcal{O}(1-10 \text{ TeV})$, the gauge couplings unify around 2×10^{16} GeV. Thus SUSY provides a good framework for the study of GUTs.

1.4.8   Open questions

Though the MSSM provides a good framework for addressing big questions within particle physics, it also raises a few of its own.

- **How is SUSY broken?**

SUSY must be broken. The soft masses generated by SUSY breaking determine much of the low energy phenomenology of a supersymmetric theory. However the mechanism of SUSY breaking is unknown. The challenge for theorists is twofold. Firstly there is a need to produce models of SUSY breaking from more fundamental theories such as string models. Such models would determine the parameters of $\mathcal{L}_{soft}$ in terms of fewer more fundamental parameters. Secondly it is important to understand the links between the soft parameters and the phenomenology. This will allow theorists to use the experimental evidence gathered by the LHC and other future experiments to constrain the parameters of $\mathcal{L}_{soft}$ thus gives information about the structure of SUSY breaking.

- **The μ problem**

Eq. 1.18 requires $\mu \sim m_{H_{u,d}}$ for REWSB to reproduce the Z mass. As μ appears as a SUSY preserving Higgs mass term it can have no connection to the soft masses. This raises a question and a problem. The question is, could μ be generated by more fundamental physics than suggested by the MSSM? In some Next to Minimal Supersymmetric Standard Models (NMSSMs), μ is generated via the VEV of some new field $\mu \approx \langle N \rangle$. The problem for the MSSM is, as μ is unrelated to the soft masses, we must resort to a degree of fine-tuning between μ and the soft masses if we are to satisfy the condition in Eq. 1.18. This fine-tuning will never be of the order required to achieve the correct Higgs (mass)^2 in the Standard Model. However, the larger the soft masses and μ are required to be (for example if no light superpartners are found at the LHC), the larger the degree of fine-tuning required. This

fine-tuning directly reduces SUSY's claim to provide a natural mechanism for electroweak symmetry breaking. In Chapter 2 we introduce a measure to quantify this fine-tuning. We use this measure to study the naturalness of REWSB within a general MSSM model in Chapter 3 and a string model in Chapter 4.

- **Why should nature choose the MSSM?**

Here we have considered the supersymmetric extension to the Standard Model with the minimal field content (the MSSM). Why should nature choose such a model? The are no good theoretical reasons other than Occam's Razor. We shouldn't introduce new fields to our theories without good reason. However theorists have managed to come up with many reasons to add new fields and so have created a range of supersymmetric theories that go beyond the MSSM. These reasons range from explaining inflation to family symmetries between generations of matter to explaining the origin of μ. Here we just consider the MSSM but note that SUSY could appear in a different form to that considered here.

Chapter 2

Constraining the MSSM

In the previous chapter we introduced the Minimal Supersymmetric Standard Model. Within the MFV approximation, and after requiring radiative electroweak symmetry breaking, the MSSM is fully specified by the parameters:

$$a_{MSSM} \in \left\{ \mathrm{m}_{\tilde{Q}}^2,\ \mathrm{m}_{\tilde{u}}^2,\ \mathrm{m}_{\tilde{d}}^2,\ \mathrm{m}_{\tilde{L}}^2,\ \mathrm{m}_{\tilde{e}}^2,\ m_{H_u}^2,\ m_{H_d}^2,\ M_1,\ M_2,\ M_3, \right.$$
$$\left. A_u,\ A_d,\ A_e,\ \tan\beta,\ \mathrm{sign}(\mu) \right\}, \tag{2.1}$$

where the mass matrices $\mathrm{m}_{\tilde{f}}^2$ are taken to be diagonal.

This is still an enormous parameter space to study. We make progress in two ways:

- Use theory to impose structures on $\mathcal{L}_{soft}$ so that we can determine a_{MSSM} in terms of fewer parameters.

- Use experiment to constrain the values of a_{MSSM}.

In this chapter we introduce the methods used to study the phenomenology of the MSSM. In section 2.1 we summarise the numerical codes used to

31

relate the parameters a_{MSSM} to experimental data. In section 2.2 we summarise the experimental bounds from particle searches, measurements of $BR(b \to s\gamma)$ and SUSY contributions to $(g-2)_\mu$. We then go on to consider two of the major motivations for SUSY in more detail. In section 2.3 we look at how radiative electroweak symmetry breaking can be directly related to the soft parameters. In section 2.4 we look at how SUSY reproduces the observed dark matter density, and review the current experimental measurements. As these last two conditions are not only bounds on the MSSM, but phenomena the theory is expected to explain, we also require that it satisfy these conditions *naturally*. In section 2.5.1 we introduce a measure to quantify the fine-tuning required for the MSSM to provide REWSB. In section 2.5.2 we introduce an analogous measure to quantify the fine-tuning required for the MSSM to reproduce the observed dark matter density. These measures lie at the core of our studies of naturalness within the MSSM and beyond.

2.1 Methodology

Theoretical studies of SUSY breaking generally specify the parameters of $\mathcal{L}_{soft}$ at some high energy scale, usually $m_{GUT} \approx 2 \times 10^{16}$ GeV. To relate these theories to the low energy physics studied in colliders or in direct dark matter detectors we must run the parameters of the theory using the MSSM RGEs[1]. To do this we use the publicly available numerical code SOFTSUSY v.1.9.1 [18].

---

[1]For a comprehensive list of the MSSM RGEs see the appendix of [17].

SOFTSUSY takes a_{MSSM} as inputs. It starts by running the Standard Model masses and gauge couplings to m_Z. These values are then used as constraints. The programme then makes a first guess at the Yukawa couplings before running both the Yukawa couplings and gauge couplings up to the point at which gauge coupling unification is achieved. This sets m_{GUT}. Here the soft parameters are set to agree with the values provided as inputs. The whole set-up is then evolved back down to low energy where the condition of radiative electroweak symmetry breaking is imposed. The size of μ is calculated and $\tan \beta$ is set. At m_Z the SUSY corrections to the gauge and Yukawa couplings are calculated and the whole process is repeated with the new values. This loop is iterated until a user defined degree of accuracy is achieved. Once this is satisfied, the pole masses of the Higgs bosons and the sparticles are calculated and output.

Once we have the particle spectrum for a given model point we can impose a number of experimental constraints. Firstly, at this point we can rule out a model point if it fails to produce REWSB, shown in SOFTSUSY by the calculated value of μ^2 being negative. We can also rule out a model point if it results in a tachyon. At this stage we also impose the experimental limits on the particle masses. Finally we rule out a region of parameter space if it results in an LSP that is not the lightest neutralino.

In the remaining parameter space we calculate the SUSY contribution to $BR(b \rightarrow s\gamma)$ and $(g-2)_\mu$, as well as the predicted dark matter relic density. These calculations are involved and we use the public code micrOMEGAs v.1.3.6 [19]. This interfaces with SOFTSUSY via the format laid out in the SUSY Les Houches Accord (SLHA) [20]. This computational structure al-

lows us to produce numerical scans of the parameter space that directly relate a_{MSSM} to low energy phenomenology. We consider all of the constraints we impose, and their relation to the soft parameters, in the following sections.

2.2 Experimental bounds

2.2.1 Particle searches

Experiments have been looking for BSM particles for years. It was hoped that they would show up at LEP or the Tevatron. The lack of any evidence for SUSY at these experiments puts stringent bounds on sparticle masses. The tightest bounds come from run 2 of the Large Electron Positron Collider (LEP2) at CERN. The results of SUSY searches at the four separate LEP experiments, ALEPH, DELPHI, L3 and OPAL, have been combined by the LEP2 SUSY Working Group and are compiled on their web pages [21].

The exact structure of a given SUSY theory affects how likely it would be for a given experiment to see a superpartner of a given mass. Therefore the LEP experiments do not generally place a direct cut on the mass of a given superpartner. For example, consider the case of a model in which the lightest neutralino $\tilde{\chi}_1^0$ is the LSP and the next to lightest superpartner (NLSP) is a slepton. Now the slepton will decay to a neutralino via the process $\tilde{l} \rightarrow \tilde{\chi}_1^0 + l$. If the mass difference between the LSP and the NLSP is small then the lepton produced will have very low energy. As we decrease the mass difference between the LSP and NLSP, at some point the energy of the lepton drops below the sensitivity of the detector. Therefore the LEP2

bounds on slepton masses only apply when the mass difference between the slepton and the lightest neutralino is greater than a few GeV. Equally, different choices of MSSM parameters can change the coupling strengths altering the interaction cross-sections that go into calculating the LEP2 bounds. Within this work we generally place a conservative lower limit on the masses of the superpartners. Where there are clear exceptions, such as in the case of a nearly degenerate $\tilde{l}$ and $\tilde{\chi}_1^0$ we include this check into our application of the mass bounds.

Of all of the unseen particles predicted by the MSSM the lightest Higgs h^0 deserves a special mention. The present mass bound on the lightest Higgs within the Standard Model is $m_{h^0} > 114$ GeV. However the mass limits on the lightest Higgs boson in the MSSM are somewhat lower. We take a conservative bound of $m_{h^0} > 111$ GeV throughout[2].

2.2.2 $BR(b \to s\gamma)$

The variation of $BR(b \to s\gamma)$ from the value predicted by the Standard Model is highly sensitive to SUSY contributions. To date, no variation from the Standard Model has been detected. The present experimental measurement of this value comes from BELLE [23], CLEO [24] and ALEPH [25]. We follow the analysis of [85] and take the value to be:

$$BR(b \to s\gamma) = (3.25 \pm 0.54) \times 10^{-4}. \tag{2.2}$$

We calculate the SUSY contribution to the branching ratio using `micrOMEGAs`.

---

[2]For a more sophisticated treatment of the Higgs bound in numerical studies see, for example, [70].

Within microOMEGAs all 1-loop effects and some 2-loop contributions are included. There is a detailed discussion of their implementation in [19].

The 1-loop SUSY contributions to $BR(b \rightarrow s\gamma)$ involve loops with a charged Higgs and a top quark and loops with a chargino and a squark. Contributions from a charged Higgs are large if the charged Higgs is light. Contributions from charginos and squarks are enhanced when either squarks or charginos are light. They are also enhanced when a chargino and squark are close in mass. The individual contributions depend upon the exact composition of the charginos. As the mass and composition of the chargino is determined by μ, M_2 and β, we expect the scale of the SUSY contribution to be sensitive to these parameters.

To summarise, $BR(b \rightarrow s\gamma)$ depends primarily on the soft squark masses m_0^2, the soft Higgs masses $m_{H_{u,d}}^2$, M_2, μ and $\tan \beta$. There is also some dependence on M_1 and M_3 through running effects.

2.2.3 $(g-2)$ of the muon

Present measurements of the value of the anomalous magnetic moment of the muon a_μ deviate from the theoretical calculation of the SM value. However questions remain around the exact form of the Standard Model calculation, specifically whether we should use τ or e^+e^- data in the analysis of the hadronic vacuum polarisation. At ICHEP '04 [26] there was general agreement that the τ data should be disregarded though that agreement has been challenged by recent measurements[3]. Here we take the result obtained by

---

[3]Note that the SND Collaboration recently reported a result that was out of line with the e^+e^- results from other groups, being more consistent with the τ data. However very recently an error was reported in their analysis, and now the most recent result from SND is completely consistent with the e^+e^- results from other groups [27]. This effectively will serve to increase the discrepancy of the muon $g-2$ with the Standard Model beyond

using the e^+e^- data and consider its implications for a SUSY theory. With the present experimental value from [28] and the theoretical calculation of the SM value from [29] there is a discrepancy:

$$(a_\mu)_{exp} - (a_\mu)_{SM} = \delta a_\mu = (2.52 \pm 0.92) \times 10^{-9}. \qquad (2.3)$$

This amounts to a 2.7σ deviation from the Standard Model.

The SUSY contributions to a_μ come from penguin diagrams of two types. One is mediated by a chargino and a muon sneutrino, the other is mediated by a neutralino and a smuon. For a detailed discussion of these contributions, see [30]. For our purposes it is enough to note that there will be enhancements to the SUSY contribution whenever smuons, mu-sneutrinos, charginos and neutralinos become light.

The form of the penguin diagrams mean that we expect the value of δa_μ to increase for small $\left(m_{\tilde{e}}^2\right)_{22}$, M_1, M_2, μ as these set the masses of the particles in the loops. M_1 and M_2 should also be small as they provide positive contributions to the mass of the smuon through running effects. From the details of the calculation we also find an enhancement for large $\tan\beta$ and large negative A_e. Finally, the relative sign between M_1, M_2 and μ is important for the calculation of δa_μ.

2.3   Radiative electroweak symmetry breaking

One requirement of any SUSY theory is that it break electroweak symmetry radiatively (REWSB). We recall from Eq. 1.18 that the condition for

---

2.7σ, but since the new analysis has not yet been performed here we shall continue to conservatively assume the 2.7σ deviation.

electroweak symmetry breaking with two Higgs doublets can be written:

$$\mu^2(t) = \frac{m_{H_d}^2(t) - m_{H_u}^2(t)\tan^2\beta}{\tan^2\beta - 1} - \frac{1}{2}m_Z^2(t). \tag{2.4}$$

where $t = \log Q$ and Q is the energy scale at which we want to determine μ. For REWSB to exist in a given model, we must have a positive value of μ^2 at the low energy scale $Q \sim m_Z$. We rule out any point that doesn't satisfy this criteria.

To see how the soft masses affect μ^2, we must consider the RGE evolution from the GUT scale. As the Higgs doublets have many couplings, their RGEs are complicated. This is one reason why we use sophisticated codes such as SOFTSUSY. However it is possible to calculate μ^2 approximately as a function of the high energy soft parameters [31] for a given value of $\tan\beta$. We consider regions with $\tan\beta = 10$ extensively throughout this work. Taking this value, the low energy value of μ^2 is approximately related to the GUT scale soft parameters via the relation:

$$
\begin{aligned}
\frac{m_Z^2}{2} = \quad & -0.94\mu^2 + 0.010 m_{H_d}^2 - 0.19 M_2^2 - 0.0017 M_1^2 - 0.63 m_{H_u}^2 + 0.38\left(m_{\tilde{Q}}^2\right)_{33} \\
& +0.38\left(m_{\tilde{U}}^2\right)_{33} + 0.093 A_t^2 - 0.011 A_t M_1 - 0.070 A_t M_2 - 0.30 A_t M_3 \\
& +2.51 M_3^2 + 0.0059 M_1 M_2 + 0.028 M_1 M_3 + 0.195 M_2 M_3, \tag{2.5}
\end{aligned}
$$

where m_Z and μ are defined at (m_Z) and the rest of the masses are defined at (m_{GUT}).

To calculate this dependence we have used the 1-loop RGEs. We have also simplified the calculation by noting that the Yukawa couplings are dom-

inated by the third family. This allows us to make the approximation that only the third families contribute to the Higgs running. When we perform our numerical scans using SOFTSUSY we use the full 2-loop RGEs and don't assume third family dominance. Therefore Eq. 2.5 should not be taken as an exact result, but instead can be used to understand the dominant contributions from the soft mass terms at the GUT scale to the size of μ at m_Z.

The dominant positive contributions arise from M_3, the gluino mass, and $\left(m_{\tilde{Q}}^2\right)_{33}$, $\left(m_{\tilde{U}}^2\right)_{33}$, the third family squark (mass)^2. These terms all push $m_{H_u}^2$ negative, helping to satisfy Eq. 2.4. Unsurprisingly the dominant negative contribution is $m_{H_u}^2$. If $m_{H_u}^2$ is large and positive at the GUT scale, larger running effects are required to push it small or negative at the electroweak scale. Therefore to achieve REWSB we need small $m_{H_u}^2$ and/or large $\left(m_{\tilde{Q}}^2\right)_{33}$, $\left(m_{\tilde{U}}^2\right)_{33}$, M_3.

Eq. 2.5 also shows that fine-tuning is necessary if soft masses greatly exceed m_Z (as they must). If we have a large positive contribution due to large M_3^2 (for example), this must be cancelled by large contributions from the negative terms. This condition allows us to determine the size of μ^2, resulting in $|\mu|$ being an output of SOFTSUSY. However, the larger the contributions from the soft masses, the larger $|\mu|$, and so the greater the degree of fine-tuning required to fit the measured value of m_Z. We consider this point in more detail in section 2.5.1.
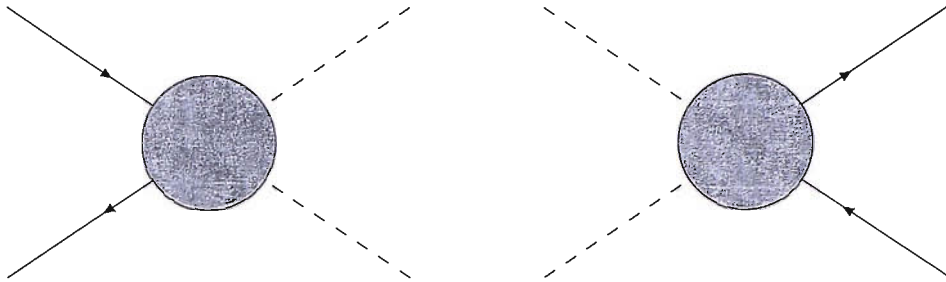
Figure 2.1: Diagrams by which Standard Model matter (solid) annihilates to superpartners (dashed) and vice versa.

2.4 Dark matter

Experiments require the existence of a substantial density of non-baryonic, massive, electrically (and colour) neutral dark matter in the universe. To explain such observations within particle physics we not only need a candidate particle with the correct properties, but we also need the theory to naturally produce a relic density of the observed magnitude.

The relic density is determined by a combination of particle physics and cosmology. In the early universe there is a period in which the temperature is such that $T \gg m_{LSP}$ and both processes in Fig. 2.1 occur at equal rates resulting in the LSP being in equilibrium with Standard Model matter. Once the universe expands and cools to an era in which $T < m_{LSP}$, processes of the form shown in the left hand diagram of Fig. 2.1 are kinematically disallowed. In this era the LSPs annihilate in pairs to SM matter, decreasing the number density of superpartners in the universe. Finally when $T \ll m_{LSP}$, this annihilation rate becomes vanishingly small. As R-parity conservation ensures the LSP is stable, this results in a stable LSP relic density. The exact magnitude of the relic density is governed by the annihilation that occurs just after the LSP falls out of equilibrium. It is the details of this

process that determine whether or not a supersymmetric theory naturally explains the observed relic density.

In section 2.4.1 we summarise the experimental evidence for dark matter and the present experimental bounds on the relic density. In section 2.4.2 we consider the candidates for dark matter within the MSSM and motivate the neutralino as the best candidate. In section 2.4.3 we briefly cover the details of the calculation of the relic density and highlight its dependence on the MSSM soft parameters.

2.4.1 Evidence for dark matter

In 1933 Zwicky studied the velocity dispersion of galaxies in the Coma cluster and inferred that there must be 400 solar masses per solar luminosity [7], requiring the majority of matter in a galaxy cluster to be non-luminous. This provided the first evidence for dark matter. Since then a number of different sources have provided evidence for dark matter. For a good review of the present experimental evidence see [32]. The evidence can be divided up according to distance scale.

- **Galactic scales**

The smallest distance scale for dark matter evidence is that of galaxies. The mass distribution within a galaxy can be measured in two ways. Firstly the mass can be estimated from the luminosity of the galaxy. Secondly, the mass distribution can be calculated through its effect on the motion of the stars. If a star at radius r has velocity v then we can use Newtonian
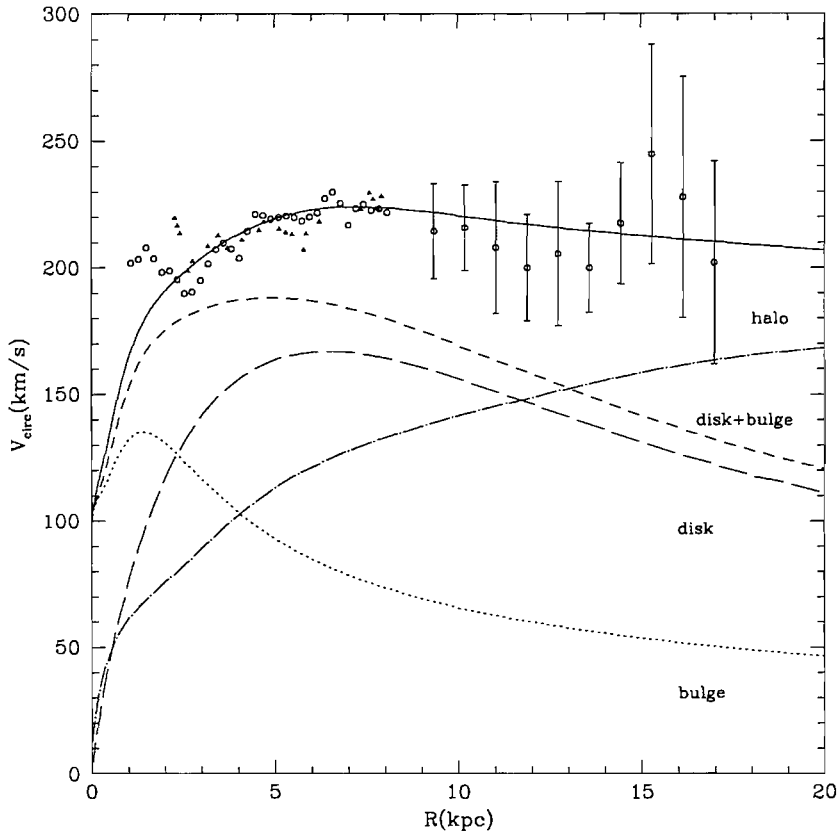
Figure 2.2: An example of using a spherical halo of dark matter to fit the observed rotation curves of the Milky Way, from [33]. The solid line is the rotation curve from disk + bulge + halo.

dynamics to calculate the total mass M within the radius r:

$$M = \frac{v^2 r}{G}. \tag{2.6}$$

In Fig. 2.2 we show an example of the rotation curves expected from the luminous matter in the disk and the bulge compared to the rotation curve actually measured. Not only is the total mass calculated from the luminosity too low to give the observed rotation curves, it is also distributed in the wrong regions. However if an approximately spherically symmetric halo of weakly interacting neutral dark matter with a density distribution $\rho \propto 1/r^2$ is added (the dot-dashed line in Fig. 2.2), the observed rotation

curve can be accounted for. This finding is true not just in the Milky Way, but in the vast majority of galaxies observed.

- **Galaxy clusters**

Dark matter also exists on the scale of galaxy clusters, as noted by Zwicky. As well as measuring the mass from the luminosity and movement of galaxies within clusters, it is also possible to measure the mass of a cluster via gravitational lensing. Once again the mass measurements only match up if there is a substantial quantity of dark matter.

- **Cosmological scales**

Though measurements on smaller scales prove that some quantity of dark matter is required in the universe, they only loosely constrain the total quantity of dark matter in the universe. To measure the total dark matter density we need to look on cosmological scales. The most accurate studies on these scales have been performed by the Wilkinson Microwave Anisotropy Probe (WMAP) [8, 9]. WMAP measures the cosmic microwave background (CMB), the left over radiation from the surface of last scattering in the early universe. This radiation is highly isotropic (down to the level of 10^{-5}) and fits the spectrum of black body radiation with a temperature of 2.726K. The anisotropies in this radiation give clues as to the structure and form of the early universe and it is these anisotropies that WMAP was designed to study.

These studies have been highly successful and tightly constrain cosmological models. In this work we are only interested in their implications for

the density of cold dark matter. Throughout we use the WMAP 1 year

results [8] that measure the non-baryonic cold dark matter density to be[4]:

$$\Omega_{CDM} h^2 = 0.1126 \pm 0.0081. \tag{2.7}$$

Comparison with to the measured baryonic density $\Omega_b h^2 = 0.0224$ shows

the universe contains a much larger density of dark matter than baryonic

Standard Model matter.

- **Direct detection**

The rotation curves of galaxies show that dark matter must exist in

roughly spherical halos in every galaxy. This allows us to estimate the local

dark matter density and thus the local flux. Efforts are currently underway

to detect this flux through direct detection at more than 20 experiments

around the world. The detection of WIMPs depends primarily upon the

mass of the dark matter particle and the interaction cross-section. For a

comprehensive listing of the current experimental bounds, and an interac-

tive plotting programme to display them, see [34]. No direct evidence for

dark matter has been found to date. However, present experiments are only

beginning to explore the regions of the $(\sigma, m_{\tilde{\chi}_1^0})$ parameter space in which we

would expect to find the MSSM neutralino. A direct detection signal would

allow us to constrain both the mass and composition of a dark matter parti-

cle independently of data from the LHC. These two research programmes are

therefore highly complimentary and should allow the form of BSM physics

---

[4]The WMAP three year results [9] came out during the course of this work. For consistency we stick to the 1 year values throughout but note that the three year results showed a drop in the central value of $\Omega_{CDM} h^2$ to 0.1046.

to be tightly constrained over the course of the next 10 years.

2.4.2 The candidates for particulate dark matter

We have already mentioned that if the lightest neutralino is the LSP, it makes a good dark matter candidate. However as the LSP in an R-parity conserving SUSY theory is always stable, the MSSM contains other candidates for dark matter. Firstly we can rule out any particle that carries electromagnetic charge or colour quantum numbers. Coloured dark matter would interact strongly. Charged dark matter would become trapped inside atoms, providing anomalously heavy nuclei. Such nuclei have never been observed.

Even after ruling out all charged particles we are left with four candidates within the MSSM.

- **Neutrinos**

Neutrino dark matter has an edge over the other candidates as neutrinos have been shown to exist. However we also know the approximate density of neutrinos in the universe and their masses are so low that they cannot provide the observed mass density. They are also disfavoured because they are relativistic (hot) around the time of galaxy formation which poses serious problems for models of structure formation.

- **Sneutrinos**

Just as the neutrino provides an uncharged stable candidate, so too must its superpartner, the sneutrino [35]. LEP bounds require the sneutrino mass to be $m_{\tilde{\nu}} \gtrsim 70$ GeV. This ensures that it is non-relativistic (cold) in the

early universe. However the cross-section for scattering of sneutrinos off nuclei [36] are large enough to have been ruled already by direct detection experiments[5].

- **The neutralino**

The lightest neutralino is uncharged, weakly interacting and stable (if it is the LSP). LEP bounds require that it have a mass $m_{\tilde{\chi}_1^0} \gtrsim 35$ GeV meaning it is a cold dark matter candidate [37]. Furthermore in many SUSY models it is naturally the lightest particle in the SUSY spectrum. Within this work we require that the neutralino be the LSP and rule out regions of parameter space in which this is not satisfied.

- **Dark matter beyond the MSSM**

If we are willing to venture outside the confines of the MSSM, we find a wealth of possible candidates for dark matter. Some of these arise as by products of solutions to other theoretical problems (such as the axion [38, 39], and axino [40]) whereas others do not. Though we do not wish to catalogue all the particles in the "dark matter zoo", special mention must be made of the gravitino, a particle that appears if we require SUSY to be a local symmetry.

If we require SUSY to be a local symmetry we are forced to include a spin-2 graviton in the theory. The superpartner of the graviton is the spin-3/2 gravitino. Such a particle is weakly interacting (its couplings are of

---

[5]Rick Gaitskell and Vic Mandic maintain a web page [34] that allows the generation of plots of the current experimental limits in the $(M_{DM}, \sigma(nucleon))$ plane. These pages also contain an up to date and comprehensive list of the papers reporting the current results of direct dark matter detection experiments from around the world.

the gravitational scale), massive and neutral so meets the primary require-
ments for a dark matter candidate [42], [43]. However the extremely weak
coupling of gravitino dark matter can raise its own problems. With very
weak couplings, the NLSP will be pseudo-stable, resulting in decays to the
gravitino long after supersymmetric matter decouples from Standard Model
matter. The energetic photons that are produced in this process can destroy
Big Bang Nucleosynthesis (BBN). These problems are not insurmountable,
but have lead to the gravitino being disfavoured in considerations of dark
matter. In Chapter 4 we study a model that contains a gravitino. However
other constraints mean the gravitino is never the LSP in this model.

2.4.3 Calculating the relic abundance

The number density of neutralinos in the early universe is governed by the
Boltzmann equation which can be written in the form:

$$\frac{dn}{dt} + 3Hn = -\langle \sigma v \rangle \left(n^2 - (n^{eq})^2 \right), \tag{2.8}$$

where n is the number density at time t, n^{eq} is the number density in ther-
mal equilibrium, H is the Hubble constant and $\langle \sigma v \rangle$ the annihilation cross-
section for neutralinos with an average velocity v.

For massive particles in the non-relativistic limit we can write:

$$n^{eq} = g \left(\frac{mT}{2\pi} \right)^{3/2} e^{-m/T}, \tag{2.9}$$

where m is the particle mass and T is the temperature.

For heavy states we can can simplify the calculation considerably by

expanding the cross-section in terms of v:

$$\langle \sigma v \rangle = a + b \langle v^2 \rangle + \mathcal{O}\left(\langle v^4 \rangle\right). \tag{2.10}$$

From these we can find the present number density of a relic. This gives the density as $\rho_\chi = m_\chi n_\chi$. This in turn is related to the quantity constrained by WMAP via:

$$\Omega_\chi \equiv \frac{\rho_\chi}{\rho_c}, \tag{2.11}$$

where ρ_c is the critical density required for a flat universe:

$$\rho_c \equiv \frac{3H^2}{8\pi G_N}. \tag{2.12}$$

By solving the Boltzmann equation[6] to find n_χ we get the dark matter relic density as:

$$\Omega_{CDM} h^2 \approx \frac{1.07 \times 10^9 \text{ GeV}}{M_{Pl}} \frac{m}{T_F \sqrt{g_*}} \frac{1}{(a + 3bT_F/m)}, \tag{2.13}$$

where T_F is the freeze-out temperature and g_* is the number of relativistic degrees of freedom, evaluated at freeze-out.

This calculation is performed in detail by `micrOMEGAs` in our work. Here we are interested in the general behaviour of $\Omega_{CDM} h^2$ across the parameter space. To this end we can re-write Eq. 2.13 as [44]:

$$\Omega_{CDM} h^2 \approx \frac{3 \times 10^{-27} \text{cm}^3 \text{s}^{-1}}{\langle \sigma v \rangle}, \tag{2.14}$$

---

[6]For a more in depth treatment of this calculation see [32, 44].

which is useful for order of magnitude estimates. Here we see that the dark matter density is entirely set by the annihilation cross-section. To understand whether the MSSM naturally explains the observed dark matter density, we need to consider the annihilation channels that go into calculating $\langle \sigma v \rangle$.

2.4.4 Coannihilation

Griest and Seckel [45] noticed that if the NLSP were only slightly heavier than the LSP and if they shared a quantum number, then the presence of a significant quantity of NLSPs around T_f resulted in the calculation of section 2.4.3 being incorrect. In such a case we need to not only consider interactions of the form $\tilde{\chi}_1^0 \tilde{\chi}_1^0 \to X_{SM}$ (where X_{SM} is some set of Standard Model particles), but also interactions of the form $\tilde{\chi}_1^0 + X_{NLSP} \to X_{SM}$ and $X_{NLSP} + X_{NLSP} \to X_{SM}$. Obviously if there is more than one particle close in mass to the $\tilde{\chi}_1^0$, we must add in extra annihilation channels. If there are a lot of particles close in mass to the $\tilde{\chi}_1^0$, there can be a lot of annihilation channels open.

To perform a calculation similar to the one above in the case of many particles, we change Eq. 2.8 to include the number density of NLSPs as well. The larger the mass-difference between the LSP and NLSP, the lower will be n_{NLSP}. This serves to reduce the magnitude of coannihilation effects. The details of coannihilation in general can be found in [32] and in the case of the neutralino specifically in [46]. The exact form of the equations for neutralino-slepton annihilation are presented in [47]. microMEGAs automatically calculates coannihilation effects for all SUSY particles.
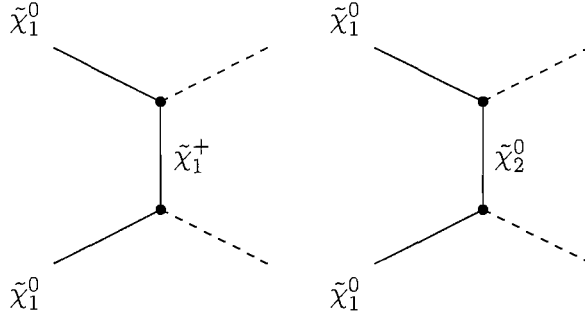
Figure 2.3: Higgsino LSPs have enhanced contributions from annihilation via the t and u-channel exchange of a neutralino or chargino where the final state particles are neutral or charged Higgs bosons respectively.

The effect of coannihilation on $\Omega_{CDM}h^2$ depends very strongly on the mass difference $\Delta m = m_{NLSP} - m_{\tilde{\chi}_1^0}$. If the lightest neutralino and the NLSP are degenerate in mass, the coannihilation contribution will often result in $\Omega_{CDM}h^2 \ll \Omega_{CDM}^{WMAP}h^2$.

2.4.5 $\Omega_{CDM}h^2$ and the composition of $\tilde{\chi}_1^0$

The annihilation cross-section for $\tilde{\chi}_1^0\tilde{\chi}_1^0 \to X_{SM}$ primarily depends upon the mass and composition of the lightest neutralino $\tilde{\chi}_1^0$ [37]. As this is determined by the parameters M_1, M_2, μ from Eq. 1.22 we can start by analysing the dark matter density in the limits in which one of these parameters is much lighter than the others.

- $\mu \ll M_1$, M_2: **higgsino dark matter**

In this limit both $\tilde{\chi}_1^0$ and $\tilde{\chi}_2^0$ are higgsino and lie close in mass. Not only this but $\tilde{\chi}_1^+$ is also higgsino and of a similar mass to $\tilde{\chi}_1^0$ and $\tilde{\chi}_2^0$. This obviously introduces a large coannihilation effect to the calculation of $\Omega_{CDM}h^2$. Secondly, neutralino annihilation via t-channel chargino or neutralino exchange, shown in Fig. 2.3, is greatly enhanced for light $\tilde{\chi}_2^0$, $\tilde{\chi}_1^+$ and enhanced couplings to final state Higgs bosons. Both of these conditions are fulfilled
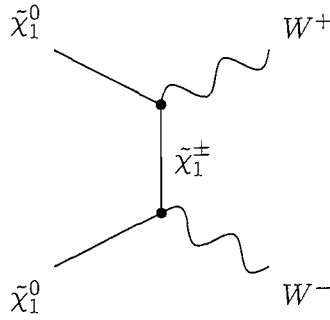
Figure 2.4: Wino LSPs have enhanced contributions from annihilation via the t and u-channel exchange of a chargino to $W^{\pm}$.

in the case of higgsino dark matter.

These effects combine to result in higgsino dark matter annihilating and co-annihilating too efficiently to account for the observed dark matter density. If we are to require MSSM matter to explain the observed dark matter density this allows us to rule out regions in which $\mu \ll M_1$, M_2.

- $M_2 \ll M_1$, μ: **wino dark matter**

In this limit the lightest neutralino is wino, as is the lightest chargino. Once again this results in a large coannihilation effect that suppresses $\Omega_{CDM}h^2$. A wino LSP also results in neutralino annihilation via t and u-channel chargino exchange to W bosons (as in Fig. 2.4) being greatly enhanced. Once again the combination of these effects results in a value of $\Omega_{CDM}h^2$ well below that measured by experiment.

- $M_1 \ll M_2$, μ: **bino dark matter**

In this limit the LSP is bino. $\tilde{\chi}_2^0$ and $\tilde{\chi}_1^+$ both depend on M_2 and μ and so will both have a much larger mass that the LSP, removing any coannihilation effects from these particles. Across most of the parameter space, the dominant contribution to bino annihilation is via t-channel sfermion ex-
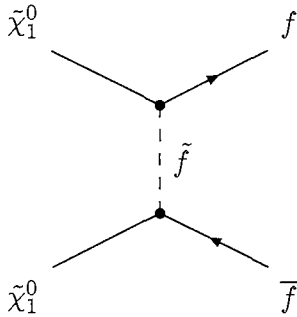
Figure 2.5: Annihilation to fermions via t,u-channel sfermion exchange. This channel dominates bino annihilation across most of the parameter space.

change shown in Fig. 2.5. This contribution is inversely proportional to the sfermion mass.

The only regions in which this annihilation channel can provide a large enough contribution to $\langle \sigma v \rangle$ to account for the observed relic density is when there are very light sfermions and a light neutralino. This is known as the bulk region. Across much of the parameter space, such regions are ruled out by LEP bounds.

If we do not have light sleptons to mediate processes such as those in Fig. 2.5, bino dark matter will generally result in a dark matter density far in excess of that observed by WMAP. Any region that predicts such a value of $\Omega_{CDM} h^2$ is ruled out absolutely as it would overclose the universe[7].

Another means of enhancing the bino annihilation cross-section is through on-shell production of a Z^0, h^0, H^0 or A^0 (Fig. 2.6). This is possible whenever $2m_{\tilde{\chi}_1^0} \approx m_{Z,h,H,A}$. In general these processes result in a very large contribution to the annihilation cross-section, often resulting in a value of $\Omega_{CDM} h^2$ well below the measured value. However with just enough of a contribution from these channels, we can have bino dark matter that results

---

[7]By resorting to exotic early universe cosmologies it is possible to reduce the dark matter density independently of properties of the neutralino. We do not consider such models here but see for example [48].
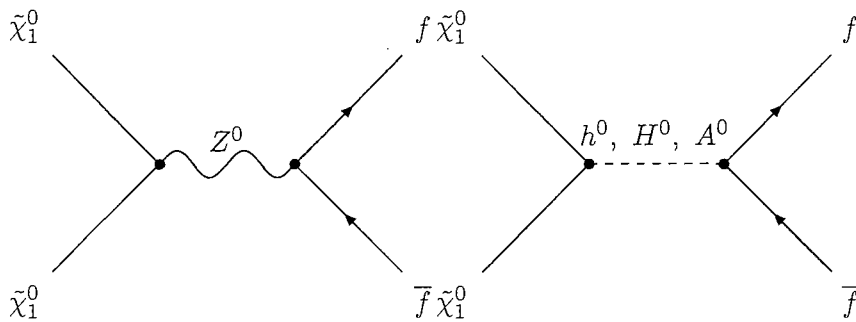
Figure 2.6: Examples of annihilation to Standard Model fields via the on-shell production of a Z or a Higgs boson. These annihilation channels can greatly enhance the decay rate of a bino LSP.

in a relic density in agreement with measurement.

Finally, if there are sleptons that are close in mass to the bino LSP, coannihilation effects can reduce the predicted value of $\Omega_{CDM}h^2$. The magnitude of these contributions depends primarily on the mass difference between the sfermion in question and the LSP.

- **"Well-tempered" dark matter**

As well as enhancements to the annihilation cross-section of bino dark matter, we can also fit the observed $\Omega_{CDM}h^2$ by moving away from the LSP being pure bino, wino or higgsino. As wino and higgsino LSPs generally produce $\Omega_{CDM}h^2 \ll \Omega_{CDM}^{WMAP}h^2$, whereas bino LSPs generally result in $\Omega_{CDM}h^2 \gg \Omega_{CDM}^{WMAP}h^2$, there must be regions in which the LSP is just the right mixture of either bino/wino or bino/higgsino to satisfy dark matter constraints. Arkani-Hamed, Delgado and Giudice [49] christened such regions "well-tempered". In [69], we extended this to the case of bino/wino/higgsino regions which we refer to as "maximally-tempered".

Region	Condition
Well-tempered bino/wino	$M_1 \approx M_2$ at m_{SUSY}
Well-tempered bino/higgsino	$M_1 \approx \mu$ at m_{SUSY}
Maximally-tempered bino/wino/higgsino	$M_1 \approx M_2 \approx \mu$ at m_{SUSY}
Bulk region (t-channel $\tilde{f}$ exchange)	light $\tilde{\chi}_1^0$ and $\tilde{f}$
sfermion coannihilation	$m_{\tilde{\chi}_1^0} \approx m_{\tilde{f}}$
Resonant annihilation	$2m_{\tilde{\chi}_1^0} \approx m_{Z,h,H,A}$

Table 2.1: The list of annihilation channels that allow the MSSM to fit the observed relic density. Note that as wino or higgsino LSPs annihilate too efficiently, the last three channels generally require a bino LSP.

2.4.6 Summary of dark matter allowed regions

Taking all of these considerations into account we can list the regions that we expect to reproduce the observed dark matter density within the MSSM. These are shown in Table 2.1. Each of these regions requires a different pattern of the input parameters a_{MSSM}.

The low energy phenomenology of each of these regions will have a distinctive form. Signals of SUSY at the LHC are determined by the parameters a_{MSSM}. Therefore we can relate the dark matter regions to distinct signals. In the case of direct dark matter detection the only SUSY particle involved is the LSP, here considered to be the neutralino. Direct detection signals are solely sensitive to the mass and composition of the neutralino and thus to M_1, M_2 and μ. Therefore a signal in a direct detection experiment will provide clear information about which region of Table 2.1 neutralino dark matter must occupy to fit the observed data.

2.5 Fine-tuning in the MSSM

In this work we are not only interested in finding MSSM models that satisfy all experimental constraints. The aim of this work is to move beyond this to

consider how naturally any given MSSM model explains two of the key questions that are left unanswered by the Standard Model, namely the source of electroweak symmetry breaking and the source of the observed dark matter density.

Questions of naturalness are interesting for two reasons. Firstly, the fact that SUSY can explain both electroweak symmetry breaking and the observed dark matter density has been a significant motivation for taking SUSY seriously. If we were to find that a region of the MSSM parameter space required an enormous amount of fine-tuning of the input parameters to fit the observed dark matter density or provide electroweak symmetry breaking, these motivations would be significantly weakened. Regions that exhibit low fine-tuning are better motivated[8]. Secondly, if the LHC finds evidence to suggest a specific pattern of soft parameters that require fine-tuning, the structure of this fine-tuning can act as a guide to more fundamental theories such as theories of SUSY breaking, just as the fine-tuning required to stabilise the Higgs mass in the Standard Model motivates the move to SUSY.

For these reasons we wish to study the degree of fine-tuning required in the MSSM for both dark matter, and electroweak symmetry breaking. To do this we need to define a measure.

2.5.1 Electroweak fine-tuning

The naturalness of radiative electroweak symmetry breaking from SUSY has been extensively studied [50]-[63]. In such studies, the following measure is

---

[8]Note we do not believe that just because a point exhibits large fine-tuning, and is therefore less theoretically motivated than another, it will not be found by experiment.

commonly used to quantify the degree of fine-tuning required for a given model point:

$$\Delta_a^{\text{EW}} = \left| \frac{\partial \ln \left(m_Z^2 \right)}{\partial \ln \left(a \right)} \right|, \qquad (2.15)$$

where a includes all the soft parameters m_{soft} at the GUT scale together with $\tan \beta$[9]. We take the total tuning of a point to be equal to the largest individual tuning[10] $\Delta^{EW} = \max(\Delta_a^{EW})$. The value of this measure gives the percentage change in m_Z^2 under a 1% change in the parameter a. If $\Delta_a^{EW} = 100$, a 1% change in a results in a 100% change in m_Z^2. Such a point therefore requires us to precisely fix the value of a to fit the experimental Z mass.

To understand how Δ^{EW} depends on the soft parameters, consider this measure in the context of the explicit expression for m_Z^2, Eq. 2.5. If, for example, we are interested in the sensitivity of m_Z^2 to M_3 we calculate the quantity $\Delta_{M_3}^{EW}$ and find:

$$\Delta_{M_3}^{EW} = \left| \frac{10 M_3^2}{m_Z^2} \right|. \qquad (2.16)$$

Thus even if $M_3 \sim m_Z$ we would still have a tuning $\Delta_{M_3}^{EW} \approx 10$. As we increase M_3 (as we are required to do to fit experimental bounds) we quickly increase the degree of tuning required to fit the observed Z mass. This general behaviour is true of all the soft parameters in Eq. 2.5. As the soft masses increase, so too does Δ^{EW}. If we want to avoid such fine-tuning we

---

[9]We also include the top Yukawa in our set of input parameters for Δ^{EW}. Though it is not a soft parameter, it is an input of the theory that we later set by requiring the masses of the quarks to agree with experiment. In theory we should include all of the Yukawa couplings in our calculation but in practise it is only the top Yukawa provides a significant contribution.

[10]There is a divide in the literature as to whether $\Delta = \max(\Delta_a)$ or $\Delta = \sqrt{\sum_a \Delta_a^2}$. Which definition one takes to be more accurate is a matter of taste. Throughout this work we take $\Delta = \max(\Delta_a)$.

would have to impose a structure on the soft masses such that positive and negative terms in Eq. 2.5 automatically cancel. As μ^2 is independent of the soft masses within the MSSM we cannot use such a tactic to remove Δ^{EW}. However if we keep the other contributions small, μ will be small and so Δ^{EW} will be small. Therefore we can predict that regions with low μ will provide low fine-tuning.

We use the sensitivity parameters Δ^{EW} to quantify the degree of fine-tuning required of the parameters for a given model point to agree with experiment. However the assumption that sensitivity directly quantifies fine-tuning is not a trivial statement. There are almost as many concepts of what is considered to be fine-tuning as there are physicists. However, we do not use the measure Δ^{EW} as a hard bound on the parameter space, rather it is to be used as a guide. Therefore a precise definition of fine-tuning in terms of sensitivity parameters is not required and we consider a point that exhibits a large sensitivity of the output (here M_Z^2) to small changes in the inputs to be fine-tuned. Therefore large Δ^{EW} corresponds to large fine-tuning for our purposes.

It is worth addressing one specific criticism of these sensitivity parameters and their relation to fine-tuning before we move on. In [64]-[66] an alternative measure of fine-tuning was proposed that arguably gives a more reliable estimate of fine-tuning. They define a fine-tuned point in parameter space to be a point in which the output (such as M_Z^2) is *unusually* sensitive to the inputs. Thus the authors of [64]-[66] claim that to provide a reliable measure of fine-tuning we must normalise the sensitivity parameters to some average value of sensitivity for a given parameter. Thus they advocate using

instead the fine-tuning parameter γ_a defined by,

$$\gamma_a = \frac{\Delta_a}{\overline{\Delta}_a}, \qquad (2.17)$$

where the average value $\overline{\Delta}_a$ is defined as discussed in [64]-[66]. The definition in Eq. 2.17 gives a different sense to the numerical value of the sensitivity parameter. For example it may be the case that all values of the sensitivity parameter are large over the entire theoretically allowed range of input parameters. Fine-tuning then corresponds to some unusually high levels of sensitivity above the typical values, where the typical values are themselves high.

We do not agree with this definition of fine-tuning. In the present work it is sufficient to consider the unnormalised sensitivity parameters Δ_a as a reasonable guide to fine-tuning. Our purpose is to compare fine-tuning across different regions of parameter space. For this purpose the simpler measure of Eq. 2.15 is sufficient.

2.5.2 Dark matter fine-tuning

Whereas the naturalness of electroweak symmetry breaking has been extensively studied, the fine-tuning required for dark matter has not[11]. In [49] Arkani-Hamed, Delgado and Giudice consider the conditions required to access each of the regions in Table 2.1 and conclude that, with the exception of the bulk region, the MSSM does not provide natural dark matter. We take

---

[11]A similar measure to Eq. 2.18 was previously defined and used to study the CMSSM in [67], [68]. One motivation of these studies was to study the sensitivity that the LHC would need to achieve to give a corresponding accuracy in the predicted dark matter density. This is an interesting question and our results can also be applied in this context, though we do not focus on that here.

up this challenge and provide the first quantitative analysis of naturalness in the case of MSSM dark matter. To study this we use an analogous measure to Eq. 2.15 to quantify the degree of fine-tuning required to reproduce the observed dark matter density:

$$\Delta_a^\Omega = \left| \frac{\partial \ln \left(\Omega_{CDM} h^2 \right)}{\partial \ln \left(a \right)} \right| . \tag{2.18}$$

Though the measures are analogous, the calculations of radiative electroweak symmetry breaking and the calculation of the relic density of dark matter have important differences. In the case of electroweak symmetry breaking, the MSSM inputs a_{MSSM} provide a complete set of inputs. This is not the case for dark matter. The calculation of the present day relic density necessarily involves some assumptions about the cosmology of the early universe[12]. These assumptions are:

- At some point in the universe's history (after inflation) there was a radiation dominated period in which $T \gg m_\chi$, where m_χ is the mass of the LSP.

- There are no exotic non-thermal production methods for dark matter.

If the first assumption holds then there was a period in the history of the universe in which Standard Model matter and supersymmetric matter (particularly the LSP) were in equilibrium. As the universe expands and cools a relic of stable SUSY particles is left behind. No further assumptions are required in the calculation of this relic density.

---

[12]The calculation of the dark matter relic density will also depend upon the Yukawa couplings, as did Δ^{EW}. Due to the difficulty of implementing this within the computer codes we use, this is not done for Δ^Ω.

If the second assumption holds then the LSP relic density is the only dark matter present in the universe. In this work we stay within such a cosmological framework. In such a framework the inputs of the MSSM, a_{MSSM}, provide the complete set of parameters for calculating the relic density of dark matter. As a result, we can use Eq. 2.18 to quantify the naturalness of dark matter. In more exotic cosmologies, the set of input parameters a_{MSSM} would need to be expanded to include variations in the details of early universe cosmology, but such models are beyond the scope of this work.

As the calculation of the relic density is significantly more convoluted than the calculation of electroweak symmetry breaking, we can't extract any straightforward estimates as we did for $\Delta_{M_3}^{EW}$. Instead we have written a code to numerically find the value of the derivative in Eq. 2.18 for each model point. To understand the naturalness of dark matter within the MSSM we must take sets of parameters that reproduce the observed dark matter density through each of the channels identified in section 2.4.6. By calculating the values of Δ^{Ω} in each of these regions we will find out whether the MSSM really does provide natural dark matter as has been claimed.

Chapter 3

How Natural is MSSM Dark Matter?

3.1 Introduction

To study the naturalness of dark matter within the MSSM, we need to consider specific structures of the MSSM input parameters a_{MSSM} that provide access to the dark matter annihilation channels in Table 2.1. There is an extensive literature on using dark matter to constrain the MSSM parameter space [70]-[99], however ours is the first study to consider the naturalness of dark matter outside the Constrained Minimal Supersymmetric Standard Model (CMSSM) [100]. In section 3.2 we begin by considering the CMSSM. In this model all the parameters a_{MSSM} are determined in terms of 4 free parameters:

$$a_{CMSSM} \in \left\{ m_0, m_{1/2}, A_0, \tan\beta \right\}, \tag{3.1}$$

61

and the sign of μ. Here m_0 is the common scalar mass that determines all the diagonal entries of the squark and slepton mass matrices. $m_{1/2}$ is the universal gaugino mass. A_0 is the common trilinear coupling. Finally $\tan\beta$ is the ratio of the Higgs VEVs as defined previously.

Such a model is motivated via its close ties to minimal Supergravity (mSUGRA) models, as well as its simplicity. As a result, the CMSSM has been extensively studied in the literature[1]. We use it as a datum to which we can compare less constrained models. Within the CMSSM we can access well-tempered bino/higgsino dark matter (the Focus Point region), $\tilde{\chi}_1^0 - \tilde{\tau}$ coannihilation and $\tilde{\chi}_1^0$ annihilation via the production of an on-shell pseudoscalar Higgs A^0 (the Funnel region). We find the $\tilde{\tau}$-coannihilation channel to be the least fine-tuned whereas both the Focus Point region and the Funnel region exhibit significant fine-tuning.

Taking the CMSSM as our starting point we go on to relax the universalities imposed the soft parameters at the GUT scale. In section 3.3 we allow non-universality between the 3rd family squark and slepton soft masses and the 1st and 2nd families. Dark matter with non-universal third family scalar masses has been considered in [85] motivated by purely phenomenological consideration, or in [86], [88] motivated by specific GUT models. The collider phenomenology of such models has also been studied in [87]. For our purposes it is interesting as such models allow access to $\tilde{e}_R - \tilde{\chi}_1^0$ and $\tilde{\mu}_R - \tilde{\chi}_1^0$ coannihilation channels, the edge of the bulk region and a bino/higgsino region that agrees with δa_μ at 1σ.

In section 3.4 we consider the effect of allowing non-universal gaugino

---

[1]See [70], [71] for a recent comprehensive analysis of the CMSSM parameter space.

masses at the GUT scale. Such models naturally arise in SUGRA models with non-minimal kinetic terms, models with gauge mediated SUSY breaking and models with anomaly mediated SUSY breaking. The dark matter phenomenology of models with non-universal gaugino masses has previously been studied in [72]-[78] and particular high energy models that give rise to non-universal gauginos have been analysed in [79]-[84], [88]. Non-universal gaugino masses are clearly interesting for studying natural dark matter. By varying M_1 and M_2 we directly control the wino and bino components of the LSP. This allows us to study the naturalness of the bino/wino well-tempered region. Within these models we are also able to access the bulk region, the h^0 resonance and the Z^0 resonance.

In section 3.5 we perform the first study of a model in which we have both non-universal scalar and gaugino masses. This allows us to study the robustness of our previous results to further non-universality. We are also able to access the maximally tempered bino/wino/higgsino region.

Finally, in section 3.6 we summarise our conclusions on the naturalness of dark matter within the MSSM.

3.2   CMSSM

The simplest model of SUSY breaking is the CMSSM. In such a model all soft mass matrices are diagonal at the high scale, taken here to be M_{GUT}, and have a universal mass squared, m_0^2, between generations. The gauginos also have a universal soft mass $m_{1/2}$. As such the model is defined by the parameters a_{CMSSM} defined in Eq.3.1.

Studies of the CMSSM find three regions that satisfy dark matter bounds.
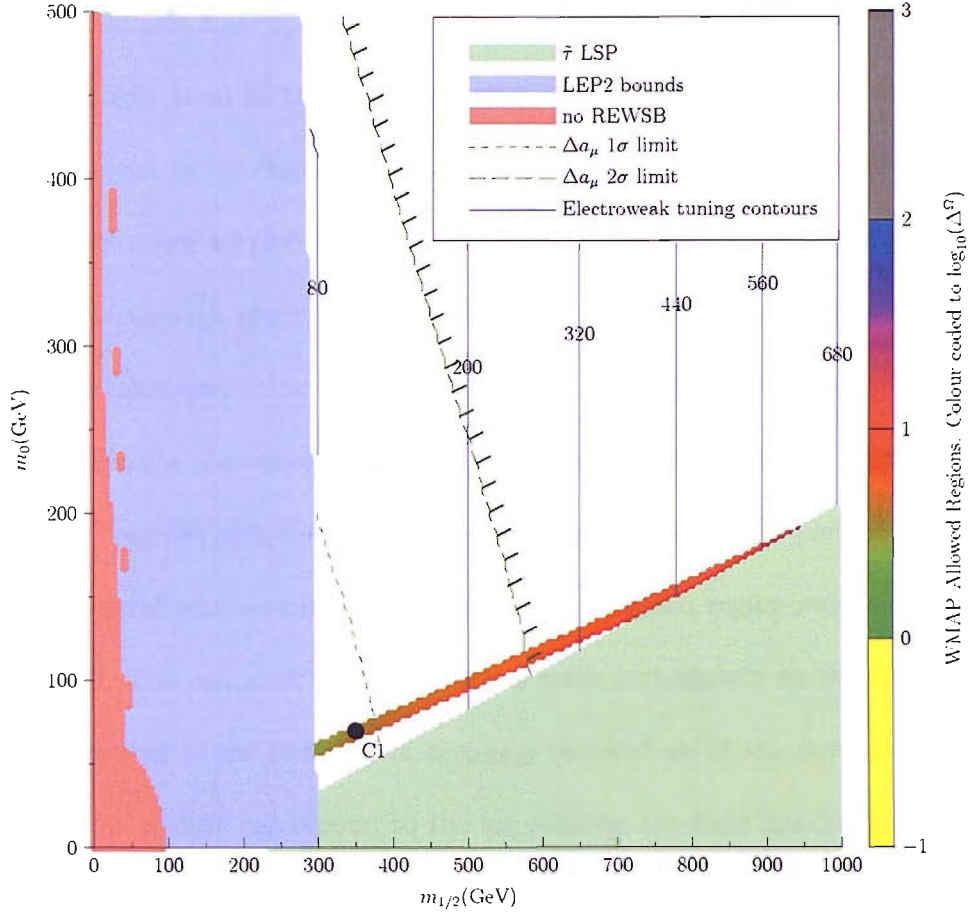
Figure 3.1: The $(m_{1/2}, m_0)$ plane for the CMSSM with $A_0 = 0$, $\tan\beta = 10$.

At large m_0, μ can become very small which in turn results in a bino/higgsino neutralino - the Focus Point region. At large $\tan\beta$ (≈ 50) and moderately large $m_{1/2}$ the pseudoscalar Higgs boson becomes light giving rise to region in which $2m_{\tilde{\chi}_1^0} \approx m_A$. Here neutralino annihilation proceeds through s-channel exchange of a pseudoscalar Higgs boson, known as the Higgs Funnel. The third region that reproduces the observed value of $\Omega_{CDM}h^2$ is where we have coannihilation of the neutralino with the lightest stau. This region appears at low values of m_0 and $m_{1/2}$ where $m_{\tilde{\tau}} \approx m_{\tilde{\chi}_1^0}$. This region has a light SUSY spectrum and satisfies δa_μ and $BR(b \to s\gamma)$ at 1σ.

In Fig. 3.1 we study the CMSSM in the $(m_{1/2}, m_0)$ plane with $A_0 = 0$,

$\tan \beta = 10$ and $\text{sign}(\mu)$ positive. Low $m_{1/2}$ values are excluded by LEP2 bounds (light blue) on the lightest Higgs mass. Low m_0 values are excluded as they result in the stau becoming the LSP (light green). In the remaining parameter space we plot the 1 and 2σ bounds on δa_μ. $BR(b \to s\gamma)$ is satisfied at 1σ through the entire parameter space and so does not appear. We plot the calculated value of the electroweak tuning required using contours (blue). Finally, the region in which the calculated dark matter relic density $\Omega_{CDM}h^2$ agrees with the WMAP measurement within 2σ is plotted as a multicoloured stripe running alongside the light green region representing a $\tilde{\tau}$ LSP. The colour of the dark matter strip corresponds to the degree of fine-tuning of the parameters a_{CMSSM} required to fit the dark matter data. The colours correspond to the log scale on the right hand side. We have considered relatively low values of m_0 and $m_{1/2}$ as it is only in these regions that the CMSSM can satisfy δa_μ and it allows us to study the $\tilde{\tau}$ coannihilation region in detail.

The coannihilation strip is the only viable dark matter region for the range of parameters in Fig. 3.1. The thinness of the stau coannihilation strip indicates that some degree of tuning is required. From the colour coding we can see that the total fine-tuning of the coannihilation strip varies from $\Delta^\Omega \approx 3$ at low m_0 to $\Delta^\Omega \approx 15$ at large m_0. To understand the origin of this tuning we need to consider the general form of dark matter in the CMSSM.

The ratio of $M_1 : M_2$ at the low energy scale determines the wino and bino components of the LSP. In the CMSSM, the gauginos have a universal soft mass at the GUT scale. The running of the gaugino masses is almost identical to the respective gauge couplings. This is very straightforward

and allows us to use a useful rule of thumb, $M_1(m_Z) \approx 0.4M_1(m_{GUT})$ and $M_2(m_Z) \approx 0.8M_2(m_{GUT})$. Therefore if $M_1 = M_2$ at the GUT scale, $M_1 \approx 0.5M_2$ at the electroweak scale and the LSP will be bino. The only exception is when we have small μ. In the CMSSM this only occurs for very large m_0, not visible in Fig. 3.1. Therefore throughout the displayed parameter space the lightest neutralino is bino. As mentioned in 2.4.5, bino dark matter alone generally results in a dark matter density greatly in excess of that measured by experiment. Thus in Fig. 3.1 values of m_0 above the coloured WMAP strip are ruled out as they overclose the universe.

Without coannihilation effects the dominant annihilation process is via t-channel $\tilde{\tau}$ exchange. However this on its own is not efficient enough and we end up with $\Omega_{CDM}h^2 \approx \mathcal{O}(1)$. The addition of coannihilation[2] reduces this by an order of magnitude. Coannihilation is generally considered to require a large degree of fine-tuning so the low values of fine-tuning of the coannihilation strip in Fig. 3.1 are something of a surprise.

The magnitude of coannihilation effects depends critically on $\Delta m = m_{NLSP} - m_{\tilde{\chi}_1^0}$. Any variation in either m_{NLSP} or $m_{\tilde{\chi}_1^0}$ will lead to a considerably larger variation in Δm. Therefore, unless $m_{\tilde{\chi}_1^0}$ and m_{LSP} are coupled in some manner we would expect coannihilation regions to be finely-tuned. In the case of Fig. 3.1, the coannihilation is between a bino LSP and a $\tilde{\tau}$. The first has its mass set at the soft scale by $m_{1/2}$ whereas the latter's soft mass is set by m_0. These are independent parameters so we would expect to see a larger fine-tuning than that discovered here.

To understand this unexpected result we take the point C1 with $m_0 =$

---

[2]For a detailed study of coannihilation within the CMSSM see [47], [109].

Parameter	Value
	C1
$\Delta^{\Omega}_{m_0}$	3.5
$\Delta^{\Omega}_{m_{1/2}}$	3.4
$\Delta^{\Omega}_{\tan\beta}$	1.4
$\Delta^{\Omega}_{A_0}$	0
Δ^{Ω}	3.5
Δ^{EW}	160

Table 3.1: Fine-tuning sensitivity parameters in the CMSSM with $A_0 = 0$, $\tan\beta = 10$ at point C1 in Fig. 3.1 with $m_0 = 70$ GeV, $m_{1/2} = 350$ GeV.

70 GeV, $m_{1/2} = 350$ GeV, $A_0 = 0$ and $\tan\beta = 10$ and consider all of the separate sensitivities Δ^{Ω}_a. The results are presented in Table 3.1.

As expected, the sensitivity comes from the parameters m_0 and $m_{1/2}$ that set the soft masses at the GUT scale. There is also a subsidiary dependence on $\tan\beta$, as this also affects the mass of the $\tilde{\tau}$. The smallness of the tuning comes from the fact that along the coannihilation strip $m_0 < m_{1/2}$. Now the running of the right handed slepton masses are strongly dependent on M_1. When m_0 is small, the dominant contribution to the low energy $\tilde{\tau}$ mass is via this running contribution from M_1. Thus in this region of the CMSSM $m_{\tilde{\tau}}$ depends strongly on $m_{1/2}$, resulting in a correlation of the masses of the neutralino and the stau. This gives considerably more natural coannihilation than would be expected.

This correlation is strongest for small values of m_0. Also, as we move to smaller m_0, contributions from t-channel $\tilde{\tau}$ exchange are enhanced. In these regions we need less coannihilation to satisfy $\Omega_{CDM}h^2$. This has the effect of reducing the total sensitivity to m_0. These effects combine to give low values of Δ^{Ω} for low m_0 and $m_{1/2}$ within the CMSSM, regions which also give a SUSY contribution to $(g-2)_\mu$ that explain δa_μ. Equally, if the
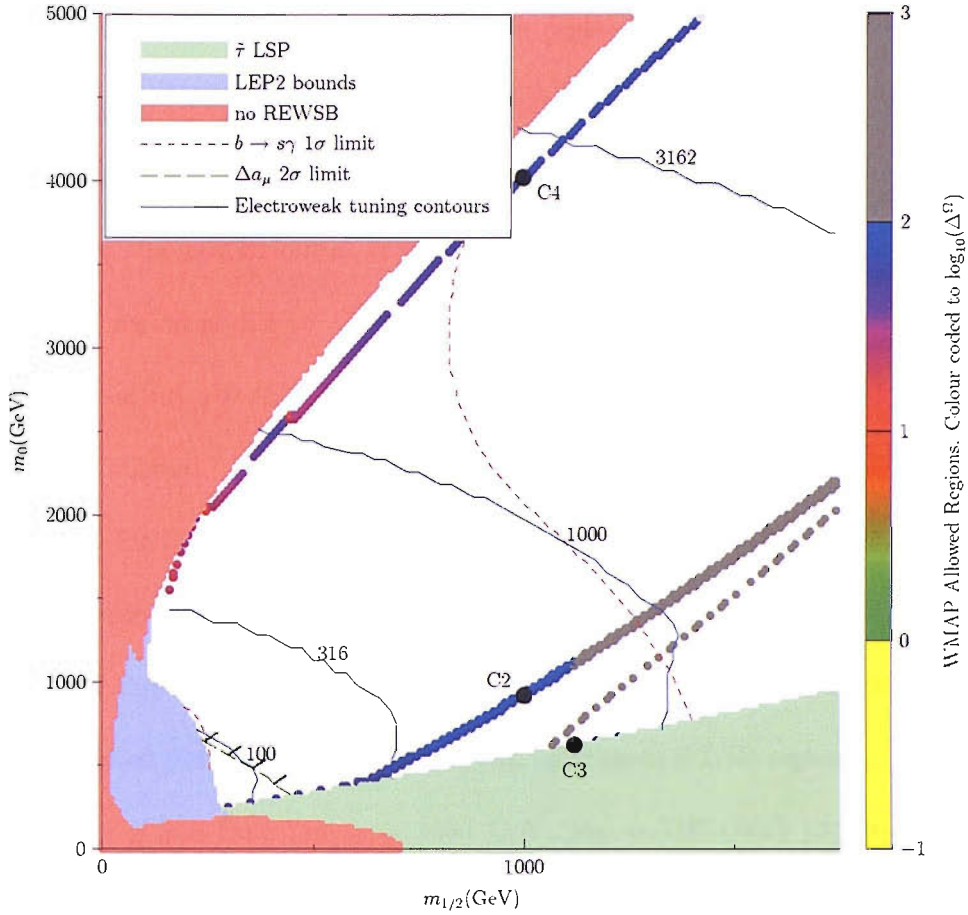
Figure 3.2: The $(m_{1/2}, m_0)$ plane for the CMSSM with $A_0 = 0$, $\tan\beta = 50$.

measured value of $(g-2)_\mu$ is found to agree with the Standard Model value, the CMSSM will be forced to larger values of m_0 and $m_{1/2}$ and we will have to accept a greater degree of fine-tuning to fit $\Omega_{CDM}^{WMAP} h^2$.

Finally, note the behaviour of Δ^{EW} across the parameter space. The primary dependence is on $m_{1/2}$, This is to be expected from 2.5 as the term with the largest coefficient is M_3^2. Therefore moving to larger values of $m_{1/2}$ will also increase the degree of electroweak fine-tuning required.

In Fig. 3.2 we move to $\tan\beta = 50$ and expand the ranges of m_0 and $m_{1/2}$ that we scan over. This allows us access to new dark matter regions beyond just $\tilde{\tau}$-coannihilation. There are a number of interesting features

in this plot. For large m_0, REWSB fails (light red) as we are unable to drive $m_{H_u}^2$ small enough through RGE effects. Along the edge of this region μ is small, resulting in a neutralino with significant higgsino component. Therefore the multicoloured WMAP strip that runs along the edge of the light red region is due to a well-tempered bino/higgsino LSP. The kink in this strip at $m_{1/2} \approx 450$ GeV is where $m_{\tilde{\chi}_1^0} \approx m_t$ and the process $\tilde{\chi}_1^0 \tilde{\chi}_1^0 \to t\bar{t}$ becomes allowed.

As in Fig 3.1, low values of m_0 are ruled out by a $\tilde{\tau}$ LSP. Along the edge of this region there is a $\tilde{\tau}$-coannihilation strip. However this strip is very thin and this scan struggles to resolve it. The strip appears as a series of disconnected points along the edge of the light green $\tilde{\tau}$ LSP region.

Along a line from $(m_{1/2} = 1050$ GeV, $m_0 = 700$ GeV$)$ to $(m_{1/2} = 1750$ GeV, $m_0 = 2100$ GeV$)$ the mass of the LSP is such that $2m_{\tilde{\chi}_1^0} = m_A$ and the LSP annihilates via an on-shell pseudoscalar Higgs A^0. When $2m_{\tilde{\chi}_1^0} = m_{A^0}$ is exactly true, the contribution from resonant annihilation is too large, resulting in $\Omega_{CDM} h^2 \ll \Omega_{CDM}^{WMAP} h^2$. Therefore we only fit the measured dark matter density $\Omega_{CDM}^{WMAP} h^2$ on the either edge of the resonance.

In these three separate channels we find a wide range of fine-tunings. The well-tempered bino/higgsino region exhibits tuning ranging from $\Delta^{\Omega} = 30$ at the low $m_{1/2}$ end to $\Delta^{\Omega} = 60$ at large $m_{1/2}$. The coannihilation region here has a tuning $\Delta^{\Omega} \approx 40$. However the Higgs Funnel clearly exhibits the greatest tuning with much of it plotted in grey corresponding to $\Delta^{\Omega} > 100$. To understand how these tunings arise we take the points C2, C3 and C4 for the Higgs Funnel, $\tilde{\tau}$-coannihilation and well-tempered regions respectively and study the different contributions to Δ^{Ω}. The results are presented in

Parameter	Value		
	C2	C3	C4
$\Delta^{\Omega}_{m_0}$	6.9	38	63
$\Delta^{\Omega}_{m_{1/2}}$	11	30	37
$\Delta^{\Omega}_{\tan\beta}$	91	49	10
$\Delta^{\Omega}_{A_0}$	0	0	0
Δ^{Ω}	91	49	63
Δ^{EW}	600	750	2800

Table 3.2: Fine-tuning sensitivity parameters in the CMSSM with $A_0 = 0$, $\tan\beta = 50$ from Fig. 3.1. C2 has $m_0 = 920$ GeV, $m_{1/2} = 1000$ GeV. C3 has $m_0 = 625$ GeV, $m_{1/2} = 1120$ GeV. C4 has $m_0 = 4025$ GeV, $m_{1/2} = 1000$ GeV.

Table 3.2.

Point C2 represents a point where neutralino annihilation is dominantly to the pseudoscalar Higgs. It is unsurprising that a process that proceeds via resonant production of a particle should be fine-tuned. Here the tuning depends primarily on $\tan\beta$ as it is this parameter that dominates the determination of the pseudoscalar Higgs mass.

At point C3 the relic density calculation is dominated by coannihilation between the $\tilde{\tau}$ and the $\tilde{\chi}^0_1$. In this region the tunings with respect to $m_{1/2}$ and m_0 have risen. This is to be expected as the contribution from t-channel $\tilde{\tau}$ exchange is negligible for these large values. Also large m_0 reduces the correlation between $m_{\tilde{\chi}^0_1}$ and $m_{\tilde{\tau}}$. However the primary contribution to the total tuning is due to $\tan\beta$. This is because when $\tan\beta$ is large the stau mass has a strong dependence on $\tan\beta$. On the other hand, $m_{\tilde{\chi}^0_1}$ is entirely independent of $\tan\beta$. Therefore, in this case, there is no correspondence between $m_{\tilde{\chi}^0_1}$ and $m_{\tilde{\tau}}$. As a result we have large fine-tuning, just as would be expected for coannihilation between two unrelated particles.

Finally point C4 represents the bino/higgsino well-tempered region. This

point exhibits a large sensitivity to m_0 and a smaller sensitivity to $m_{1/2}$. This channel directly depends upon the higgsino fraction in $\tilde{\chi}_1^0$. This is determined by the ratio $\mu : M_1$. As it is the Higgs masses that determine μ at tree level, the large sensitivity to m_0 is unsurprising, especially as the low energy value of M_1 has no dependence on m_0. The fact that $\Delta_{m_{1/2}}^{\Omega}$ is smaller is worth a comment. To understand this consider Eq. 2.5. Though Eq. 2.5 is for $\tan\beta = 10$, it does show that $\mu^2 \propto M_3^3$. Therefore as we increase $m_{1/2}$ we not only increase M_1, we also increase μ and so varying $m_{1/2}$ does not change the ratio $\mu : M_1$ as drastically as might be expected.

The points C1-C4 serve as datums to which we can compare models in which we relax the universalities of the CMSSM. We will start by breaking the universality between the sfermion generations.

3.3 Non-universal Third Family Scalar Masses

The first deviation we take from universality of the CMSSM is to allow the 3rd family sfermion mass squared to vary independently of the 1st and 2nd families. This results in a model with five parameters and a sign:

$$a_{CMSSM+m_{0,3}} \in \left\{ m_0,\ m_{0,3},\ m_{1/2},\ \tan\beta,\ A_0 \right\} \qquad (3.2)$$

and the sign of μ. These determine the soft masses of the squarks, sleptons, Higgs and gauginos at M_{GUT} to be:

$$m_{\tilde{Q}}^2, m_{\tilde{L}}^2, m_{\tilde{u}}^2, m_{\tilde{d}}^2, m_{\tilde{e}}^2 \; = \; \begin{pmatrix} m_0^2 & 0 & 0 \\ 0 & m_0^2 & 0 \\ 0 & 0 & m_{0,3}^2 \end{pmatrix}$$

$$m_{H_u}^2 = m_{H_d}^2 \; = \; m_{0,3}^2$$

$$M_\alpha \; = \; m_{1/2}$$

where $\alpha = 1, 2, 3$ labels the three gauginos. We have set the Higgs soft masses to be equal to the third family soft mass $m_{0,3}$ since it seems reasonable that all soft masses involved in EWSB should be of the same order. This is also the case in certain string models [101], [103].

From a purely phenomenological point of view, we gain a lot by allowing ourselves this extra freedom, as pointed out in [85]. Firstly, the size of μ is highly sensitive to the third family squark masses and the Higgs masses as shown in Eq. 2.5. On the other hand δa_μ is sensitive to the first and second family slepton masses. If we allow the 3rd generation soft masses to vary independently of the 1st and 2nd, we can access regions with low μ in which the neutralino is a bino/higgsino mix and which still agree with δa_μ at 1σ.

However we have to be careful with low values of μ. Small μ results in light charginos which enhance the SUSY contribution to $BR(b \rightarrow s\gamma)$. However the charginos appear in loops with stops, and with a large value of $m_{0,3}$, the stops become heavy and help to suppress this contribution. Thus in this model, $BR(b \rightarrow s\gamma)$ will be problem at large $m_{0,3}$ but not as much as might be initially expected.
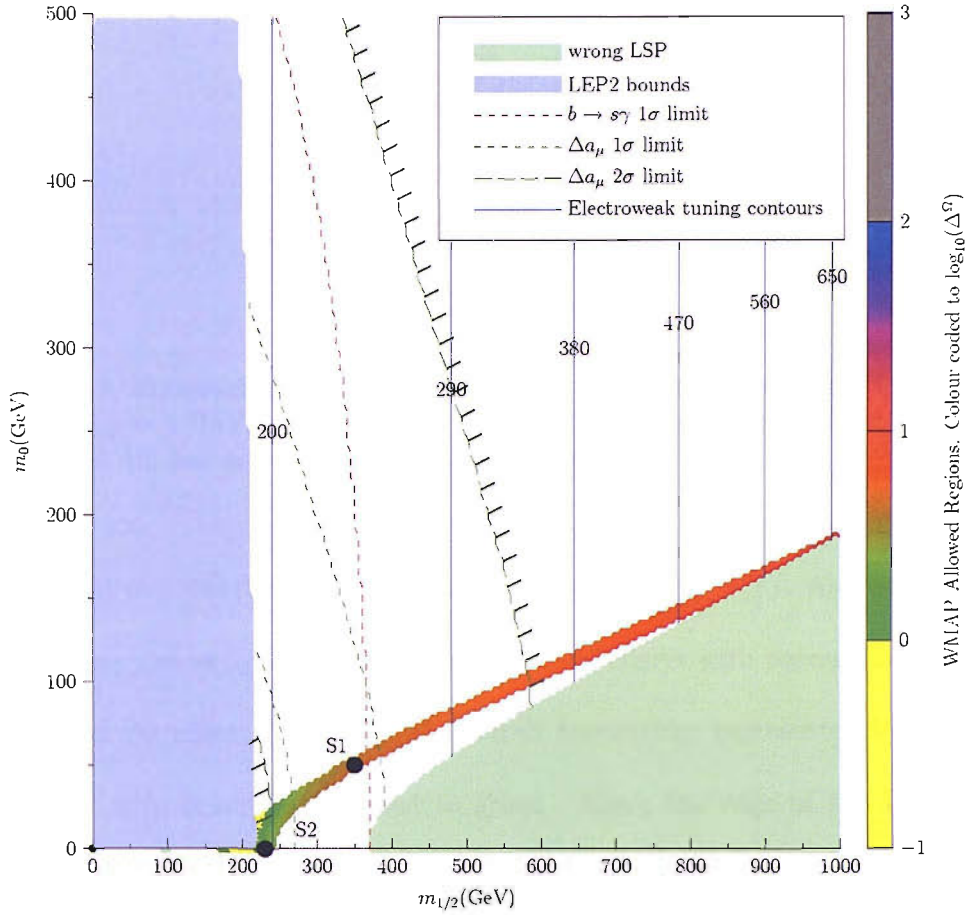
Figure 3.3: The $(m_{1/2}, m_0)$ plane for non-universal sfermion masses with $m_{0,3} = 1$ TeV, $A_0 = 0$, $\tan\beta = 10$.

In Fig. 3.3 we take the same range for m_0 and $m_{1/2}$ as we did for Fig. 3.1 but we now set $m_{0,3} = 1000$ GeV. With a large value of $m_{0,3}$ the stau is no longer the lightest slepton, we now have a normal mass hierarchy (NMH) in the sfermions. The immediate result of this is that the coannihilation strip at low m_0 is now coannihilation with selectrons and smuons rather than staus. This also means that we can now access $m_0 = 0$ without ending up with a charged LSP. This happens at $m_{1/2} = 230$ GeV. The lower bound on $m_{1/2}$ from LEP2 constraints on the lightest Higgs also changes between Fig. 3.1 and Fig. 3.3 from 300 GeV to $m_{1/2} \approx 200$ GeV.

As we can access low values of both $m_{1/2}$ and m_0, we can access regions

Parameter	Value	
	S1	S2
$\Delta^{\Omega}_{m_0}$	2.4	0
$\Delta^{\Omega}_{m_{0,3}}$	0.15	0.30
$\Delta^{\Omega}_{m_{1/2}}$	4.2	1.8
$\Delta^{\Omega}_{\tan\beta}$	0.061	0.033
$\Delta^{\Omega}_{A_0}$	0	0
Δ^{Ω}	4.2	1.8
Δ^{EW}	240	200

Table 3.3: Fine-tuning sensitivity parameters for different points in Fig. 3.3 with $m_{0,3} = 1$ TeV, $A_0 = 0$, $\tan\beta = 10$. S1 has $m_0 = 50$ GeV, $m_{1/2} = 350$ GeV. S2 has $m_0 = 0$ GeV, $m_{1/2} = 230$ GeV

with light sleptons that in turn mediate the process $\tilde{\chi}^0_1 \tilde{\chi}^0_1 \rightarrow f\bar{f}$. As we move to low m_0 and $m_{1/2}$ this process becomes competitive with coannihilation. This has the effect of reducing the overall fine-tuning, represented by the WMAP strip changing from red to green. Along the edge of the LEP2 bounds there is even the hint of yellow, representing points where $\Delta^{\Omega} < 1$. However accessing this region comes at a cost. For low m_0 and $m_{1/2} < 250$ GeV the smuons become so light that the SUSY contribution to δa_μ is too large. This large contribution could be reduced if we were to allow M_1 and M_2 to have different signs. Finally the dashed red line is also an early warning. For $m_{1/2} < 350$ GeV the charginos are light enough that we violate the bounds on $BR(b \rightarrow s\gamma)$, though only at 1σ.

To understand the tuning of a $\tilde{e}_R$, $\tilde{\mu}_R$-coannihilation region and t-channel sfermion exchange we consider two points on the successful dark matter strip: S1 at $m_0 = 50$ GeV, $m_{1/2} = 350$ GeV; and S2 at $m_0 = 0$ GeV, $m_{1/2} = 230$ GeV. The fine-tuning of these points with respect to our 5 parameters is shown in Table 3.3.

We choose point S1 to allow direct comparison with the CMSSM. Once

again we find a tuning of around 25% with respect to $m_{1/2}$ though the dependence on $m_{0,3}$ is minimal. This shouldn't be surprising as the neutralino annihilation channels in question depend primarily on the mass of the smuon, selectrons and the neutralino, none of which are sensitive to $m_{0,3}$. From this region, there is nothing to suggest that selectron and smuon coannihilation channels are any more natural that the stau coannihilation channel in the CMSSM.

Point S2 is considerably more interesting. Here there is a dramatic decrease in the sensitivity to the soft parameters. The primary reason for this is that there are more channels at work than just coannihilation. At $m_0 = 0$, the selectron and smuon are light enough that t-channel slepton exchange in the process $\tilde{\chi}_1^0 \tilde{\chi}_1^0 \rightarrow e^+ e^-$ or $\mu^+ \mu^-$ becomes competitive. Indeed at this point such processes account for 60% of the annihilation of SUSY matter whereas coannihilation processes only account for 40%.

This combination of annihilation channels is responsible for the drastic decrease in dark matter sensitivity to the soft parameters. By decreasing $m_{1/2}$ we decrease the mass of the neutralino and to lesser extent the selectron and the smuon. This increases the mass splitting between the states, suppressing coannihilation effects. However lower slepton masses enhance the cross-section for t-channel slepton exchange. This has the effect of smearing out the region of successful dark matter in the $m_{1/2}$ direction.

If $m_0 = 0$, $\Delta_{m_0}^\Omega = 0$ automatically[3]. However we would also expect $\Delta_{m_0}^\Omega$ to be small whenever m_0 is small. Whenever $m_0 \ll m_{1/2}$ the masses of

[3]Due to the definition of Δ^Ω, whenever $a = 0$, $\Delta_a^\Omega = 0$. However we have checked that this has not resulted in an artificially low Δ by taking a number of points of decreasing m_0. From this we conclude that as $m_0 \rightarrow 0$, $\Delta_{m_0}^\Omega \rightarrow 0$ smoothly.

both the sleptons and the neutralino are going to be primarily dependent upon $m_{1/2}$. Therefore the low energy phenomenology will be dominated by $m_{1/2}$ so neither t-channel slepton exchange or coannihilation should depend strongly on m_0 when m_0 is small.

This particular combination of channels smears out critical dependence on the soft parameters. Moreover, both channels will naturally occur in any model with light m_0 and reasonably light $m_{1/2}$. However light selectrons and smuons also enhance δa_μ and, as a result, point S2 slightly exceeds the 2σ bound on δa_μ[4].

Having access to $m_0 = 0$ also permits a solution to the SUSY flavour changing neutral current (FCNC) problem, at least for the first two generations, where it is most severe. Being zero at high energies, non-zero elements of the low energy upper block of the squark and slepton mass matrices proportional to the unit matrix are generated via gaugino running effects, giving a universal form involving the first two families, greatly suppressing the most severe FCNCs. This mechanism is analogous to "gaugino mediated SUSY breaking" [104], [105] but applies here to only the first two families. It was first studied in the framework of a particular brane setup in [106] where it was referred to as "brane mediated SUSY breaking".

As in Fig. 3.1, the electroweak tuning is primarily dependent upon variations in $m_{1/2}$ through the contributions of M_3 to the running of the Higgs masses. We have slightly larger values of Δ^{EW} throughout because we have set $m_{0,3} = 1$ TeV.

Having considered the behaviour of a model with $m_{0,3} = 1$ TeV, we now

---

[4]As mentioned earlier this can be avoided if we allow a relative sign between M_1 and M_2.
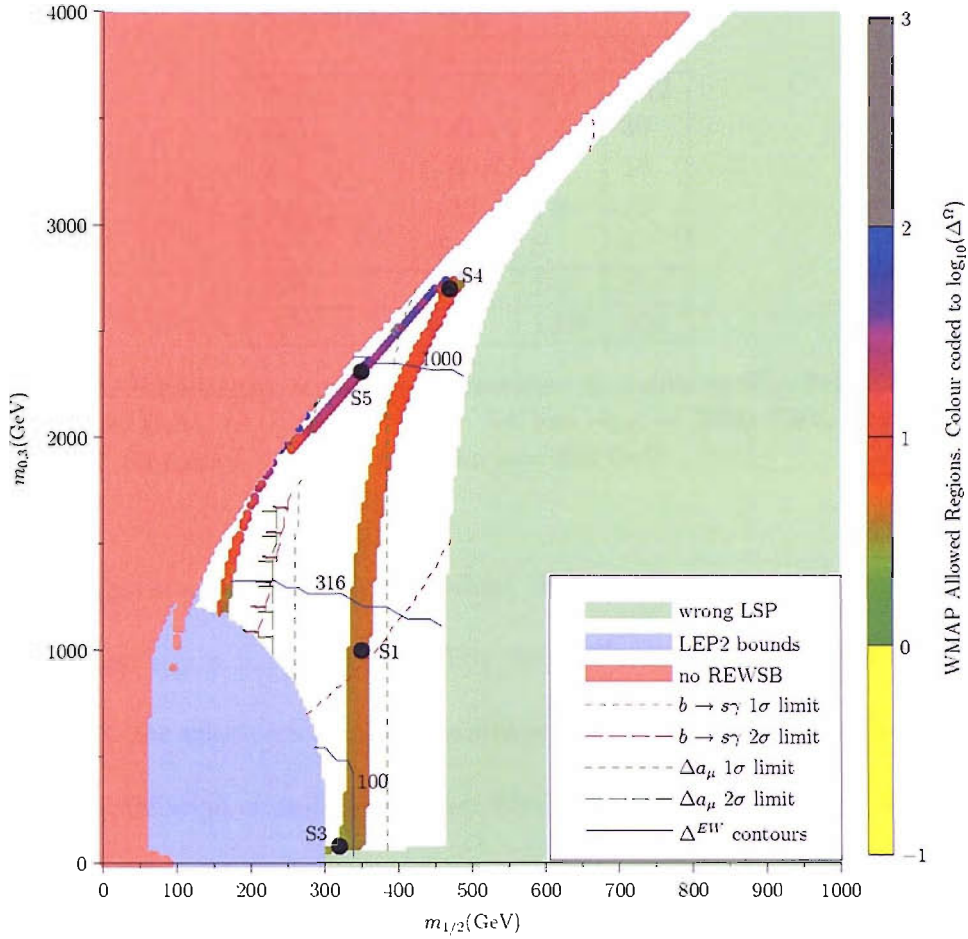
Figure 3.4: The $(m_{1/2}, m_{0,3})$ plane for non-universal sfermion masses with $m_0 = 50$ GeV, $A_0 = 0$, $\tan\beta = 10$.

go on to consider the case of general $m_{0,3}$ in Fig. 3.4. We fix $m_0 = 50$ GeV and allow $m_{0,3}$ to vary from 1 to 4 TeV. For the majority of the plot, the light shaded (green) region represents the region ruled out due to a smuon or selectron LSP. The dark matter strip that runs parallel to it is due to coannihilation with smuons and selectrons, as exemplified by point S1 studied previously in Fig. 3.4.

As we mentioned earlier, if we increase $m_{0,3}$ enough we lower μ^2 to the point where it becomes negative and REWSB fails. As we approach the region in which REWSB fails, $|\mu|$ decreases and therefore we steadily increase

Parameter	Value		
	S3	S4	S5
$\Delta^{\Omega}_{m_0}$	1.5	0.67	0.12
$\Delta^{\Omega}_{m_{0,3}}$	0.41	2.4	30
$\Delta^{\Omega}_{m_{1/2}}$	2.4	2.8	18
$\Delta^{\Omega}_{\tan\beta}$	0.23	1.0	12
$\Delta^{\Omega}_{A_0}$	0	0	0
Δ^{Ω}	2.4	2.8	30
Δ^{EW}	91	1300	950

Table 3.4: Fine-tuning sensitivity parameters at points in Fig. 3.4. S3 has $m_{0,3} = 80$ GeV, $m_{1/2} = 320$ GeV. S4 has $m_{0,3} = 2700$ GeV, $m_{1/2} = 470$ GeV. S5 has $m_{0,3} = 2308$ GeV, $m_{1/2} = 350$ GeV

the higgsino component of the neutralino. This results in an analogue of the Focus Point region in the CMSSM. The main difference here is that as m_0 is still small, the selectrons and smuons still provide a substantial contribution to the annihilation cross-section. Therefore point S5 is not solely due to the LSP being bino/higgsino as is the case for the focus point in the CMSSM.

The last band in Fig. 3.4 that agrees with $\Omega_{CDM}h^2$ is at low $m_{1/2} \approx$ 160 GeV and $m_{0,3} \approx 1.2$ to 2 TeV. In this region the selectron and smuons are light enough to mediate t-channel sfermion exchange. However this region is ruled out at 2σ by $BR(b \rightarrow s\gamma)$ and δa_μ so we do not study it further here.

To study the naturalness of the dark matter regions in more detail, we take the points S3-S5 as shown in Fig. 3.4 and Table 3.4. Point S1 also shown in Fig. 3.4 was considered previously. This allows a comparison of the Focus Point region with its well-tempered neutralino in point S5 to the smuon/selectron coannihilation region of point S1. We also take points S3 and S4 where these regions meet. Having found a hint of natural dark matter in point S2 in which we had more than one annihilation channel at

work, S3 and S4 allow us to study tuning in regions that exhibit different combinations of annihilation channels.

Point S3 lies on the point at which selectrons, smuons and staus all contribute to annihilation rates equally. We also have a 47% contribution from t-channel slepton exchange. Because the stau coannihilation depends almost solely on $m_{0,3}$ and the selectron and smuon coannihilation depends on m_0, the sensitivity to either of these parameters is reduced. In addition, if we increase either $m_{0,3}$ or m_0 we are increasing the mass of either the staus or the smuons and selectrons, which always leaves at least one light slepton to mediate t-channel slepton exchange. As a result S3 has a lower fine-tuning than either primarily stau coannihilation (as with C1) or selectron and smuon coannihilation (as with S1).

Point S4 also lies on an intersection in annihilation channels. This time it is the intersection of the bino/higgsino well-tempered strip and the selectron, smuon coannihilation strip. The quoted Δ_a^Ω values should therefore be compared to S5 and S1 respectively. The selectron, smuon coannihilation strip is primarily sensitive to m_0 and $m_{1/2}$ through their effect on the sparticle masses. In contrast the bino/higgsino strip, represented by point S5, is highly sensitive to $m_{0,3}$ and $m_{1/2}$ through their effects on the low energy values of μ and M_1. Once again by combining channels we reduce our dependence on any one parameter. In this case we manage to achieve a low degree of fine-tuning while also having a well-tempered neutralino. However with $m_{0,3} = 2700$ GeV and $\Delta^{EW} \approx 1000$ we are in peril of reintroducing fine-tuning complaints in the electroweak sector.

Finally, note that in both the CMSSM and this model with non-universal

third family scalars, the tuning of the well-tempered bino/higgsino is larger than the tuning required for the slepton coannihilation regions. In [49] the well-tempered neutralino is suggested as some of the most plausible options for dark matter within a general SUSY theory. However here we have shown that, at least in certain models, such well-tempered regions are more fine-tuned with respect to soft parameters than the coannihilation regions rejected in [49].

In summary, allowing $m_{0,3}$ to vary independently of the first and second family masses, and in particular to become independently large, we find the following features:

- Access to $m_0 = 0$, and hence a solution to the SUSY FCNC problem for the 1st and 2nd families, with lower Δ^Ω than in the CMSSM at the expense of large SUSY contributions to $(g-2)_\mu$.

- Access to the well tempered bino/higgsino region which agrees with δa_μ at 1σ, but this well tempered point involves 3% dark matter fine-tuning.

- We can access certain regions such as S3, S4 in which we have a number of different annihilation channels at work and these lead to lower values of Δ^Ω and more natural solutions to the dark matter problem.

- Large $m_{0,3}$ implies a high degree of fine-tuning for REWSB, as expected, so a fully natural model is not possible in this case.

3.4 Non-universal Gaugino Masses

As with high 3rd family masses, there are good reasons for allowing the soft gaugino masses to be non-universal. From a theoretical point of view, non-universal gaugino masses are interesting as they naturally occur in SUGRA models with non-minimal gauge kinetic terms, which arise from many string constructions (see e.g. [101], [103]). They also naturally occur in gauge mediated SUSY breaking [107] and anomaly mediated SUSY breaking [108].

From a phenomenological point of view, non-universal gauginos are extremely useful. By allowing M_1 and M_2 to take different values, we can directly change the bino/wino balance in the neutralinos allowing access to wino and well-tempered bino/wino LSP states. M_3 allows us to vary the squark sector independently of the sleptons through its effects on the running masses. μ also depends on M_3 as shown in Eq. 2.5. Therefore by allowing our gaugino masses to be non-universal we gain control over M_1, M_2 and to a lesser extent μ.

To be precise we consider the parameters:

$$a_{CMSSM+M_i} \in \{m_0, \ M_1, \ M_2, \ M_3, \ \tan\beta, \ A_0\} \tag{3.3}$$

and the sign of μ.

In Fig. 3.5 we keep $M_2 = M_3 = 350$ GeV, $\tan\beta = 10$ and $A_0 = 0$, but allow m_0 and M_1 to vary. As we have a unified mass for the sfermions, the light shaded (green) region at low m_0 is excluded by a stau LSP. The LEP2 bound at $M_1 \approx 100$ GeV is due to the neutralino becoming too light. The LEP bound for low m_0 and low $m_{1/2}$ is a bound on the mass of the $\tilde{\tau}$. With
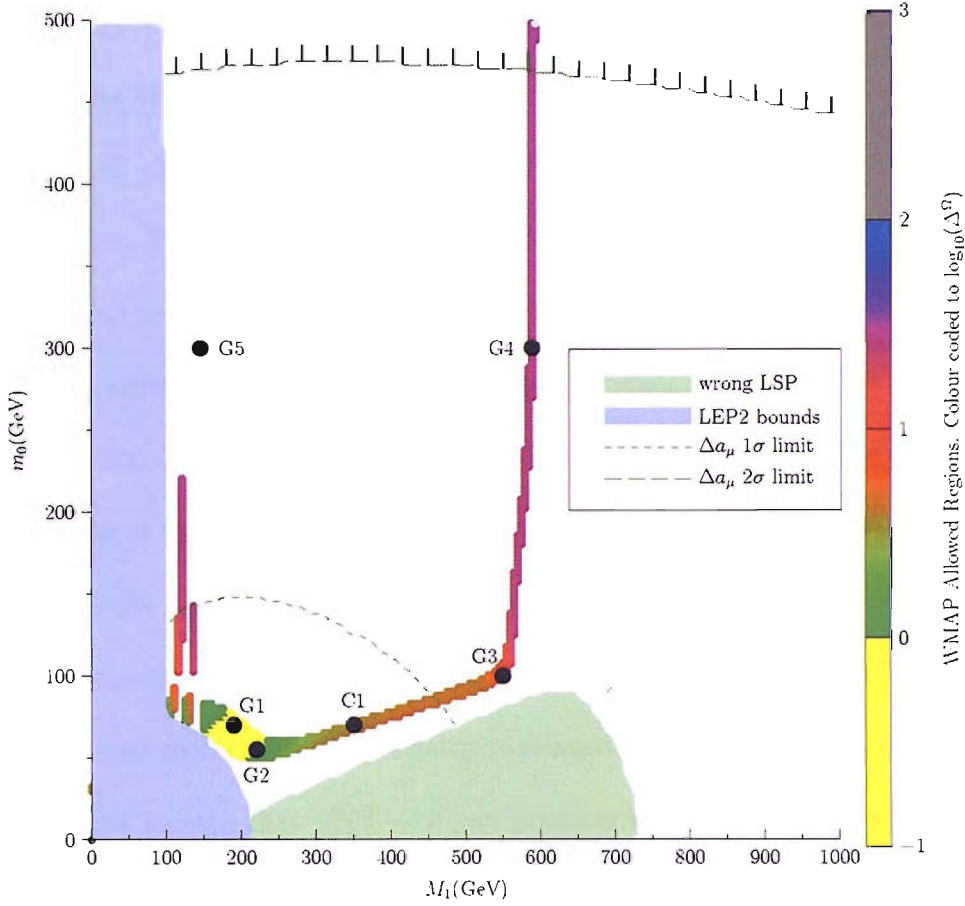
Figure 3.5: The (M_1, m_0) plane for non-universal gauginos with $M_2 = M_3 = 350$ GeV, $A_0 = 0$, $\tan\beta = 10$.

$M_3 = 350$ GeV the Higgs mass is above the LEP limit across the whole scan[5].

The most striking feature of Fig. 3.5 is the multitude of different regions that satisfy $\Omega_{CDM}h^2$. There is the coannihilation strip for 300 GeV $< M_1 <$ 500 GeV containing the point C1 at $M_1 = 350$ GeV which coincides with the CMSSM point considered previously, with bino dark matter and a stau coannihilation channel. In addition there is the well tempered bino/wino LSP at $M_1 \approx 600$ GeV containing the point G4. When $M_1 = 700$ GeV, $M_1(m_{GUT}) = 2M_2(m_{GUT})$ and so, through our rule of thumb $M_1(m_{SUSY}) \approx$

---

[5]In parallel to Fig. 3.1, we can take M_3 down to 300 GeV without violating the LEP2 bound on the lightest Higgs mass. This also results in the lowest value of μ.

$M_2(m_{SUSY})$. As we approach $M_1 = 700$ GeV, we steadily increase the wino proportion of the LSP. When $M_1 \approx 600$ GeV, there is just enough wino in the LSP to satisfy dark matter constraints, the so called well-tempered bino/wino. The two vertical lines at $M_1 = 130$ GeV and $M_1 = 140$ GeV correspond to the points at which $2m_{\tilde{\chi}_1^0} = m_Z, m_{h^0}$ respectively and we have resonant s-channel annihilation. The Higgs resonance stretches all the way to $m_0 > 500$ GeV but the resolution of the scan is such that it can't resolve the width of the resulting dark matter lines. However the most interesting region is the bulk region plotted in yellow containing the point G1 which arises from the very low values of 150 GeV $< M_1 < 250$ GeV, which are allowed now that gaugino universality is relaxed, which allows the sleptons to be light enough that $\tilde{\chi}_1^0 \tilde{\chi}_1^0 \rightarrow l\bar{l}$ can produce the observed relic density on its own. The colour coding allows us to gauge the total tuning of these different regions. The most natural region is the bulk region with $\Delta^\Omega < 1$. This is followed by the coannihilation region with a tuning comparable to that of the CMSSM. The well-tempered bino/wino region exhibits a tuning $\Delta^\Omega \approx 30$ throughout, comparable to that of the lower end of the Z and Higgs resonance. The only region we can't see in detail here is the Higgs resonance for large m_0. To study this region, and understand the sources of tuning in the other regions in more detail, we take the points C1, G4, G5, and G1 in each region and for points G2, G3 where two annihilation processes contribute equally. The results are presented in Table 3.5[6].

It is striking that two of the points in Table 3.5, namely G1 and G2, have

---

[6]Though point C1 has the same values for the soft parameters as in Table 3.1, here we allow the gaugino masses to vary independently. Therefore the tuning is calculated using the parameters $a_{CMSSM+M_i}$ rather than a_{CMSSM} and so C1 here does not represent the CMSSM. This is the point at which a model with non-universal gauginos makes contact with the CMSSM.

Parameter	Value					
	G1	G2	G3	G4	G5	C1
$\Delta^\Omega_{m_0}$	0.83	0.97	3.0	0.65	5.7	3.5
$\Delta^\Omega_{M_1}$	0.80	0.51	8.0	28	1100	2.7
$\Delta^\Omega_{M_2}$	0.23	0.36	3.4	26	4.8	0.64
$\Delta^\Omega_{M_3}$	0.24	0.44	2.3	5.8	91	1.4
$\Delta^\Omega_{\tan\beta}$	0.20	0.50	1.2	0.20	4.1	1.4
$\Delta^\Omega_{A_0}$	0	0	0	0	0	0
Δ^Ω	0.83	0.97	8.0	28	1100	3.5
Δ^{EW}	110	110	111	111	110	160

Table 3.5: Fine-tuning sensitivity parameters for points taken from Fig. 3.5 with $M_2 = M_3 = 350$ GeV, $A_0 = 0$, $\tan\beta = 10$. G1 has $m_0 = 70$ GeV, $M_1 = 190$ GeV. G2 has $m_0 = 55$ GeV, $M_1 = 220$ GeV. G3 has $m_0 = 100$ GeV, $M_1 = 550$ GeV. G4 has $m_0 = 300$ GeV, $M_1 = 590$ GeV. G5 has $m_0 = 300$ GeV, $M_1 = 146.15$ GeV.

a dark matter sensitivity parameter below unity, corresponding to "supernatural" dark matter (i.e. no fine-tuning required at all to achieve successful dark matter). Point G1 lies in the middle of the bulk region in which annihilation proceeds through t-channel sfermion exchange. As this process depends directly upon the mass of the sleptons that are exchanged, it is unsurprising that the majority of the dependence is on m_0 and M_1. However it is clear that the dependence is significantly lower than in the CMSSM. This is because the cross-section for $\tilde{\chi}^0_1 \tilde{\chi}^0_1 \rightarrow l\bar{l}$ varies slowly with $m_{\tilde{l}}$ in comparison to coannihilation processes that depend upon precise mass differences between particles. In the neighbouring point G2 both coannihilation and t-channel slepton exchange are competitive. Here the sensitivity to m_0 increases slightly (due to the coannihilation channel) but the sensitivity to M_1 decreases significantly for the same reasons as point S2 in the the case of non-universal scalars.

The advantage of combining annihilation channels is shown by comparing the point G3 and G4. G4 has been chosen to lie on the well-tempered

bino/wino line. As with the bino/higgsino region, as we move away from a pure bino LSP the annihilation and coannihilation cross-section rise dramatically, leading to a sharp drop in $\Omega_{CDM}h^2$. Here, as before, such well-tempered regions exhibit Δ_a^Ω values of ≈ 30, values well in excess of slepton coannihilation regions with low m_0. G3 lies in the region in which we have both coannihilation with staus and a significant wino component in the neutralino. This results in a region that is both well-tempered and exhibits lower values of Δ^Ω.

Finally we briefly consider the naturalness of s-channel annihilation regions. As these are sharply peaked whenever $2m_{\tilde{\chi}_1^0} = m_{Z,h}$, we expect there to be a substantial dependence on any parameter that directly affect the neutralino mass. As point G5 shows, this dependence is extreme. If we were to find ourselves to be living in this part of parameter space we would have to look for some further theoretical justification. A Δ^Ω value greater than 1000 cannot be considered natural.

Note that there are no contours of electroweak tuning in Fig. 3.5. This is because neither M_1 or m_0 greatly affect Δ^{EW} in this region. We find $\Delta^{EW} \approx 110$ across the parameter space displayed.

Once again, these studies of naturalness can only be considered in the case of a given model. In this model with non-universal gaugino masses we have showed that the well-tempered region is considerably more fine-tuned than t-channel slepton exchange or even slepton coannihilation regions. However the tuning in the well-tempered region pales in significance when we consider the amount of tuning required to land us on the edge of the light Higgs annihilation channel.

However the fate of the bino/wino dark matter strip could be considered to be better than that of the bino/higgsino neutralino. The reason for this is that the bino/higgsino region depends precisely on M_1/μ whereas the bino/wino region depends on M_1/M_2. In the latter case to guarantee that we land in the bino/wino well-tempered strip it is only necessary to have a model that requires $M_1(m_{GUT}) \approx 1.7 M_2(m_{GUT})$. In such a model the large dependence on M_1 and M_2 in G4 would disappear and a bino/wino neutralino could provide a dark matter candidate. However there is no magic ratio at the high scale that will obviously reproduce the relevant bino/higgsino ratio at the low scale. To see this it is enough to consider the dependence of μ on the soft parameters. To guarantee a given ratio between μ and M_1 it would be necessary to have a model that relates all the parameters in Eq. 2.5 in just the right way.

Leaving aside such questions of models of SUSY breaking, the most vivid results of allowing non-universal gaugino masses are:

- The bulk region involving bino annihilation via t-channel slepton exchange can be accessed, since low M_1 is possible leading to light sleptons. This allows "supernatural" dark matter exemplified by the points G1 and G2.

- Low m_0 and M_1 also allow us to fit δa_μ at 1σ.

- A well tempered bino/wino neutralino scenario is possible, for example point G4, but this requires 3% fine tuning similar to the well tempered bino/higgsino of point S5.

- Combinations of annihilation channels on the edge of such regions such

as point G3 lead to lower fine-tuning.

- To achieve the observed value of $\Omega_{CDM} h^2$ through resonant annihilation such as at point G5 through a light Higgs requires extremely large fine-tuning for large m_0.

3.5 Non-universal Gauginos and Third Family Scalar Masses

Having considered non-universal gauginos and the situation in which we allow the third family sfermion and Higgs masses to be large, we now consider the effect of including both of these extensions to the CMSSM at once. This results in a model with 7 free soft parameters and a sign:

$$a_{non-univ} \in \{m_0, \ m_{0,3}, \ M_1, \ M_2, \ M_3, \ \tan\beta, \ A_0\} \qquad (3.4)$$

and the sign of μ.

It is clear from the two previous sections that the mechanics of dark matter annihilation can be sensitive to many of these parameters. To get a true handle of the sensitivity of these regions to the soft parameters, we should allow all of the different parameters to vary at once. In addition, by allowing all parameters to vary simultaneously, we open up the possibility of accessing new regions in which we satisfy dark matter that have even lower Δ^Ω values than we have found so far. However having large $m_{0,3}$ clearly means that REWSB will be fine-tuned. Nevertheless a new result of having both types of non-universality together is that we can access a maximally

Figure 3.6: The (M_1, m_0) plane for non-universal gaugino and sfermion masses with $M_2 = M_3 = 350$ GeV, $m_{0,3} = 1000$ GeV, $A_0 = 0$, $\tan \beta = 10$.

tempered bino/wino/higgsino neutralino.

In Fig. 3.6 we take $M_{2,3} = 350$ GeV, $\tan \beta = 10$ and $A_0 = 0$ as in Fig. 3.5 but set $m_{0,3} = 1$ TeV. The introduction of a high 3rd family mass has had the same general effects as in Fig. 3.3. The light shaded (green) excluded region is now due to smuon and selectron LSPs rather than staus which once again allows access to $m_0 = 0$. The lack of a light stau has also reduced the $\tilde{\chi}_1^0 \tilde{\chi}_1^0 \rightarrow l\bar{l}$ cross-section across the entire parameter space. Thus we need lower values of m_0 and M_1, and thus lighter smuons and selectrons, to access a region in which t-channel slepton exchange alone can satisfy dark matter constraints. As a result much of the bulk region is once again ruled out by

Parameter	Value	
	SG1	SG2
$\Delta^{\Omega}_{m_0}$	0.35	1.6
$\Delta^{\Omega}_{m_{0,3}}$	0.10	0.15
$\Delta^{\Omega}_{M_1}$	0.04	8.9
$\Delta^{\Omega}_{M_2}$	0.028	7.7
$\Delta^{\Omega}_{M_3}$	0.036	0.89
$\Delta^{\Omega}_{\tan\beta}$	0.014	0.056
$\Delta^{\Omega}_{A_0}$	0	0
Δ^{Ω}	0.35	8.9
Δ^{EW}	240	240

Table 3.6: Fine-tuning sensitivity at points taken from Fig. 3.6 with $M_2 = M_3 = 350$ GeV, $m_{0,3} = 1000$ GeV, $A_0 = 0$, $\tan\beta = 10$. SG1 has $m_0 = 25$ GeV, $M_1 = 205$ GeV. SG2 has $m_0 = 85$ GeV, $M_1 = 585$ GeV.

LEP particle searches.

Apart from these details, the general features remain the same as in Fig. 3.5. We cannot access $M_1 < 100$ GeV due to LEP2 bounds on the lightest neutralino. At low M_1 we have thin lines corresponding to the light Higgs and Z resonances. The line is broken due to the resolution of the grid used to scan the space - a testament to extreme sensitivity of these regions to M_1. At low M_1 and low m_0 we have dominant contributions from t-channel slepton exchange. For moderate values of M_1 we have coannihilation with selectrons and smuons and when $M_1 \approx 600$ GeV we get bino/wino dark matter. Once again Δ^{EW} varies slowly across the parameter space so there are no contours displayed. In general $\Delta^{EW} \approx 250$ throughout.

In our hunt for natural dark matter, we consider points in which many different annihilation channels contribute. We take point SG1 at the intersection of the selectron, smuon coannihilation region and the t-channel slepton band. Point SG2 is taken in the region where bino/wino dark matter also coannihilates with selectrons and smuons. SG1 once again shows
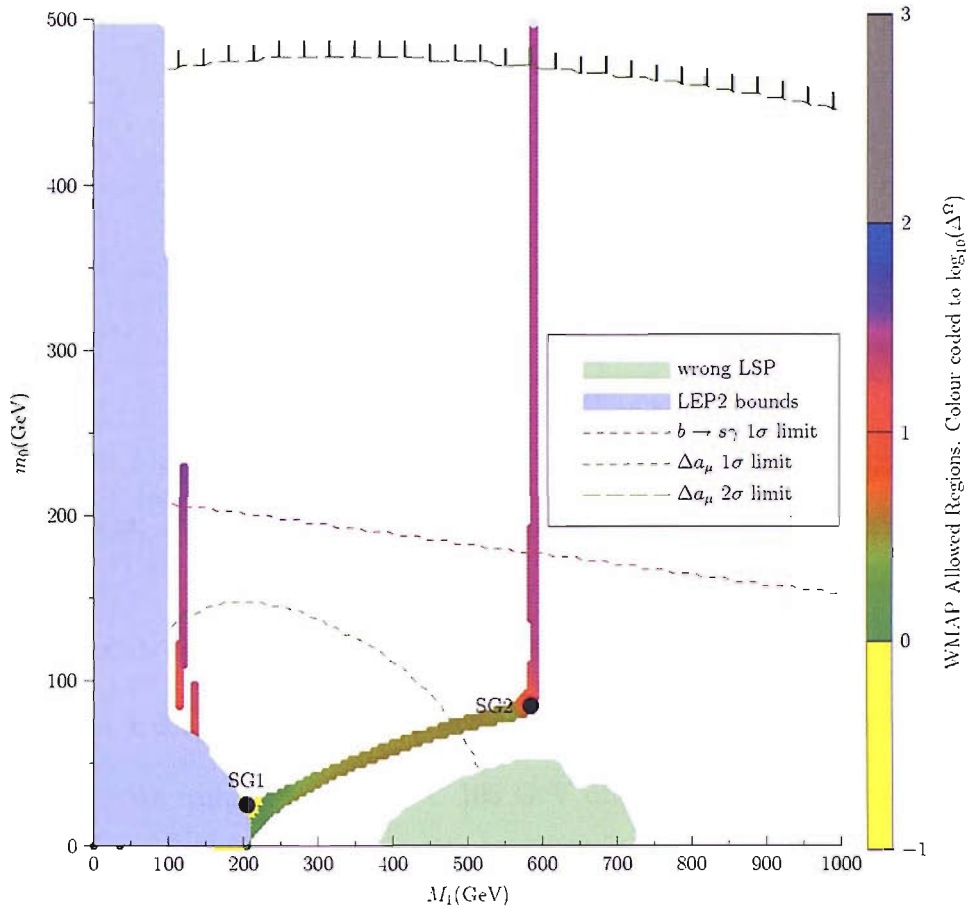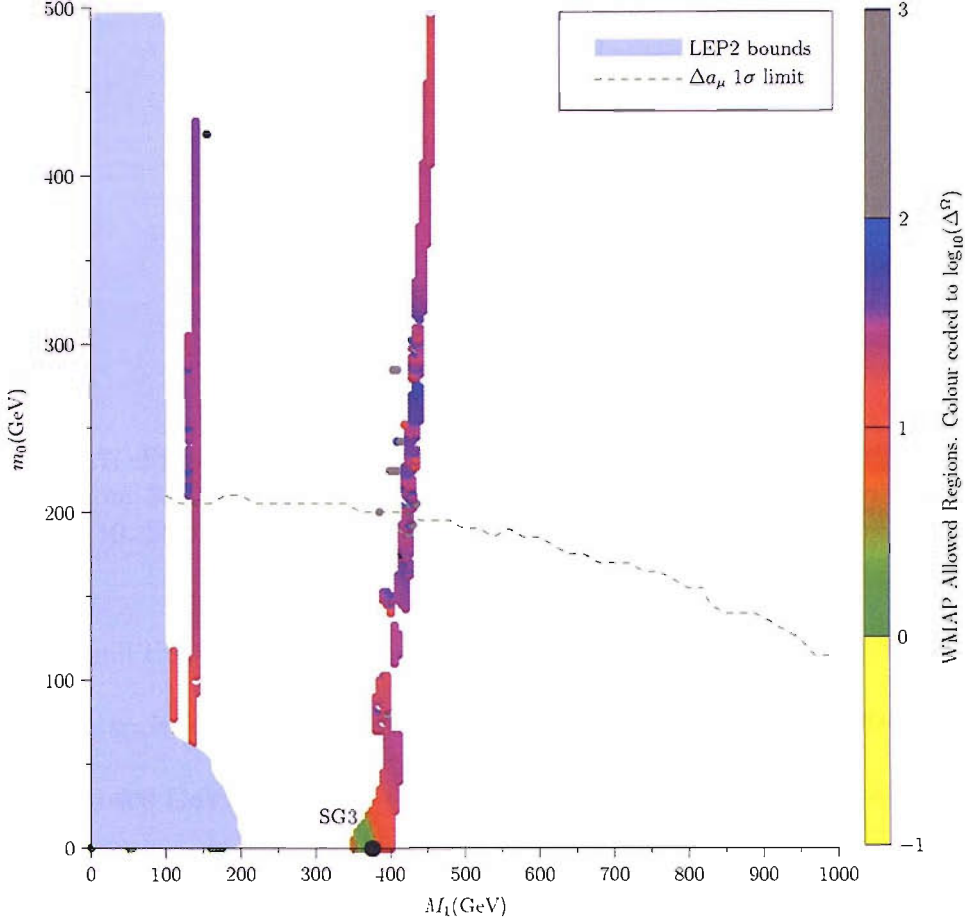
Figure 3.7: The (M_1, m_0) plane for non-universal gaugino and sfermion masses with $M_2 = M_3 = 350$ GeV, $m_{0,3} = 2250$ GeV, $A_0 = 0$, $\tan \beta = 10$.

that regions with low m_0 and M_1 exhibit small fine-tuning. Here the dark matter band appears at lower m_0 and lower M_1 in Fig. 3.6 than in Fig. 3.3. The result, through a combination of the effects discussed earlier, is an order of magnitude decrease in the sensitivity of this region in comparison to the most favourable region of the CMSSM. Point SG1 again provides a supernatural solution to dark matter[7].

Fig. 3.7 contains the maximally tempered neutralino at point SG3. With $M_2 = M_3 = 350$ GeV, we take $m_{0,3} = 2250$ GeV to achieve small enough μ.

---

[7]In this region we also agree with δa_μ in contrast to $m_0 = 0$ point in section 3.3. This is because $M_2 = 350$ GeV which avoids charginos that are too light and keeps δa_μ at the correct level.

Parameter	Value
	SG3
$\Delta^{\Omega}_{m_0}$	0.064
$\Delta^{\Omega}_{m_{0,3}}$	3.8
$\Delta^{\Omega}_{M_1}$	2.0
$\Delta^{\Omega}_{M_2}$	0.52
$\Delta^{\Omega}_{M_3}$	3.7
$\Delta^{\Omega}_{\tan\beta}$	1.0
$\Delta^{\Omega}_{A_0}$	0.015
Δ^{Ω}	3.8
Δ^{EW}	240

Table 3.7: Fine-tuning sensitivity at the maximally tempered point SG3 taken from 3.7 with $M_2 = M_3 = 350$ GeV, $m_{0,3} = 1000$ GeV, $A_0 = 0$, $\tan\beta = 10$. SG3 has $m_0 = 0$ GeV, $M_1 = 375$ GeV.

Once again this raises questions of fine-tuning in the electroweak sector but we leave such concerns aside for the time being. The region of interest lies at $M_1 \approx 400$ GeV. This line is rather disjointed as SOFTSUSY has difficulty calculating the spectrum in regions where μ is small. In this band the neutralino has significant portions of bino, wino and higgsino. This results in all of the neutralinos and charginos being close in mass and so results in a large number of annihilation and coannihilation processes in the early universe. In Table 3.7 we study point SG3 at $m_0 = 0$ GeV, $M_1 = 375$ GeV.

The maximally-tempered neutralino at point SG3 exhibits dramatically lower fine-tuning than either the bino/wino (G4) or bino/higgsino (S5) regions. By allowing the neutralino to be maximally mixed, we decrease the degree of tuning required to satisfy dark matter by an order of magnitude with respect to merely well-tempered cases. Note that this is particular to low m_0, as we move to larger m_0 we return to degrees of fine-tuning of the same order as the bino/wino region ion Fig. 3.5 or the bino/higgsino region of Fig. 3.3.

As with the case of non-universal gaugino masses alone, or just a high third family scalar mass, we find that there are certain points in parameter spaces where different annihilation channels contribute with roughly equal strength. These regions are characterised by a sharp drop in the fine-tuning of soft parameters required to reproduce $\Omega_{CDM}h^2$. By allowing both non-universal soft gaugino masses and non-universal 3rd family scalar masses we find that not only are these regions stable against further non-universalities, but also that we can access values of Δ_a^Ω an order of magnitude smaller than in the CMSSM.

3.6   Conclusions

We have explored regions of MSSM parameter space with non-universal gaugino and third family scalar masses in which neutralino dark matter may be implemented naturally. In order to examine the relative naturalness of different regions we employed a dark matter fine-tuning sensitivity parameter, which we use in conjunction with the similarly defined sensitivity parameter used for EWSB. Employing these quantitative measures of fine-tuning we find that $\tilde{\tau}$-coannihilation channel in the CMSSM may involve as little as 25% tuning, due to renormalisation group (RG) running effects.

For non-universal third family scalar masses in which $m_{0,3}$ is allowed to become independently large, we find that we have access to $m_0 = 0$, and hence a solution to the SUSY FCNC problem, with lower Δ_a^Ω than in the CMSSM at the expense of large SUSY contributions to $(g-2)_\mu$. Alternatively, with non-universal third family scalar masses, we can also access the well tempered bino/higgsino region which agrees with δa_μ at 1σ,

but this well tempered point involves 3% dark matter fine-tuning. We can access certain regions in which we have a number of different annihilation channels at work and these lead to lower values of dark matter fine tuning. However large $m_{0,3}$ implies a high degree of fine tuning for REWSB, as expected, so a fully natural model is not possible in this case.

With non-universal gauginos the bulk region involving bino annihilation via t-channel slepton exchange can be accessed, since low M_1 is possible leading to light sleptons. This allows supernatural dark matter (for example at points G1, G2) with minimal EWSB fine-tuning, depending on how low M_3 is taken consistently with the LEP Higgs bound. Low m_0 and M_1 also allow us to fit δa_μ at 1σ. Alternatively, with non-universal gauginos, the well tempered bino/wino neutralino scenario is also possible, but again requires 3% fine-tuning as in the case of the well tempered bino/higgsino. However combinations of annihilation channels on the edge of such regions such as point G3 lead to lower fine-tuning. To achieve the observed value of $\Omega_{CDM}h^2$ through resonant annihilation such as at point G5 through a light Higgs requires extremely large fine-tuning.

With both non-universal third family masses and non-universal gauginos, a new feature appears: the maximally-tempered bino/wino/higgsino neutralino where the LSP consists of roughly equal amounts of bino, wino and higgsino (for example point SG3). Although the maximally tempered neutralino has quite low fine-tuning for low m_0, the large value of $m_{0,3}$ inherent in this approach always means that EWSB will be very fine-tuned.

In general, having non-universal third family and gaugino masses opens up new regions of MSSM parameter space in which dark matter may be im-

Region	Typical Δ^{Ω}
Well-tempered bino/wino	~ 30
Well-tempered bino/higgsino	$30 - 60$
Maximally-tempered bino/wino/higgsino	$4 - 60$
Bulk region (t-channel $\tilde{f}$ exchange)	< 1
slepton coannihilation (low M_1, m_0)	$3 - 15$
slepton coannihilation (large M_1, m_0)	~ 50
Z-resonant annihilation	~ 10
h^0-resonant annihilation	$10 - 1000$
A^0-resonant annihilation	$80 - 300$

Table 3.8: The general tunings found for the different neutralino annihilation channels within the MSSM.

plemented naturally. In particular allowing non-universal gauginos opens up the bulk region that allows bino annihilation via t-channel slepton exchange, leading to "supernatural" dark matter corresponding to no fine-tuning at all with respect to dark matter. By contrast we find that the recently proposed well-tempered neutralino regions involve substantial fine-tuning of MSSM parameters in order to satisfy the dark matter constraints, although the fine-tuning may be ameliorated if several annihilation channels act simultaneously. Although we have identified regions of "supernatural" dark matter in which there is no fine-tuning to achieve successful dark matter, the usual MSSM fine-tuning to achieve EWSB always remains.

Within these patterns of MSSM parameters, we have found that the fine-tuning of dark matter primarily depends on the channel involved, rather than the magnitude of the parameters. This is in contrast to Δ^{EW} in which the tuning is almost always directly proportional to the magnitude of the input parameters. The exception is that for very low m_0, the slepton coannihilation channels become significantly more natural, due to the emergence of a correspondence between $m_{\tilde{\chi}_1^0}$ and $m_{\tilde{l}}$ for bino dark matter. Using the

general results of these scans we can categorise the regions in Table 2.1. We

present these results in Table 3.8.

Chapter 4

Dark Matter from a String

Model

4.1 Introduction

Though such a non-universal MSSM provides a general framework for study-
ing natural dark matter regions, it may not be realistic to regard the mass
terms in the soft SUSY breaking Lagrangian as fundamental inputs since
the soft masses merely parameterise the unknown physics of SUSY break-
ing. In any realistic model of SUSY breaking the soft breaking terms in
the Lagrangian should be generated dynamically. It is the parameters that
define the mechanism of SUSY breaking that should be taken as the funda-
mental inputs. As we have mentioned, this is a problem as the true origin of
SUSY breaking is unknown. In string theory the unknown SUSY breaking
dynamics may be manifested as F-term vacuum expectation values (VEVs)
of hidden sector moduli fields appearing in the theory. Therefore the val-
ues of these F-terms may be regarded as being more fundamental input

parameters than the soft mass terms of the MSSM. Although the values of the F-terms are unknown, they may be parameterised in terms of so called Goldstino angles which describe the relative magnitude of the F-terms associated with the different moduli fields, as was done for example in type I string theories in [110]. A more reliable estimate of fine-tuning sensitivity should therefore result from using such Goldstino angles, together with the gravitino mass $m_{3/2}$, and some other undetermined electroweak parameters such as the μ parameter and the ratio of Higgs vacuum expectation values $\tan\beta$ as inputs. Therefore fine-tuning should more properly be calculated with respect to these inputs. It is possible that fine-tuning when calculated in terms of such inputs could yield very different results.

In this chapter we extend the previous analysis of the non-universal MSSM to a semi-realistic type I string theory model of the form originally proposed in [102] and phenomenologically analysed in [103] (see also [101], [102], [113]). Using such a string model we can address two questions. Firstly, how does the fine-tuning of a particular dark matter region in the non-universal MSSM compare to a similar region in the string model? Secondly, do some regions of SUSY breaking parameter space in the string model more naturally explain dark matter and electroweak symmetry breaking than others? The model we use to address these points is the type I string inspired model in [102] in which we can obtain SUSY breaking from any of twisted (Y) moduli, untwisted (T) moduli or the dilaton (S). The phenomenology of SUSY breaking in this model has been studied in [103]. Neutralino dark matter has not so far been studied in this string model, or any string model involving twisted moduli, although it has been studied in other

string models [82], [114]-[116]. However in none of these cases has the question of the naturalness of the predicted dark matter density been addressed and, as discussed, one of the main motivations for the present study is to explore how such results obtained in the non-universal MSSM translate to the case of a "more fundamental" string theory where such non-universality arises automatically. The main motivation for revisiting the model in [102], [103] is that it exhibits non-universal gaugino masses and non-universality between the 3rd family and the 1st and 2nd family squarks and sleptons, similar to the structures analysed in Chapter 3. This allows a direct comparison between the non-universal MSSM and a corresponding type I string model, since the latter shares many of the dark matter regions previously considered. We will find that dark matter constraints close off much of the parameter space of the type I string model, for example the benchmark points suggested in [103] are either ruled out ($\Omega_{CDM}h^2 \gg \Omega_{CDM}^{WMAP}h^2$) or disfavoured ($\Omega_{CDM}h^2 \ll \Omega_{CDM}^{WMAP}h^2$). However we will find new successful regions of dark matter in the string model, which mirror some of those found in the non-universal MSSM, some of which exhibit degrees of fine-tuning in agreement with previous results [69], and some which vary significantly.

The layout of this chapter is as follows. In section 4.2 we summarise the string model of [103] and analyse the structures of the GUT scale soft masses specifically with respect to their implications for dark matter. In section 4.3 we use numerical scans to study the fine-tuning of dark matter within such a model. In section 4.4 we present our conclusions from the string model.
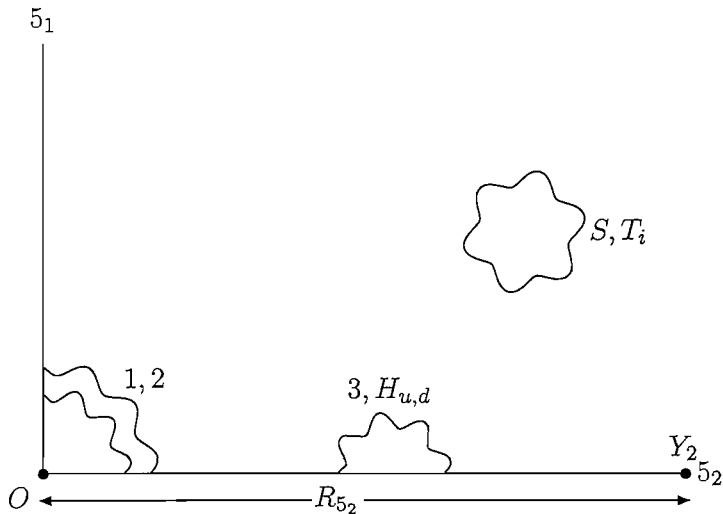
Figure 4.1: The brane set-up from [102], [103].

4.2 The Model

4.2.1 The brane set-up

Type I string theory not only contains open and closed strings, but also contains extended objects to which the ends of opens strings are attached. These are known as Dp-branes where the brane extends in p+1 dimensions. From a model building perspective D-branes are extremely useful. A given stack of D-branes will have a set of open strings confined to move on its surface. By identifying a given field with a given open string, we fix its properties and the number of dimensions in which it can propagate.

We start with the brane set-up shown in Fig. 4.1, originally proposed in [102], [103]. Here we have two perpendicular intersecting stacks of D5 branes 5_1 and 5_2. Each holds a copy of the MSSM gauge group. To maintain gauge coupling unification at the GUT scale we take the limit of single brane dominance $R_{5_2} \gg R_{5_1}$. The twisted moduli Y_2 is trapped at a fixed point in the D5$_2$-brane. The untwisted moduli T_i and the dilaton propagate in the

99
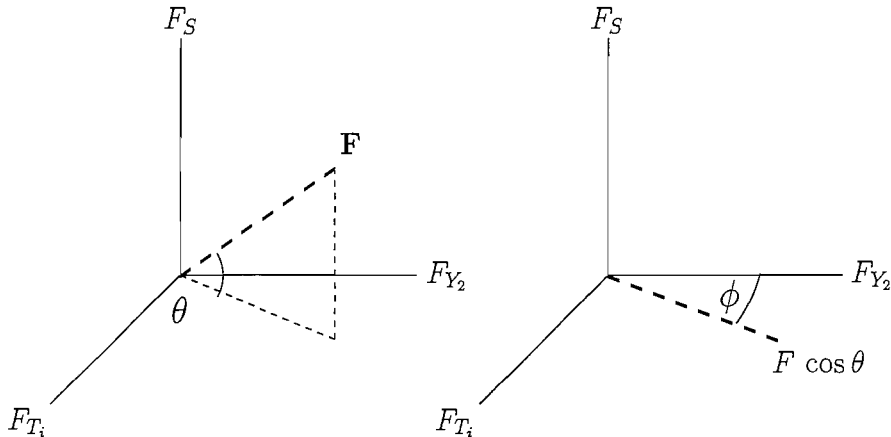
Figure 4.2: The Goldstino angles are defined to parameterise the F-term SUSY breaking coming from the S,T and Y moduli. $(\theta, \phi) = (0, 0)$ corresponds to twisted moduli (Y_2) SUSY breaking. $(\theta, \phi) = (0, \pi/2)$ corresponds to untwisted moduli (T_i) SUSY breaking. $\theta = 0$ corresponds to dilaton (S) SUSY breaking.

10D bulk. We identify the first and second families with open strings with one end on the 5_1 brane and the other on the 5_2 brane. This localises them at the intersection of the branes and effectively sequesters them from the twisted moduli. The third family and the Higgs bosons are identified with strings on the 5_2 brane.

In such a model the SUSY breaking can come from the twisted moduli (Y_2) localised at a fixed point in the 5_2 brane, the untwisted moduli (T_i) in the bulk or the dilaton (S). Each of these forms of SUSY breaking gives rise to distinct GUT scale soft masses and so to distinct low energy phenomena. As the exact form of their contribution to the SUSY breaking F-terms is not known, we use Goldstino angles [110] to parameterise the relevant contributions of each. These angles are defined as shown in Fig. 4.2.

4.2.2 GUT scale soft masses

The model determines the soft masses at the GUT scale to be [102], [103]:

$$
m_{\tilde{Q}}^2, m_{\tilde{L}}^2, m_{\tilde{u}}^2, m_{\tilde{d}}^2, m_{\tilde{e}}^2 \;=\; \begin{pmatrix} m_0^2 & 0 & 0 \\ 0 & m_0^2 & 0 \\ 0 & 0 & m_{0,3}^2 \end{pmatrix}, \tag{4.1}
$$

$$
m_{H_u}^2 = m_{H_d}^2 \;=\; m_H^2, \tag{4.2}
$$

where m_0^2 is defined as:

$$
\begin{aligned}
m_0^2 \;=\; & m_{3/2}^2 \left[1 - \frac{3}{2}\sin^2\theta - \frac{1}{2}\cos^2\theta\,\sin^2\phi \right. \\
& - \left(1 - e^{-(T_2+\bar{T}_2)/4} \right)\cos^2\theta\,\cos^2\phi \\
& - \frac{X}{3}\cos^2\theta\,\sin^2\phi\,\delta_{GS}\left(1 - e^{-(T_2+\bar{T}_2)/4} \right) \\
& + \frac{X^2}{96}\cos^2\theta\,\sin^2\phi\,e^{-(T_2+\bar{T}_2)/4}(T_2+\bar{T}_2)^2 \\
& - \frac{1}{16\sqrt{3}}\cos^2\theta\,\cos\phi\,\sin\phi\,e^{-(T_2+\bar{T}_2)/4}\left\{ 8(T_2+\bar{T}_2) + \delta_{GS}\,X \right\}X \\
& \left. + \; \mathcal{O}\left[\frac{\delta_{GS}\,e^{-(T_2+\overline{T}_2)/4}}{(T_2+\overline{T}_2)} \right] \right], \tag{4.3}
\end{aligned}
$$

with $X = Y_2 + \overline{Y}_2 - \delta_{GS}\ln(T_2 + \overline{T}_2)$, where δ_{GS} is the Green-Schwartz parameter. $m_{0,3}^2$ and m_H^2 are defined as:

$$
m_{0,3}^2 \;=\; m_{3/2}^2 \left(1 - \cos^2\theta\,\sin^2\phi \right), \tag{4.4}
$$

$$
m_H^2 \;=\; m_{3/2}^2 \left(1 - 3\sin^2\theta \right). \tag{4.5}
$$

The soft gaugino masses and trilinears are:

$$
M_\alpha = \frac{\sqrt{3}\, m_{3/2}\, g_\alpha^2}{8\pi} \cos\theta \left[\frac{\sin\phi}{\sqrt{3}} \left\{ T_2 + \bar{T}_2 + \frac{s_\alpha}{4\pi}\delta_{GS} \right\} \right.
$$
$$
\left. - \cos\phi \left\{ \frac{\delta_{GS}}{T_2 + \bar{T}_2} - \frac{s_\alpha}{4\pi} \right\} + \mathcal{O}\left[\left(\frac{\delta_{GS}}{T_2 + \bar{T}_2} \right)^2 \right] \right], \qquad (4.6)
$$
$$
\mathcal{A} = -m_{3/2} \left(\cos\theta\, \sin\phi + \mathcal{O}\left[\frac{\delta_{GS}}{(T_2 + \bar{T}_2)^2} \right] \right), \qquad (4.7)
$$

where we follow [117] in taking the parameter s_α to be equal to the MSSM

1-loop β-function coefficients: $s_\alpha = \beta_\alpha$ where $\beta_\alpha = 2\pi \{33/5, 1, -3\}$. Note

that all the soft masses scale as $m_{3/2}$ as expected in any SUGRA theory.

4.2.3   Fine-tuning and the set of input parameters

Given the form of our measure of fine-tuning, Eq. 2.18, it is clear that the

value of Δ^Ω depends directly on our choice of inputs. In the non-universal

MSSM studied previously we took our inputs at the high energy (GUT)

scale as $a = a_{non-univ}$ where:

$$
a_{non-univ} \in \{ m_0, m_{0,3}, M_1, M_2, M_3, A_0, \tan\beta \}, \qquad (4.8)
$$

and the sign of μ.

Within the present type I string model we take $a = a_{string}$ where:

$$
a_{string} \in \{ m_{3/2}, \delta_{GS}, T_2 + \overline{T}_2, Y_2 + \overline{Y}_2, \theta, \phi, \tan\beta \}, \qquad (4.9)
$$

and the sign of μ.

Here $\tan\beta$ and $\text{sign}(\mu)$ are as in the general MSSM study as they result

from the requirement that the model provide radiative electroweak sym-

metry breaking. θ and ϕ are the Goldstino angles that parameterise the different contributions to SUSY breaking from the moduli and the dilaton. The remaining parameters are directly related to the moduli. The untwisted moduli T_i determine the radii of compactification. $T_2 + \overline{T}_2$ parameterises the compactification radius in the 5_2 direction via the relation [110]:

$$R_{5_2} = \frac{1}{2}\sqrt{T_2 + \overline{T}_2}. \qquad (4.10)$$

As the twisted moduli are trapped at the fixed point at one end of the 5_2 brane and the 1st and 2nd families of scalars are trapped at the other end of the brane, the radius of compactification, and therefore $T_2 + \overline{T}_2$, governs the degree of sequestering. This is evident in the limits of Eq. 4.3: as $T_2 + \overline{T}_2 \to \infty$, $m_0^2 \to 0$.

Within this paper we follow [103] in taking $T_2 + \overline{T}_2 = 50$ and $Y_2 + \overline{Y}_2 = 0$. This maintains the validity of the series expansion in $\delta_{GS}/(T_2 + \overline{T}_2)$ used to determine the F-terms. However, as these VEVs are essentially arbitrary, we include them in our set of parameters for determining dark matter fine-tuning.

δ_{GS} is a model dependent parameter that depends upon the details of the anomaly cancellation in the twisted sector. This calculation is beyond the scope of this paper and we set $\delta_{GS} = -10$ throughout. However this value can vary and so we include it in our calculation of fine-tuning parameters.

Region	ϕ	$M_1 : M_2 : M_3$
Twisted moduli (Y_2) dominated	0	$3.5 : 0.7 : -1.3$
Untwisted moduli (T_i) dominated	$\pi/2$	$5.7 : 26 : 38$

Table 4.1: The ratio of the GUT scale gaugino masses in the twisted moduli (Y_2) and untwisted moduli (T_i) SUSY breaking limits.

4.2.4   The structure of the neutralino

The studies of the previous chapter clearly showed that the principle factors in the determination of the dark matter relic density are the mass and composition of the lightest neutralino. These are determined by the ratio between M_1, M_2 and μ at the low energy scale. Though we cannot predict the size of μ from the form of the soft masses, we can find M_1 and M_2. The values of M_i at m_{GUT} can be simplified from Eq. 4.6 once we have set $T_2 + \overline{T}_2$ and δ_{GS}:

$$M_1 = 0.03 m_{3/2} \cos \theta \, (5.7 \sin \phi + 3.5 \cos \phi)$$

$$M_2 = 0.03 m_{3/2} \cos \theta \, (26 \sin \phi + 0.7 \cos \phi) \, . \qquad (4.11)$$

$$M_3 = 0.03 m_{3/2} \cos \theta \, (38 \sin \phi - 1.3 \cos \phi)$$

The overall magnitude of the gaugino masses is set by $m_{3/2}$ and $\cos \theta$. The ratio of GUT scale gaugino masses is determined by ϕ, as shown in Table 4.1. To analyse the low energy gaugino mass ratio, and so study the composition of the $\tilde{\chi}_1^0$, we once again use the rule of thumb that $M_1(M_{SUSY}) \approx 0.4 M_1(m_{GUT})$ and $M_2(M_{SUSY}) \approx 0.8 M_2(m_{GUT})$. This allows us to see that in the twisted moduli dominated limit, in the absence of small μ, we have wino dark matter. In the untwisted moduli dominated limit, again without small μ, we have bino dark matter. To find the bino/wino well-tempered

Point	θ	ϕ	$m_{3/2}$(TeV)	$\tan\beta$	$\tilde{\chi}_1^0$	$\Omega_{CDM}h^2$
A	0	0	5	4	wino	$\Omega_{CDM}h^2 \ll \Omega_{CDM}^{WMAP}h^2$
B	0.1	0.1	2	10	bino	$\Omega_{CDM}h^2 \gg \Omega_{CDM}^{WMAP}h^2$
C	0.6	0.1	2	20	bino	$\Omega_{CDM}h^2 \gg \Omega_{CDM}^{WMAP}h^2$

Table 4.2: Benchmark points from [103]. B and C overclose the universe and so are ruled out by dark matter. A lies in a region inaccessible within our studies as the parameter space is ruled out by LEP2 bounds on the lightest Higgs for $m_t = 172.7$ GeV. However even if the parameter space were allowed, the LSP would be wino and so could not reproduce the observed dark matter density.

region we need to find the value of ϕ that gives $M_1(m_{SUSY}) \approx M_2(m_{SUSY})$.
This occurs when $M_1(m_{GUT}) \approx 2M_2(m_{GUT})$ and so the switch from bino to wino dark matter will occur around $\phi \approx 0.05$. Therefore to study bino/wino "well-tempered" dark matter we should consider low values of ϕ. At lower values of ϕ dark matter will be wino and so will annihilate too efficiently to explain the observed dark matter. At larger ϕ, dark matter will be bino or bino/higgsino.

In Table 4.1 we have not included the dilaton dominated limit $\theta = \pi/2$ for two reasons. Firstly, as $\theta \to \pi/2$, $M_i \to 0$ and the parameter space will be ruled out by LEP bounds on the neutralinos, charginos and the gluino. As $\cos\theta$ is a common coefficient, the degree of dilaton contribution only affects the overall mass scale of the gauginos, not their composition. Secondly we are forbidden from accessing $\theta = \pi/2$, the dilaton dominated limit, by Eq. 4.5. Here we keep the squared Higgs mass positive at the GUT scale throughout and so limit our studies to $\theta < sin^{-1}\left(1/\sqrt{3}\right)$. Therefore the dilaton contribution can only suppress the gaugino masses by a factor of 0.8 at the most. The primary effect of θ on the phenomenology is through the sfermion and Higgs masses.

By considering the mass and composition of the lightest neutralino we

can quickly analyse the implications of dark matter for the benchmark points proposed in [103]. In Table 4.2 we list the soft parameters that define the three benchmark points and note the resulting composition of the LSP. Point A corresponds to the twisted moduli dominated limit and the LSP is wino. Remember that wino dark matter annihilates efficiently in the early universe resulting in a relic density far lower than that observed today. For point A to remain valid, there would have to be non-thermal production of SUSY dark matter or some other, non-SUSY, particle responsible for the observed relic density[1].

Points B and C both result in bino dark matter. For the density to be in agreement with its measured value, we need to look for regions in which annihilation channels are enhanced. This can happen if (i) the NLSP is close in mass to the neutralino, allowing for coannihilation, (ii) neutralinos can annihilate to a real on-shell Higgs or Z or (iii) there exist light sfermions that can mediate neutralino annihilation via t-channel sfermion exchange. None of these mechanisms exist in the case of points B or C, resulting in a predicted dark matter density far in excess of that measured by WMAP.

Having noted that the previously proposed benchmark points fail to account for the observed dark matter we go on to scan the parameter space to find regions that agree with the WMAP measurement of $\Omega_{CDM}h^2$.

---

[1]As we will show in section 4.3.1, this point is also ruled out by LEP2 bounds on the lightest Higgs if we take $m_t = 172.7$ GeV, as we do throughout this paper.

Soft Mass	Value
m_0	$3.7 \times 10^{-6} \ m_{3/2}$
$m_{0,3}$	$m_{3/2}$
m_H	$m_{3/2}$
M_1	$0.1 \ m_{3/2}$
M_2	$0.02 \ m_{3/2}$
M_3	$-0.04 \ m_{3/2}$
A	0

Table 4.3: In the twisted moduli (Y_2) dominated limit, $\theta = \phi = 0$, the soft masses take the form shown. This limit is characterised by the exponential suppression of the 1st and 2nd family scalar soft masses and a light wino LSP.

4.3 The a_{string} parameter space

4.3.1 Twisted moduli dominated SUSY breaking

In the twisted moduli dominated limit ($\theta = \phi = 0$) the soft masses simplify to the values shown in Table 4.3. In this regime the 1st and 2nd family scalars have exponentially suppressed soft masses due to their sequestering from the twisted moduli. The third family scalars and the Higgs bosons have a universal soft mass equal to $m_{3/2}$. Finally the lightest neutralino is wino and very light.

In Figs. 4.3(a)-(d) we examine the phenomenology of the parameter space as T-moduli contributions are gradually switched on by slowly increasing ϕ from 0. In the twisted moduli dominated limit (Fig. 4.3(a)) the parameter space is either closed off by LEP bounds on the lightest Higgs and chargino or because $\mu^2 < 0$, resulting in a failure of radiative electroweak symmetry breaking. This disagrees with [103] because we take $m_t = 172.7$ GeV as opposed to $m_t = 178$ GeV. Therefore the twisted moduli dominated limit is ruled out by experimental bounds for the present top mass.

In Fig. 4.3(b)-(d) we take incrementally larger values of $\phi = 0.05, 0.07$
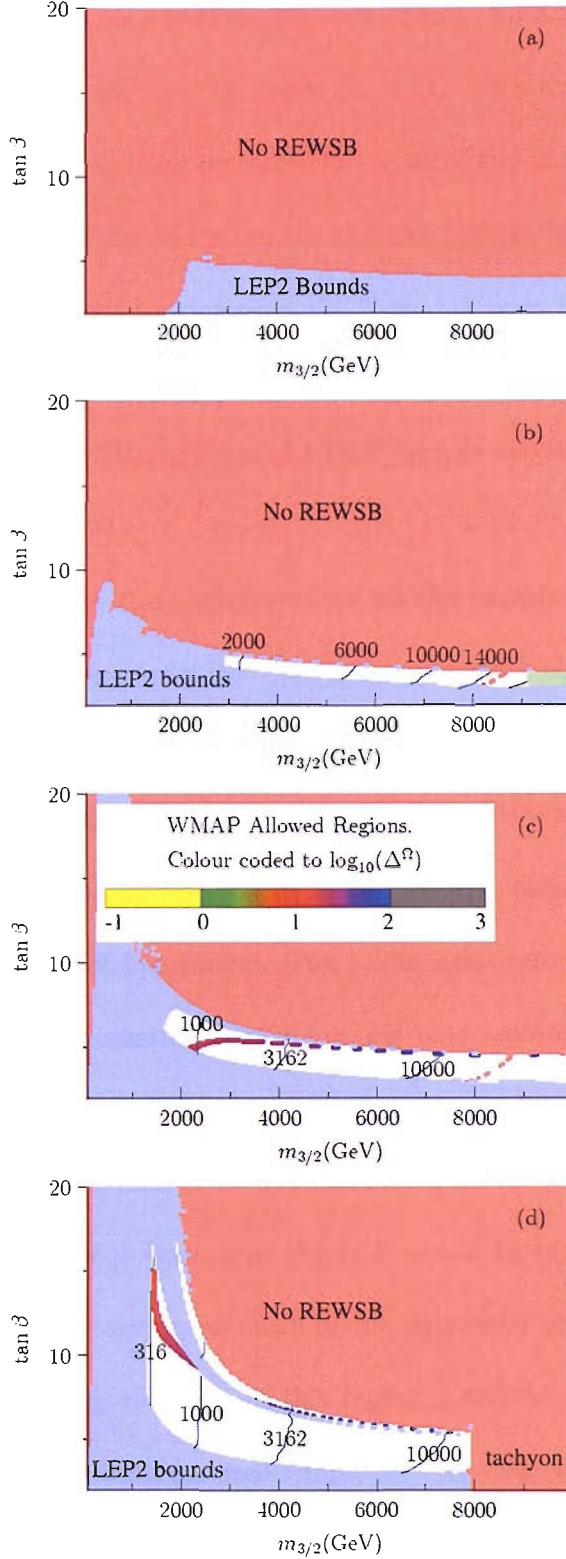
Figure 4.3: Panel (a) shows the twisted moduli dominated limit $\theta = \phi = 0$. As we switch on contributions from T-moduli, the LEP and REWSB bounds recede. In (b) $\phi = 0.05$, (c) $\phi = 0.07$ and (d) $\phi = 0.1$. $\theta = 0$ throughout. In panels (c) and (d) there are regions allowed by WMAP. These regions are plotted in varying colours corresponding to the degree of fine-tuning they require. In panel (c) we present a legend for this colour coding. Finally, we represent EW tuning by contours in panels (b)-(d). $BR(b \rightarrow s\gamma)$ agrees with measurement at 1σ across the open parameter space but $(g-2)_\mu$ agrees with the Standard Model value. The low energy SUSY spectra corresponding to these panels are discussed in [103].

and 0.1 respectively. This has three primary effects. Firstly M_2 increases, and to a lesser extent so does M_1 from Eq. 4.11. This changes the LSP from wino to bino and quickly increases the mass of the charginos, helping to satisfy LEP bounds. Secondly the 1st and 2nd family soft scalar masses receive a substantial contribution from the T-moduli from Eq. 4.3. Finally M_3 becomes positive and then steadily increases in size, helping to mitigate the bounds from REWSB and from the LEP bounds on the lightest Higgs boson.

The combination of these effects opens up the parameter space as we increase ϕ, where the area of parameter space consistent with collider phenomenology is shown as white space in the figures, and within this white space the area consistent with WMAP allowed neutralino dark matter is shown as thin coloured bands, where once again the colour coding corresponds to the degree of fine-tuning. The colour scale remains the same as before with green representing low tuning and blue representing large tuning. The first evidence of the model providing a dark matter density in agreement with that measured by WMAP is in Figs. 4.3(c) and 4.3(d). In both of these scans, if μ were large the LSP would be bino, with a small proportion of wino. However as much of the parameter space is closed off because $\mu^2 < 0$, along the edge of this region μ will be of a comparable magnitude to M_1 resulting in "well-tempered" bino/higgsino dark matter. In such regions, co-annihilation with $\tilde{\chi}_2^0$ and $\tilde{\chi}_1^+$ become significant and reduces the dark matter density to the magnitude observed. However the well-tempered region visible at $4 - 8$ TeV is plotted in dark blue, corresponding to a fine-tuning $\Delta^\Omega \approx 60$. This is comparable in magnitude to the

tuning found for bino-higgsino regions previously studied. As μ is sensitive to $\tan\beta$ and M_1 is not, there is no reason for these masses to be correlated as is required for bino/higgsino dark matter. Therefore it is unsurprising that the tuning is large and the majority of the tuning is due to $\tan\beta$, which strongly affects the size of μ.

As we move to lower values of $m_{3/2}$, the colour of the dark matter strip moves from blue to red. This corresponds to a drop in Δ^Ω. To understand this we need to once again consider the composition of the LSP. Away from the region with low μ, the neutralino is primarily bino with a small but significant wino component. This results in $\tilde{\chi}_2^0$ and $\tilde{\chi}_1^+$ being slightly heavier than $\tilde{\chi}_1^0$. Across much of the parameter space this mass difference is large enough that co-annihilation effects are unimportant. However, as the overall mass scale drops, so does the absolute value of the mass difference between the LSP and the NLSPs. Below $m_{3/2} = 4$ TeV, the mass difference is small enough for there to be an appreciable number density of $\tilde{\chi}_1^+$ and $\tilde{\chi}_2^0$ at freeze out to co-annihilate with the LSP. The efficiency of coannihilation is primarily sensitive to the mass difference between the LSP and the NLSP. This mass difference scales slowly with $m_{3/2}$ resulting in a bino/wino well-tempered region that exhibits low fine-tuning $\Delta^\Omega \approx 10$, lower than the tuning required for bino/wino regions considered in the previous chapter.

In Fig. 4.3(b), though there is a region of parameter space that satisfies LEP bounds and REWSB, there is no WMAP allowed strip. This is because here the wino component of the LSP is already too large and dark matter annihilates too efficiently in the early universe. This is unfortunate as it is only for low ϕ that we have exponentially suppressed soft masses for the

1st and 2nd families. We would like to be able to access such a region of parameter space as light 1st and 2nd family sleptons can provide neutralino annihilation via t-channel slepton exchange and low fine-tuning. Such a region is not available in this string model because as soon as we move away from $\phi = 0$ the first and second families gain substantial masses. As soon as we can access bino dark matter, the sleptons are already too heavy to contribute significantly to neutralino annihilation. Though we fail to find a light slepton bulk region in this limit, in the limit of untwisted moduli dominated SUSY breaking we will find a light $\tilde{\tau}$ bulk region.

Finally we note that the electroweak fine-tuning is large right across this parameter space. This is a direct result of the large values of $m_{3/2}$ that are required to satisfy LEP bounds. When $\phi = 0$, $M_2 = 0.02\ m_{3/2}$ from Eq. 4.11 and charginos are too light. As we increase ϕ, the coefficient of proportionality between M_2 and $m_{3/2}$ increases but remains small for small ϕ. To reach low $m_{3/2}$ we need to move to regimes in which $\sin\phi \approx \mathcal{O}(1)$, away from the twisted moduli dominated limit. These large values of $m_{3/2}$ are responsible for large electroweak tuning as before. To access regions with low EW fine-tuning we need to access low $m_{3/2}$, and that means taking large ϕ, as we consider next.

4.3.2 T-moduli dominated SUSY breaking

In the limit in which all the SUSY breaking comes from the untwisted T-moduli ($\theta = 0$, $\phi = \pi/2$), the soft masses take the form shown in Table 4.4. In the gaugino sector, as $M_1 < M_2$, the lightest neutralino will have no wino component. Unless there is a part of the parameter space with low μ,

Soft Mass	Value
m_0	$131\ m_{3/2}$
$m_{0,3}$	0
m_H	$m_{3/2}$
M_1	$0.17\ m_{3/2}$
M_2	$0.78\ m_{3/2}$
M_3	$1.14\ m_{3/2}$
A	$-m_{3/2}$

Table 4.4: The soft masses in the untwisted moduli (T_i) dominated limit, $\theta = 0, \phi = \pi/2$. This limit is characterised by vanishing 3rd family scalar masses and a bino LSP.

the LSP will be bino. As bino dark matter on its own generally annihilates extremely inefficiently there would need to be other contributions to the annihilation cross-section to satisfy WMAP bounds. The other defining feature of this limit is that $m_{0,3} = 0$. As the third family particles all pick up masses through loop corrections, they will not be massless at the low energy scale. However these corrections are smallest for $\tilde{\tau}_1$ and will leave it light. This opens up the possibility that t-channel stau exchange and stau co-annihilation will help to suppress the bino dark matter density.

As the 1st and 2nd family particles have a large soft mass, they will not provide a contribution to the muon $(g - 2)$ value. Therefore this limit will not agree with the measured deviation δa_μ from the standard model value [26]. In this limit, the model predicts a value of $(g - 2)_\mu$ in agreement with the Standard Model.

In Figs. 4.4(a)-(d) we gradually switch on twisted moduli contributions by slowly decreasing ϕ from $\pi/2$ while keeping $\theta = 0$. This immediately gives a non-zero mass to the 3rd family squarks and sleptons. Writing $\phi = \pi/2 - \delta$, for small δ we can write the 3rd family scalar mass:

$$m_{0,3} \approx \frac{\delta}{\sqrt{2}} m_{3/2}.$$ (4.12)
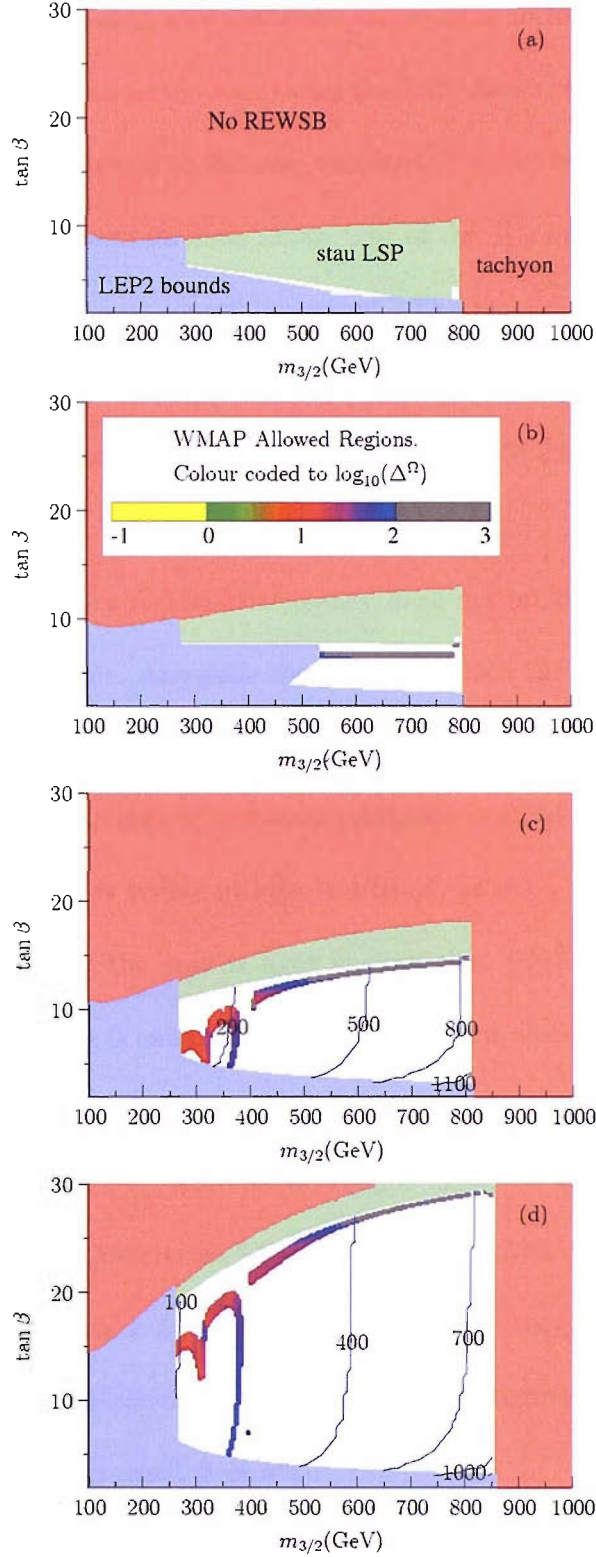
Figure 4.4: Panel (a) shows the T-moduli dominated limit $\theta = 0, \varphi = \pi/2$ in which the parameter space is entirely closed off by experimental bounds. As soon as we move away from $\phi = \pi/2$, the parameter space opens up and we find dark matter allowed regions. In (b) $\phi = 15\pi/32$, (c) $\phi = 7\pi/16$ and (d) $\phi = 3\pi/8$. Once again we switch off the dilaton contributions by taking $\theta = 0$ throughout. In panel (a) we label the different bounds that rule out the parameter space. In panel (b)-(d) the WMAP allowed regions are plotted in varying colours corresponding to the degree of fine-tuning. EW fine-tuning is represented by contours. $BR(b \to s\gamma)$ agrees with measurement at 1σ across the open parameter space but $(g - 2)_\mu$ agrees with the Standard Model value. The SUSY spectra corresponding to these panels are discussed in [103].

113

In Fig. 4.4(a) the parameter space of $\tan\beta < 10$ is entirely closed off by LEP bounds on the stau or the stau being the LSP. As we reduce ϕ, we give a soft mass to the stau and so increase its physical mass, helping to satisfy the LEP bound and push its mass above that of the $\tilde{\chi}_1^0$. In Figs. 4.4(c),(d) the stau LEP bound is no longer important. The remaining LEP bounds are the Higgs for low $\tan\beta$ and the lightest neutralino for $m_{3/2} < 270$ GeV. Large $\tan\beta$ is ruled out by a failure of REWSB ($\mu^2 < 0$) and the stau being the LSP.

There are 4 distinct regions that satisfy dark matter bounds in the T-moduli dominated limit. Alongside the region in which the stau is the LSP, there is a corresponding dark matter strip in which the stau is close in mass to the neutralino and $\tilde{\chi}_1^0 - \tilde{\tau}$ co-annihilation reduces $\Omega_{CDM}h^2$ to the observed value. This is visible in Figs. 4.4(b)-(d) at $m_{3/2} > 450$ GeV. For lower values of $m_{3/2}$, the stau is light enough that $\tilde{\chi}_1^0\tilde{\chi}_1^0 \to \tau^+\tau^-$ via t-channel stau exchange is enhanced to the point that it alone can account for the observed dark matter density. This $\tilde{\tau}$ bulk region is a direct analogue of the bulk region in Fig. 3.5. As we reduce $m_{3/2}$, we are also reducing the mass of the LSP. Before the LEP bounds close off the parameter space there are regions in which $2m_{\tilde{\chi}_1^0} = m_{Z,h^0}$. These lie at $m_{3/2} = 310$ GeV and $m_{3/2} = 400$ GeV respectively. In these regions, the lightest neutralino can annihilate via a real on-shell Z or h^0.

Each of these regions has a distinct measure of fine-tuning. The biggest surprise is the stau co-annihilation strip, shown in grey. In contrast to the stau co-annihilation strips we saw in the previous chapter, this co-annihilation strip exhibits fine-tuning $\Delta^\Omega > 100$. This is an order of magni-

tude increase over the typical Δ^Ω of previous stau co-annihilation regions. The reason for this is the extreme sensitivity to ϕ highlighted by Eq. 4.12. In previous studies the soft stau mass was so light that loop corrections from the gauginos dominated the determination of its low energy mass. This reduced the sensitivity to variations in the soft stau mass and resulted in the low energy stau and neutralino masses being correlated. In this model, the extreme sensitivity of the stau soft mass to ϕ (for $\phi = 1.47$, a 10% variation in ϕ results in a 150% change in $m_{0,3}$) breaks this correspondence. As a result, for $\theta = 0$, the model does not have a region in which $m_{\tilde{\tau}}$ and $m_{\tilde{\chi}_1^0}$ are correlated.

We can see this by considering the effect of changing from varying the soft mass directly to varying it via ϕ. Under a change of variables:

$$\Delta_\phi^\Omega = \sum_{a_{MSSM}} \frac{\phi}{a_{MSSM}} \frac{\partial a_{MSSM}}{\partial \phi} \Delta_{a_{MSSM}}^\Omega. \qquad (4.13)$$

When $\theta = 0$, the coefficient of proportionality between Δ_ϕ^Ω and $\Delta_{m_{0,3}}^\Omega$ is $\phi \tan \phi$, so as $\phi \to \pi/2$, $\Delta^\Omega \to \infty$. This dramatically demonstrates the model dependence of fine-tuning.

Eq. 4.13 is exact and a similar change of variables can be performed to find all of the $\Delta_{a_{string}}^\Omega$ in terms of $\Delta_{a_{MSSM}}^\Omega$. In general these expressions are convoluted and not particularly informative. However in cases such as that of the $\tilde{\tau}$ coannihilation region, we can use Eq. 4.13 to understand the change in the fine-tuning.

The bulk region is shown in red in Figs. 4.4(c),(d) corresponding to Δ^Ω of order 10. This tuning is entirely from ϕ. In the general MSSM study,

the tuning of the bulk region came equally from $\Delta^{\Omega}_{M_1}$ and $\Delta^{\Omega}_{m_0}$ where m_0 was the soft mass of the slepton that mediated t-channel annihilation. This resulted in low tuning of the bulk region $\Delta^{\Omega} < 1$. When we change variables from a_{MSSM} to a_{string}, for $\delta \approx 0.1$, $\theta = 0$, Eq. 4.13 gives $\Delta^{\Omega}_{\phi} \approx 10\Delta^{\Omega}_{m_{0,3}}$ in the bulk region. This explains the order of magnitude increase in the tuning.

Finally we consider the resonances. The lower edge of the Higgs resonance exhibits a tuning $\Delta^{\Omega} \approx 50$ whereas the edge at larger $m_{3/2}$ is so steep that the scan has failed to resolve it. What we can see of it exhibits tuning well in excess of 100. In contrast the Z resonance exhibits relatively low fine-tuning. This is because annihilation via an s-channel Z is inefficient and provides only a small contribution to the total annihilation cross-section. This is because the Z is spin 1, whereas the neutralino is a spin 1/2 Majorana fermion. This means that in the $v_{\tilde{\chi}^0_1} \to 0$ limit, the annihilation cross-section via on-shell Z production becomes negligible. As this contribution is small, it hardly affects the dark matter fine-tuning.

The electroweak fine-tuning is shown by contours on the open parameter space. As we noted in the previous section, electroweak fine-tuning depends closely on the largest 3rd family masses. As we can access low $m_{3/2}$ for large ϕ, we end up with electroweak fine-tuning of $\mathcal{O}(100)$, similar to the lowest electroweak fine-tuning found in the MSSM.

4.3.3 Switching on the dilaton.

In the limit of dilaton dominated SUSY breaking, $\theta = \pi/2$ the soft mass terms take the form shown in Table 4.5. This structure of soft masses

Soft Mass	Value
m_0^2	$-0.5\ m_{3/2}^2$
$m_{0,3}^2$	$m_{3/2}^2$
m_H^2	$-2\ m_{3/2}^2$
M_i	0
A	0

Table 4.5: The soft masses in the dilaton (S) dominated limit, $\theta = \pi/2$. This limit is characterised by vanishing gaugino masses and negative Higgs (mass)^2.

gives rise to a plethora of problems. Firstly, negative soft sfermion (mass^2) will result in tachyons. Secondly, massless gauginos are ruled out by LEP. However the biggest problem lies in the Higgs sector. If the soft term m_H^2 is negative we run the risk of breaking electroweak symmetry at the GUT scale. This happens when $m_H^2 + \mu^2 < 0$ at the GUT scale. We steer clear of such regions by constraining our parameters to give $m_H^2 > 0$. This allows us to impose the constraint $0 < \theta < 0.6$.

When we consider the maximum allowed dilaton contribution, there are two interesting limits. For $(\theta = 0.6, \phi = 0)$ we have (S, Y_2) SUSY breaking. When $(\theta = 0.6, \phi = \pi/2)$ we have (S, T_i) SUSY breaking.

For $\phi = 0$, dark matter is still wino and so cannot reproduce the observed dark matter density. The only change is that we can access large values of $\tan\beta$. Therefore we cannot have a model in which there is no T-moduli contribution to SUSY breaking and reproduce the observed dark matter density.

In Fig. 4.5(b) $\phi = \pi/2$, $\theta = 0.6$ giving $M_1 < M_2$ and hence the LSP is bino. By introducing non-zero θ we increases the stau mass and avoid the LEP bounds on the stau that ruled out $\theta = 0$, $\phi = \pi/2$. It is only for large $\tan\beta$ that the stau is light enough to contribute to neutralino

117
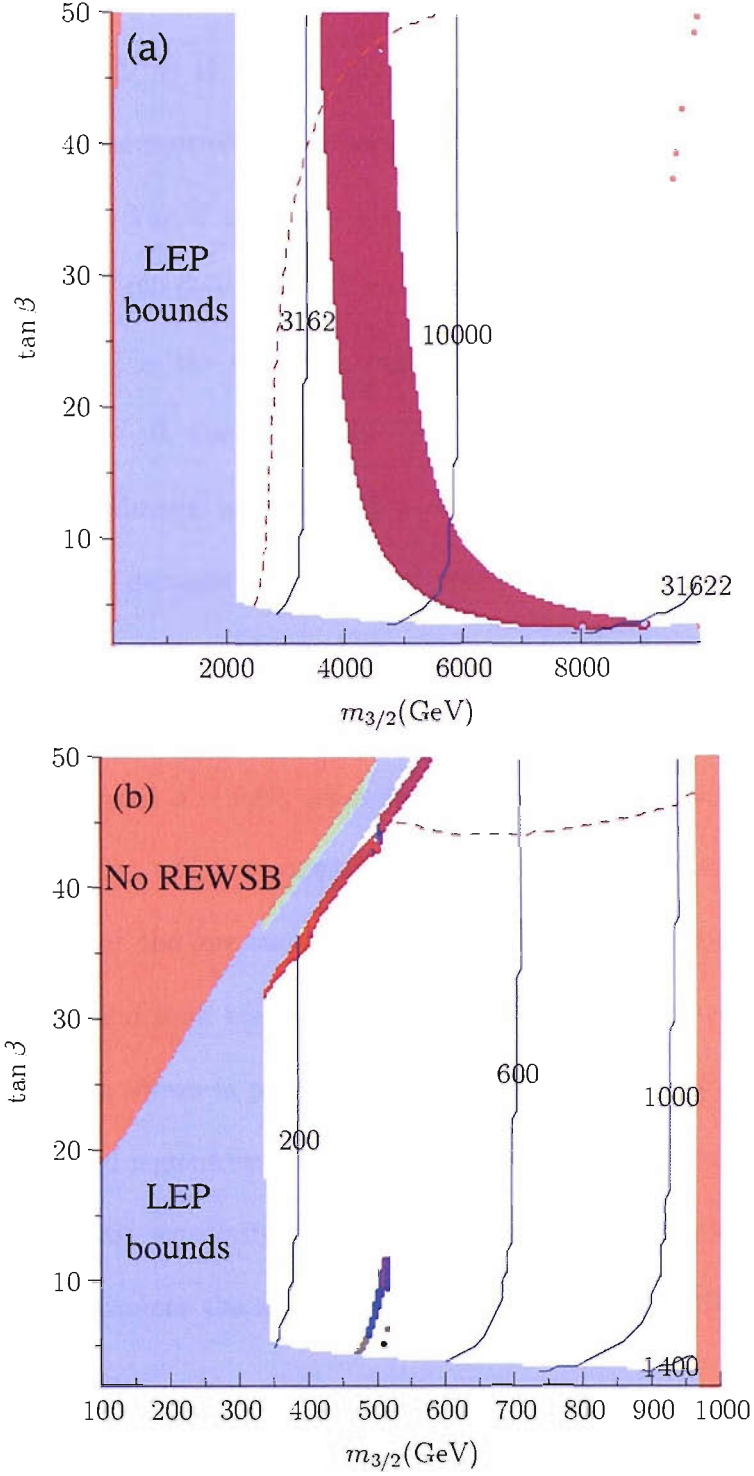
Figure 4.5: Here we show the maximum dilaton contribution $\theta = 0.6$. For larger values of θ, $m^2_{H_{1,2}} < 0$ at the GUT scale. The regions that satisfy dark matter constraints are plotted in varying colours to represent the required quantity of fine-tuning. This colour coding is as per the legend in Fig. 4.4(b). The electroweak fine-tuning is represented by contours in the open parameter space. The $BR(b \rightarrow s\gamma)$ 1σ limit is plotted as a red dashed line. In panel (a) $\phi = 0.06$, here we have maximally tempered bino/wino/higgsino dark matter, plotted in purple. In panel (b) $\phi = \pi/2$, the limit in which there is no twisted moduli (Y_2) contribution. Again $(g-2)_\mu$ agrees with the Standard Model.

annihilation via t-channel $\tilde{\tau}$ exchange. As before this region is shown in red, corresponding to $\Delta^\Omega \approx 10$. As we can still access low $m_{3/2}$, there exists a region in which the neutralinos can annihilate via the production of a real on-shell h^0 or Z. The Z resonance shows up as a small blip in the bulk region at $m_{3/2} = 400$ GeV. The h^0 resonance appears as a highly tuned region (dark blue) in the stau bulk region around $m_{3/2} = 500$ GeV and also at $\tan\beta = 5 - 10$. For $\tan\beta = 10 - 40$, even resonant annihilation via on-shell Higgs production is not enough to suppress the dark matter density.

As we steadily decrease ϕ, the staus increase in mass removing the stau bulk region. Small ϕ also reduces the gaugino masses, requiring ever larger values of $m_{3/2}$ to satisfy LEP bounds. There is no change in the dark matter phenomenology until $\phi = 0.06$, when the neutralino acquires a large wino component. In Fig. 4.5(a) we display this region of parameter space. Here $M_1 \approx M_2 \approx \mu$ at the low energy scale, resulting in maximally tempered bino/wino/higgsino dark matter. This in turn gives a wide dark matter annihilation strip shown in purple that corresponds to $\Delta^\Omega = 23$, similar to the well-tempered regions we looked at within the MSSM. The tuning arises from the soft mass sensitivity to ϕ. This dependence is understandable as it is ϕ that determines the size of the bino and wino contributions to the lightest neutralino.

The electroweak fine-tuning is dependent upon the size of $m_{3/2}$. Therefore Fig. 4.5(b) exhibits low Δ^{EW} in agreement with Fig. 4.4 and Fig. 4.5(a) exhibits large Δ^{EW} as in Fig. 4.3.

Dark Matter Region	θ	ϕ	$m_{3/2}$(TeV)	Typical Δ^Ω	Typical Δ^{EW}
bino/higgsino	0-0.6	< 0.4	1-10	60	> 3000
bino/wino	0-0.6	≈ 0.06	1-3	10	300 − 3000
bino/wino/higgsino	0-0.6	≈ 0.06	2-5	10-20	1000-6000
$\tilde{\tau}$-co-annihilation	0-0.6	> 0.8	0.4-0.9	100	500-800
t-channel $\tilde{\tau}$ exchange	0-0.6	> 0.8	0.25-0.45	10	100-200
h^0 resonance	0-0.6	> 0.4	≈ 0.4	> 80	200
Z^0 resonance	< 0.3	> 0.4	≈ 0.3	4-20	130

Table 4.6: A summary of the successful regions of parameter space in the type I string model considered here that satisfy experimental bounds on the dark matter density with corresponding typical values of Δ^Ω and Δ^{EW}.

4.4 Conclusions

In this chapter we have achieved two things. Firstly, we have used the measured dark matter relic density to constrain the type I string model of [103]. Secondly, we have studied fine-tuning in the string model for both electroweak symmetry breaking and dark matter.

We have found that dark matter constraints close off much of the parameter space of the type I string model, for example the benchmark points suggested in [103] are either ruled out ($\Omega_{CDM}h^2 \gg \Omega_{CDM}^{WMAP}h^2$) or disfavoured ($\Omega_{CDM}h^2 \ll \Omega_{CDM}^{WMAP}h^2$). However, by performing a comprehensive scan over the parameter space, we found successful regions of dark matter within the string model. As in the previous chapter, these regions fall within the dark matter channels listed in Table. 2.1. This allows a direct comparison of the degree of fine-tuning within the string model and the general MSSM parametrisation. Some regions exhibit degrees of fine-tuning in agreement with the previous results while others vary significantly. The results are summarised in Table 4.6.

From Table 4.6 it can be seen that the observed dark matter density tightly constrains the available parameter space. For $\phi > 0.07$, without un-

usual contributions to the annihilation cross-section the model predicts an over-abundance of dark matter that would over-close the universe. Equally for $\phi < 0.05$, the LSP is wino and the model predicts a dark matter abundance orders of magnitude less than that observed. By imposing dark matter constraints we have ruled out the benchmark points proposed in [103]. Instead, we propose a benchmark point within the region of lowest fine-tuning, the stau bulk region combined with on-shell Z production. The SUSY spectrum of this point is presented in Table 4.7.

In addition to constraining our models, we have been able to study how fine tuning varies between the MSSM studied in [69] and a type I string model of SUSY breaking, which was one of our main motivations for this study. From Table 4.6 it can be seen that, in the string model, the lowest dark matter fine-tuning exists in the bulk region, corresponding to t-channel $\tilde{\tau}$ exchange. The Z resonance, the well tempered bino/wino and the maximally tempered bino/wino/higgsino regions also have low dark matter fine-tuning. Of these, the lowest electroweak fine-tuning arises in the bulk (t-channel $\tilde{\tau}$ exchange) and Z resonance regions. These results are consistent with the conclusions based on the previous MSSM analysis, although the bulk region in the MSSM corresponding to first and second family slepton exchange cannot be accessed in the string model as discussed. Thus in most cases the degree of fine-tuning is found to be the same order of magnitude as found for similar dark matter regions within the MSSM. However this is not always the case. Whereas the well tempered bino/higgsino region in Table 4.6 continues to be highly fine-tuned as in the MSSM, the well tempered bino/wino in Table 4.6 has a fine tuning of about 10 as compared

to the MSSM value of about 30, making this scenario more natural in the framework of string theories such as the one considered here.

In some cases there is a sharp disagreement between the fine tuning calculated in the MSSM and in the string model, for example in the stau co-annihilation region. Due to the form of the SUSY breaking in this model, the stau mass, and so the dark matter density, is very sensitive to ϕ which leads to an order of magnitude increase in the dark matter fine-tuning in the string model as compared to the MSSM, making this region less natural in the string model. This can be understood via Eq. 4.13 which shows that, through a general change of variables, the variation of the fine-tuning between a general MSSM model and a string model can be calculated. In principle a similar change of variables is responsible for all the differences in fine tuning calculated in the MSSM and the string model. In practise however, such a change of variables is not analytically tractable, and numerical methods such as those used in the present paper are required in order to obtain quantitative results. However the results in this paper indicate a general strategy for reducing fine tuning within string models, namely to search for string models that minimise the coefficients of the tuning measures. This in turn will minimise Δ^{Ω}, providing more natural dark matter than the MSSM for a given region of parameter space. Such a strategy could also be employed to reduce electroweak fine tuning once the solution to the μ problem is properly understood within the framework of string theory.

Point	A'
θ	0
ϕ	$3\pi/8$
$m_{3/2}$	310
$\tan\beta$	13
m_{h^0}	115
m_{A^0}	550
m_{H^0}	550
$m_{H^\pm}$	556
$m_{\tilde{\chi}_1^0}$	44.5
$m_{\tilde{\chi}_2^0}$	213
$m_{\tilde{\chi}_1^\pm}$	213
$m_{\tilde{g}}$	930
$m_{\tilde{t}_1}$	546
$m_{\tilde{t}_2}$	757
$m_{\tilde{c}_L}, m_{\tilde{u}_L}$	3390
$m_{\tilde{c}_R}, m_{\tilde{u}_R}$	3390
$m_{\tilde{b}_1}$	687
$m_{\tilde{b}_2}$	739
$m_{\tilde{s}_L}, m_{\tilde{d}_L}$	3390
$m_{\tilde{s}_R}, m_{\tilde{d}_R}$	3390
$m_{\tilde{\tau}_1}$	104
$m_{\tilde{\tau}_2}$	222
$m_{\tilde{\mu}_L}, m_{\tilde{e}_L}$	3290
$m_{\tilde{\mu}_2}, m_{\tilde{e}_2}$	3280
$m_{\tilde{\nu}_e}, m_{\tilde{\nu}_\mu}$	3290
$m_{\tilde{\nu}_\tau}$	197
LSP	$\tilde{\chi}_1^0$

Table 4.7: Sample spectra for benchmark point A' corresponding to a point in Fig. 4.4(d) at $m_{3/2} = 310$ GeV and $\tan\beta = 13$. At this point we satisfy WMAP bounds on the dark matter density, $BR(b \to s\gamma)$ and all present mass bounds. This point requires a tuning to achieve electroweak symmetry breaking: $\Delta^{EW} = 125$, and a tuning to agree with WMAP: $\Delta^\Omega = 3.9$. The annihilation of neutralinos in the early universe is due to 40% $\tilde{\chi}_1^0\tilde{\chi}_1^0 \to \tau^+\tau^-$ via t-channel $\tilde{\tau}$ exchange and 60% $\tilde{\chi}_1^0\tilde{\chi}_1^0 \to f\bar{f}$ via the production of an on-shell Z. All masses are in GeV.

Chapter 5

Conclusions

In this thesis we have addressed the question of whether the Minimal Super-
symmetric Standard Model can naturally explain the observed dark matter
density. We have also addressed the question of how fine-tuning varies be-
tween the MSSM and a more fundamental string model.

In Chapter 2 we introduced a measure of fine-tuning for dark matter and
went on in Chapter 3 to use this to study the tuning required in the regions
of the MSSM that fit the observed relic density. We showed that, within the
structures of MSSM parameters we considered, there are typical tunings for
each specific region. We also showed that in certain regions of parameter
space, these tunings can vary. For example, generally slepton coannihilation
regions exhibit a tuning $\Delta^\Omega \approx 50$. However when m_0, the soft slepton mass,
is small, the physical slepton mass is dominated by loop corrections from M_1
that result in the slepton and gaugino masses being correlated. This results
in a significant decrease in the tuning required within a coannihilation region.

From this general study we found the most natural regions to be the
slepton bulk region in which neutralino annihilation proceeds via t-channel

slepton exchange. Such regions are not accessible in the CMSSM and so motivate a move to less constrained models. Slepton coannihilation regions with low m_0 and some maximally-tempered regions provide the next lowest values of Δ^Ω. Moderately large tunings, $\Delta^\Omega \approx 10 - 60$ are found for the Z resonance, and both well-tempered bino/higgsino and bino/wino regions. Finally the A^0 and h^0 resonances provide the largest tunings $\Delta^\Omega \approx 50 - 1000$.

These tunings refute recent claims that the MSSM fails to provide natural dark matter. They also provide a means of analysing the relative theoretical motivation of different regions of the MSSM parameter space.

In Chapter 4 we extended this analysis to consider how the dark matter fine-tuning varies when the MSSM is generated from more fundamental physics. Whereas in Chapter 3 we use dark matter to constrain the MSSM, in Chapter 4 we constrain a semi-realistic type I string model. We find that the majority of the tunings remain of the same order as in the general MSSM. The tunings that differ can be explained via the change of variables:

$$\Delta^\Omega_{a_{string}} = \sum_{a_{MSSM}} \frac{a_{string}}{a_{MSSM}} \frac{\partial a_{MSSM}}{\partial a_{string}} \Delta^\Omega_{a_{MSSM}} \tag{5.1}$$

This relation allows us to use the fine-tuning of dark matter as a guide when studying more fundamental theories of SUSY breaking. To minimise fine-tuning we should look for a set of parameters that minimise the coefficients of $\Delta^\Omega_{a_{MSSM}}$. Therefore, if the LHC provides evidence for a region of the MSSM that would require a large tuning, we have a means of guiding our search for a fundamental theory that really will provide a natural explanation of dark matter.

Bibliography

[1] F. Halzen and A. D. Martin, *Quarks and Leptons*, London, UK: Wiley (1984).

[2] M. E. Peskin and D. V. Schroeder, *An Introduction to Quantum Field Theory*, Reading, USA: Addison-Wesley (1995).

[3] K. Hagiwara *et al.* [Particle Data Group Collaboration], Phys. Rev. D **66** (2002) 010001.

[4] M. Kobayashi and T. Maskawa, Prog. Theor. Phys. **49** (1973) 652.

[5] S. L. Glashow, J. Iliopoulos and L. Maiani, Phys. Rev. D **2** (1970) 1285.

[6] Q. R. Ahmad *et al.* [SNO Collaboration], Phys. Rev. Lett. **89** (2002) 011301 [arXiv:nucl-ex/0204008];

Q. R. Ahmad *et al.* [SNO Collaboration], Phys. Rev. Lett. **89** (2002) 011302 [arXiv:nucl-ex/0204009].

[7] F. Zwicky, Helv. Phys. Acta **6** (1933) 110.

[8] D. N. Spergel *et al.* [WMAP Collaboration], Astrophys. J. Suppl. **148** (2003) 175 [arXiv:astro-ph/0302209].

[9] D. N. Spergel *et al.* [WMAP Collaboration], arXiv:astro-ph/0603449.

[10] R. H. Sanders and S. S. McGaugh, Ann. Rev. Astron. Astrophys. **40** (2002) 263 [arXiv:astro-ph/0204521].

[11] S. R. Coleman and J. Mandula, Phys. Rev. **159** (1967) 1251.

[12] R. Haag, J. T. Lopuszanski and M. Sohnius, Nucl. Phys. B **88** (1975) 257.

[13] H. E. Haber and G. L. Kane, Phys. Rept. **110**, (1984).

[14] D. Bailin and A. Love, *Supersymmetric Gauge Field Theory and String Theory*, Bristol, UK: IOP (1994) (Graduate Student Series in Physics)

[15] J. D. Lykken, arXiv:hep-th/9612114.

[16] S. P. Martin, arXiv:hep-ph/9709356.

[17] D. J. H. Chung, L. L. Everett, G. L. Kane, S. F. King, J. D. Lykken and L. T. Wang, Phys. Rept. **407** (2005) 1 [arXiv:hep-ph/0312378].

[18] B. C. Allanach, Comput. Phys. Commun. **143** (2002) 305 [arXiv:hep-ph/0104145].

[19] G. Belanger, F. Boudjema, A. Pukhov and A. Semenov, Comput. Phys. Commun. **149** (2002) 103 [arXiv:hep-ph/0112278].

[20] P. Skands *et al.*, JHEP **0407** (2004) 036 [arXiv:hep-ph/0311123].

[21] LEP SUSY Working Group, http://lepsusy.web.cern.ch/lepsusy/Welcome.html

[22] LEP Higgs Working Group, http://lephiggs.web.cern.ch/LEPHIGGS/www/Welcome.html

[23] K. Abe *et al.* [Belle Collaboration], Phys. Lett. B **511** (2001) 151 [arXiv:hep-ex/0103042].

[24] D. Cronin-Hennessy *et al.* [CLEO Collaboration], Phys. Rev. Lett. **87** (2001) 251808 [arXiv:hep-ex/0108033].

[25] R. Barate *et al.* [ALEPH Collaboration], Phys. Lett. B **429** (1998) 169.

[26] J. R. Ellis, Int. J. Mod. Phys. A **20** (2005) 5297 [arXiv:hep-ph/0409360].

[27] See talk by M. N. Achasov, at the International Workshop on e^+e^- Collisions from ϕ to Ψ, February 27 - March 2, 2006, BINP, Novosibirsk, Russia (web page http://www.inp.nsk.su/conf/phipsi06/).

[28] G. W. Bennett *et al.* [Muon g-2 Collaboration], Phys. Rev. Lett. **92** (2004) 161802 [arXiv:hep-ex/0401008].

[29] A. Hocker, arXiv:hep-ph/0410081.

[30] S. P. Martin and J. D. Wells, Phys. Rev. D **64** (2001) 035003 [arXiv:hep-ph/0103067].

[31] G. L. Kane and S. F. King, Phys. Lett. B **451** (1999) 113 [arXiv:hep-ph/9810374].

[32] G. Bertone, D. Hooper and J. Silk, Phys. Rept. **405** (2005) 279 [arXiv:hep-ph/0404175].

[33] A. Klypin, H. Zhao and R. S. Somerville, arXiv:astro-ph/0110390.

[34] R. Gaitskell, V. Mandic, http://dmtools.berkeley.edu/limitplots/

[35] J. S. Hagelin, G. L. Kane and S. Raby, Nucl. Phys. B **241** (1984) 638.

[36] T. Falk, K. A. Olive and M. Srednicki, Phys. Lett. B **339** (1994) 248 [arXiv:hep-ph/9409270].

[37] J. R. Ellis, J. S. Hagelin, D. V. Nanopoulos, K. A. Olive and M. Srednicki, Nucl. Phys. B **238** (1984) 453.

[38] M. S. Turner, Phys. Rept. **197** (1990) 67.

[39] G. Raffelt, Phys. Rept. **198** (1990) 1.

[40] L. Covi, J. E. Kim and L. Roszkowski, Phys. Rev. Lett. **82** (1999) 4180, [arXiv:hep-ph/9905212]; L. Covi, H. B. Kim, J. E. Kim and L. Roszkowski, JHEP **0105** (2001) 033, [arXiv:hep-ph/0101009]; L. Covi, L. Roszkowski, R. Ruiz de Austri and M. Small, JHEP **0406** (2004) 003, [arXiv:hep-ph/0402240].

[41] J. L. Feng, K. T. Matchev and F. Wilczek, Phys. Lett. B **482** (2000) 388 [arXiv:hep-ph/0004043].

[42] S. Weinberg, Phys. Rev. Lett. **48** (1982) 1303.

[43] J. R. Ellis, A. D. Linde and D. V. Nanopoulos, Phys. Lett. B **118** (1982) 59.

[44] G. Jungman, M. Kamionkowski and K. Griest, Phys. Rept. **267** (1996) 195 [arXiv:hep-ph/9506380].

[45] K. Griest and D. Seckel, Phys. Rev. D **43** (1991) 3191.

[46] J. Edsjo, M. Schelke, P. Ullio and P. Gondolo, JCAP **0304** (2003) 001 [arXiv:hep-ph/0301106].

[47] T. Nihei, L. Roszkowski and R. Ruiz de Austri, JHEP **0207** (2002) 024 [arXiv:hep-ph/0206266].

[48] G. F. Giudice, E. W. Kolb and A. Riotto, Phys. Rev. D **64** (2001) 023508 [arXiv:hep-ph/0005123].

[49] N. Arkani-Hamed, A. Delgado and G. F. Giudice, arXiv:hep-ph/0601041.

[50] R. Barbieri and G. F. Giudice, Nucl. Phys. B **306** (1988) 63.

[51] G. G. Ross and R. G. Roberts, Nucl. Phys. B **377** (1992) 571.

[52] B. de Carlos and J. A. Casas, Phys. Lett. B **309** (1993) 320 [arXiv:hep-ph/9303291].

[53] S. Dimopoulos and G. F. Giudice, Phys. Lett. B **357** (1995) 573 [arXiv:hep-ph/9507282].

[54] P. H. Chankowski, J. R. Ellis and S. Pokorski, Phys. Lett. B **423** (1998) 327 [arXiv:hep-ph/9712234].

[55] R. Barbieri and A. Strumia, Phys. Lett. B **433** (1998) 63 [arXiv:hep-ph/9801353].

[56] P. H. Chankowski, J. R. Ellis, M. Olechowski and S. Pokorski, Nucl. Phys. B **544** (1999) 39 [arXiv:hep-ph/9808275].

[57] J. L. Feng, K. T. Matchev and T. Moroi, Phys. Rev. Lett. **84** (2000) 2322 [arXiv:hep-ph/9908309].

[58] J. L. Feng, K. T. Matchev and T. Moroi, Phys. Rev. D **61** (2000) 075005 [arXiv:hep-ph/9909334].

[59] M. Bastero-Gil, G. L. Kane and S. F. King, Phys. Lett. B **474** (2000) 103 [arXiv:hep-ph/9910506].

[60] A. Romanino and A. Strumia, Phys. Lett. B **487** (2000) 165 [arXiv:hep-ph/9912301].

[61] J. A. Casas, J. R. Espinosa and I. Hidalgo, JHEP **0401** (2004) 008 [arXiv:hep-ph/0310137].

[62] B. C. Allanach and C. G. Lester, Phys. Rev. D **73** (2006) 015013 [arXiv:hep-ph/0507283].

[63] B. C. Allanach, Phys. Lett. B **635** (2006) 123 [arXiv:hep-ph/0601089].

[64] G. W. Anderson and D. J. Castano, Phys. Rev. D **53** (1996) 2403 [arXiv:hep-ph/9509212].

[65] G. W. Anderson and D. J. Castano, Phys. Rev. D **52** (1995) 1693 [arXiv:hep-ph/9412322].

[66] G. W. Anderson and D. J. Castano, Phys. Lett. B **347** (1995) 300 [arXiv:hep-ph/9409419].

[67] J. R. Ellis and K. A. Olive, Phys. Lett. B **514** (2001) 114 [arXiv:hep-ph/0105004].

[68] J. R. Ellis, K. A. Olive and Y. Santoso, New J. Phys. **4** (2002) 32 [arXiv:hep-ph/0202110].

[69] S. F. King and J. P. Roberts, arXiv:hep-ph/0603095.

[70] J. R. Ellis, S. Heinemeyer, K. A. Olive and G. Weiglein, JHEP **0502** (2005) 013 [arXiv:hep-ph/0411216].

[71] R. R. de Austri, R. Trotta and L. Roszkowski, JHEP **0605**, 002 (2006) [arXiv:hep-ph/0602028].

[72] G. Belanger, F. Boudjema, A. Cottrant, A. Pukhov and A. Semenov, Nucl. Phys. B **706** (2005) 411 [arXiv:hep-ph/0407218].

[73] H. Baer, T. Krupovnickas, A. Mustafayev, E. K. Park, S. Profumo and X. Tata, arXiv:hep-ph/0511034.

[74] H. Baer, A. Mustafayev, E. K. Park and S. Profumo, JHEP **0507** (2005) 046 [arXiv:hep-ph/0505227].

[75] S. Baek, D. G. Cerdeno, Y. G. Kim, P. Ko and C. Munoz, JHEP **0506** (2005) 017 [arXiv:hep-ph/0505019].

[76] D. G. Cerdeno and C. Munoz, JHEP **0410** (2004) 015 [arXiv:hep-ph/0405057].

[77] E. Nezri, arXiv:hep-ph/0305114.

[78] A. Birkedal-Hansen and B. D. Nelson, Phys. Rev. D **64** (2001) 015008 [arXiv:hep-ph/0102075].

[79] H. Baer, A. Mustafayev, E. K. Park, S. Profumo and X. Tata, JHEP **0604** (2006) 041 [arXiv:hep-ph/0603197].

[80] K. Huitu, J. Laamanen, P. N. Pandita and S. Roy, Phys. Rev. D **72** (2005) 055013 [arXiv:hep-ph/0502100].

[81] C. Pallis, Nucl. Phys. B **678** (2004) 398 [arXiv:hep-ph/0304047].

[82] A. Corsetti and P. Nath, Phys. Rev. D **64** (2001) 125010 [arXiv:hep-ph/0003186].

[83] U. Chattopadhyay and P. Nath, Phys. Rev. D **65** (2002) 075009 [arXiv:hep-ph/0110341].

[84] U. Chattopadhyay, A. Corsetti and P. Nath, Phys. Rev. D **66** (2002) 035003 [arXiv:hep-ph/0201001].

[85] H. Baer, A. Belyaev, T. Krupovnickas and A. Mustafayev, JHEP **0406** (2004) 044 [arXiv:hep-ph/0403214].

[86] M. R. Ramage and G. G. Ross, JHEP **0508** (2005) 031 [arXiv:hep-ph/0307389].

[87] E. Accomando, R. Arnowitt and B. Dutta, Phys. Lett. B **475** (2000) 176 [arXiv:hep-ph/9811300].

[88] D. Auto, H. Baer, A. Belyaev and T. Krupovnickas, JHEP **0410** (2004) 066 [arXiv:hep-ph/0407165].

[89] M. Olechowski and S. Pokorski, Phys. Lett. B **344** (1995) 201 [arXiv:hep-ph/9407404].

[90] F. M. Borzumati, M. Olechowski and S. Pokorski, Phys. Lett. B **349** (1995) 311 [arXiv:hep-ph/9412379].

[91] V. Berezinsky, A. Bottino, J. R. Ellis, N. Fornengo, G. Mignola and S. Scopel, Astropart. Phys. **5** (1996) 1 [arXiv:hep-ph/9508249].

[92] P. Nath and R. Arnowitt, Phys. Rev. D **56** (1997) 2820 [arXiv:hep-ph/9701301].

[93] E. Accomando, R. Arnowitt, B. Dutta and Y. Santoso, Nucl. Phys. B 585 (2000) 124 [arXiv:hep-ph/0001019].

[94] R. Arnowitt and B. Dutta, arXiv:hep-ph/0210339.

[95] R. Dermisek, S. Raby, L. Roszkowski and R. Ruiz De Austri, JHEP 0304 (2003) 037 [arXiv:hep-ph/0304101].

[96] V. Bertin, E. Nezri and J. Orloff, JHEP 0302 (2003) 046 [arXiv:hep-ph/0210034].

[97] A. Birkedal-Hansen and B. D. Nelson, Phys. Rev. D 67 (2003) 095006 [arXiv:hep-ph/0211071].

[98] U. Chattopadhyay and D. P. Roy, Phys. Rev. D 68 (2003) 033010 [arXiv:hep-ph/0304108].

[99] D. G. Cerdeno, K. Y. Choi, K. Jedamzik, L. Roszkowski and R. Ruiz de Austri, arXiv:hep-ph/0509275.

[100] G. L. Kane, C. F. Kolda, L. Roszkowski and J. D. Wells, Phys. Rev. D 49 (1994) 6173 [arXiv:hep-ph/9312272].

[101] S. F. King and D. A. J. Rayner, arXiv:hep-ph/0211242.

[102] S. F. King and D. A. J. Rayner, JHEP 0207 (2002) 047 [arXiv:hep-ph/0111333].

[103] B. C. Allanach, S. F. King and D. A. J. Rayner, JHEP 0405 (2004) 067 [arXiv:hep-ph/0403255].

[104] H. Baer, C. Balazs, A. Belyaev, R. Dermisek, A. Mafi and A. Mustafayev, JHEP 0205 (2002) 061 [arXiv:hep-ph/0204108].

[105] Z. Chacko, M. A. Luty, A. E. Nelson and E. Ponton, JHEP **0001** (2000) 003 [arXiv:hep-ph/9911323].

[106] S. F. King and D. A. J. Rayner, Nucl. Phys. B **607** (2001) 77 [arXiv:hep-ph/0012076].

[107] S. Dimopoulos, G. F. Giudice and A. Pomarol, Phys. Lett. B **389** (1996) 37 [arXiv:hep-ph/9607225].

[108] J. L. Feng and T. Moroi, Phys. Rev. D **61** (2000) 095004 [arXiv:hep-ph/9907319].

[109] J. R. Ellis, T. Falk, K. A. Olive and M. Srednicki, Astropart. Phys. **13** (2000) 181 [Erratum-ibid. **15** (2001) 413] [arXiv:hep-ph/9905481].

[110] L. E. Ibanez, C. Munoz and S. Rigolin, Nucl. Phys. B **553** (1999) 43 [arXiv:hep-ph/9812397].

[111] K. Benakli, Phys. Lett. B **475** (2000) 77 [arXiv:hep-ph/9911517].

[112] G. Shiu and S. H. H. Tye, Phys. Rev. D **58** (1998) 106007 [arXiv:hep-th/9805157].

[113] T. Higaki and T. Kobayashi, Phys. Rev. D **68** (2003) 046006 [arXiv:hep-th/0304200].

[114] S. Baek, P. Ko and H. S. Lee, Phys. Rev. D **65** (2002) 035004 [arXiv:hep-ph/0103218].

[115] D. G. Cerdeno, E. Gabrielli, S. Khalil, C. Munoz, E. Torrente-Lujan and E. Torrente-Lujan, Nucl. Phys. B **603** (2001) 231 [arXiv:hep-ph/0102270].

[116] D. Bailin, G. V. Kraniotis and A. Love, Phys. Lett. B **491** (2000) 161 [arXiv:hep-ph/0007206].

[117] L. E. Ibanez, R. Rabadan and A. M. Uranga, Nucl. Phys. B **576** (2000) 285 [arXiv:hep-th/9905098].

[118] C. H. Chen, M. Drees and J. F. Gunion, Phys. Rev. D **55** (1997) 330 [Erratum-ibid. D **60**, 039901 (1999)] [arXiv:hep-ph/9607421].